Journal of Pure and Applied Ultrasonics

VOLUME 33 NUMBER 1 JAN. TO MARCH- 2011

CONTENTS

Website : www.ultrasonicsindia.com

A Publication of — Ultrasonics Society of India

Information for authors

1. Type of Contribution

JOURNAL OF PURE AND APPLIED ULTRASONICS welcomes original research papers and articles related to the subject of ultrasonics. The contributions may be in the areas of physical ultrasonics, medical ultrasonics, ultrasonic non-destructive evaluation including NDT, high power ultrasonics, underwater acoustics, ultrasonic transducers, transducer materials & devices and any other related topic. These may fall into one of the following categories.

ResearchPapers **-** These should be on original research work contributing to scientific developments. They should be written with a wide readership in mind and should emphasize the significance of the work.

Reviews Articles **-** Includes critical reviews and survey articles.

Research and Technical notes **-** These should be short descriptions of new techniques, applications, instruments and components.

Letters to the editor **-** Letters will be published on points arising out of published articles and papers and on questions of opinion.

Miscellaneous **-** Miscellaneous contributions such as conference reports, Ph.D. thesis reviews and news items are also accepted. Recommended lengths of contributions are: Research papers 2000-4000 words, reviews articles 2000-5000 words; conference reports 500-1500 words; news items, research and technical notes up to 1000 words.

2. Manuscripts

Manuscripts should be typed on one side of the paper in double spacing with 25 mm margins on all side of A4 size paper. A soft copy of the manuscript in MS WORD for text and MS EXCEL for illustrations and a PDF file thereof may be sent by e-mail or CD/DVD. Colour images should be formatted as JPEG files. Figures submitted in colour would be published in colour. Colour should be avoided unless it is required in order to convey a message or serve a purpose in the image.

Title **-** Titles should be short and indicate the nature of the contribution. About 5 keywords may be given after the abstract.

Abstract **-** An abstract of 100-200 words should be provided on the title page of paper and review article. This should describe the full scope of the contribution and include the principal conclusions.

Mathematics **-** Mathematical expressions should be arranged to occupy the minimum number of lines consistent with clarity e.g., $(x^2+y^2)/(x-y)^{1/2}$

References **-** References should be indicated in the text by its number only. The reference number should be given as superscript. The corresponding reference shall contain the following information in order; names and initials of author(s)in bold, full title of the work, journal or book title in italic, volume number in bold, the year of publication in brackets and the page number. As example: Vasanth B.K., Palanichamy P., Jayakumar T. and Sankar B.N., Assessment of residual stresses in a carbon steel weld pad using critically refracted longitudinal (L_{CR}) waves, *J. Pure Appl. Ultrason*., 28 (2006) 66-72.

Units and Abbreviations **-** Authors should use SI units wherever possible.

3. Reprints

One copy of the issue in which the paper is published is sent to the author free of charges.

J. Pure Appl. Ultrason. 33 (2011) pp. 3-7

An ultrasonic method: A diagnostic tool to determine adulteration in liquid fuels

S. S. Tomar[1] and Radha Tomar[2]

[1]Department of Physics, S. L .P. Govt. P. G. College, Gwalior (M. P.) – 474006, India
[2]S.O.S. in Chemistry, Jiwaji University, Gwalior (M. P.) – 474011, India

Email: sstgwl@gmail.com

An ultrasonic grating acts as a sensor to evaluate adulteration in liquids. The method on physical optics in combination with ultrasonic grating has been used to diagnose adulteration in liquid mixtures for the present study. In this method separation between the diffracted dots depends upon the concentration or density or the refractive index of the adulterants. The variation of successive diffracted dots with concentration is sensitive enough to detect very small amount of adulteration. Light is diffracted due to ultrasonic grating and the separation of diffracted dots observed on the screen is a measure of adulteration in liquid mixtures.

Keywords: Acousto – Optics; Ultrasonic grating; Diffraction; Adulteration

1. Introduction & review of literature

Adulteration is a main problem in developing countries like India. Adulteration in liquids is often occurring in routine of modern life. It is an important problem which needs immediate attention for its solution. The adulterants are generally low quality liquids which are miscible with the pure samples and their presence will degrade quality of the sample. The effects of these adulterant mixtures will bring forth threat to the environment, living beings etc. The presence of kerosene and diesel oil in petrol produces enormous smoke and pollutes the atmosphere. There are several methods available to detect or to estimate adulteration in liquids. Some physical & chemical methods, such as synchronous fluorescence[1], evaluating total fluorescence quantum yield[2], FTIR spectroscopy and multivariate calibration[3], are being used as routine techniques for detecting sharing constituents in a sample, however no method can be identified as perfect for estimation of quantities of adulterants in samples. Fiber optic sensors have also been employed in testing adulteration in diesel and petrol by kerosene[4-5]. In view of the limitations of physical & chemical methods, some workers[6-11] have adopted and recommended ultrasonic interferometers for ultrasonic velocities, density, refractive index and compressibility of edible oils, petrol, diesel, kerosene and their binary mixtures to find out percentage of adulteration. The diffraction of light through liquid can be used to determine refractive index of the liquids by Laser Refractometry[12]. The ultrasonic velocity studies in petrol –kerosene mixture at low concentration is being determined by "Sing-Around Technique"[13]. An assessment of the extent of emission represented by opacity value and fuel quality tests with varied composition of fuel (Diesel) and adulterant (Kerosene) proportions in Diesel was the focus of the study[14]. Ghandoor et. Al[15] developed a new technique by using capillary tube for finding the refractive index of crude oils. Hueter & Bolt[16] generated the ultrasonic waves in the liquids by emerging the entire crystal mounted in liquid. Franco Docchio et.al[17] have presented a technique for measuring the refractive index of liquids using position- sensitive detector.

Keeping in mind these limitations and restrictions, a new method based on physical optics in combination with ultrasonic grating has been used to diagnose adulteration in liquid mixtures. In this method, the separation between diffracted dots depends upon the concentration or density or the refractive indices of adulterants. The variation of successive diffracted light dots with concentration is sensitive enough to detect very small amount of adulteration.

2. Theory & Principle of operation

Acousto–optic effect is the change in mechanical strain produced by an acoustic wave. Since the strain varies periodically in acoustic wave, the refractive index of the medium gets modulated periodically and creates refractive index grating. When light is incident

on such a grating, phenomena like diffraction occurs in either multiple or single order. The collimated light incidents upon a glass cell containing the mixture of liquids. The crystal fitted in base plate generates waves which on reflection from air-water interface produces the standing waves. Thus the standing waves are formed where nodes and antinodes act like opaque and transparent parts for the incident light. Thus these parts act as a grating producing the diffraction dots. By using a converging lens, these dots are displayed in the back focal plane of a lens. Hence grating action is produced in liquids. In this method the distance between two nodes or antinodes can be considered as grating element. According to the well known relative diffraction grating equation for normal incidence:

$$d \operatorname{Sin} \theta = n \lambda \quad (1)$$

Where n is the order of diffraction, λ is wavelength of light, d the width of grating & θ angle of diffraction.

The distance or separation between nodes or antinodes acts like grating element. Thus grating element can be written as:

$$d = \Lambda \text{ and } \operatorname{Sin} \theta = h / (F^2 + h^2)^{1/2} \quad (2)$$

Where Λ is the wavelength of ultrasonic waves and h is the distance between the first order diffraction dot and the centered dot. F is the focal length between the lens and the screen.

From equation (1) & (2)

$$\Lambda . h / (F^2 + h^2)^{1/2} = n \lambda \quad (3)$$

Or $h = n . \lambda . F . / \Lambda$

Or $h = C . (1/ \Lambda)$ (4)

Where C is constant equal to $n . \lambda . F$

Therefore it can be concluded that the separation between diffraction dots in the focal plane is inversely proportional to the sound wavelength which depends upon the liquid inside the glass cell. Density, Refractive index and velocity of variation of liquid mixtures has been calculated using Richardson[18] equations, which are as follows:

$$\begin{aligned} \rho_{12} &= \rho_1 X_1 + \rho_2 X_2 \\ n_{12} &= n_1 X_1 + n_2 X_2 \\ V_{12} &= V_1 X_1 + V_2 X_2 \end{aligned} \quad (5)$$

Where ρ_1 & ρ_2 are densities, n_1 & n_2 are refractive index, V_1 & V_2 are velocity of liquids and ρ_{12}, n_{12} and V_{12} are density, refractive index and velocity of the mixture respectively. X_1 and X_2 are the fraction of first & second constituents by volume.

3. Experimental set-up

To investigate the effect of light diffraction due to ultrasonic waves, a special cell has been designed (Fig. 1). The ultrasonic cell is made up of thick, optically flat glass walls of cubic shape which is fixed on a metallic copper plate as base. A hole of diameter equal to the crystal size is made at the center of the base plate in which the X-cut quartz crystal is cemented. On the back face of crystal a spring and a metallic plate are so placed that the tension on the crystal could be adjusted with the help of screws and the RF power leads connected to the upper and lower faces of crystal. The crystal faces are coated with gold for better electric connections. Propagation of ultrasonic waves is perpendicular to the crystal face. The crystal is excited by applying RF voltage. The natural frequency of 2 MHz for oscillating crystal has been used.

The details of experimental setup to study adulteration in liquids is given in Fig. 2. This apparatus has three parts: Collimating unit, table for ultrasonic cell and screen for photosensitive detector. Sodium light source (λ = 5890 X 10^{-8} cm) has been used. Ultrasonic diffractometer consists of a glass cell fitted with ultrasonic transducer and one movable metallic reflector facing each other and mounted on the opposite faces. Two transparent optical glass

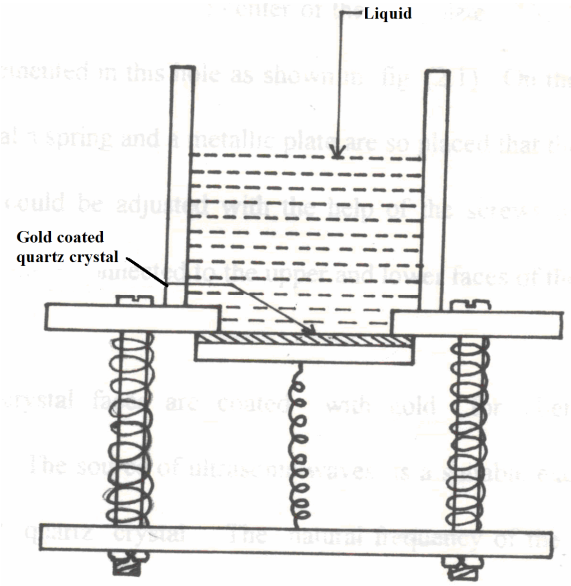

Figure 1—Ultrasonic cell filled with a liquid

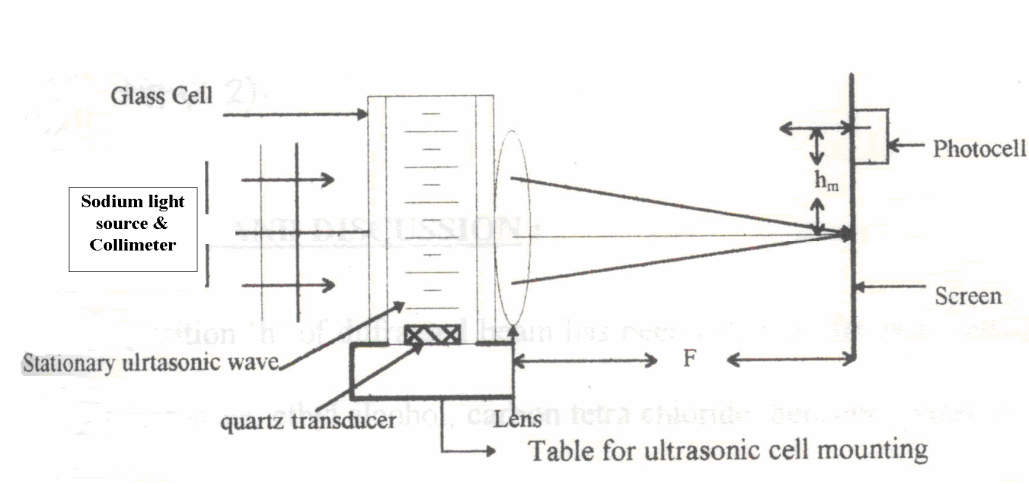

Figure 2—Experimental setup for adulteration detection and estimation in liquids of daily use

windows are also fitted on the remaining two sides of glass cell. The parallel light through optical windows from sodium light source incidents upon the glass cell. An adulterated liquid mixture is filled in the glass cell in which ultrasonic grating is set up by the transducer. Because of ultrasonic grating the light is diffracted which can be observed on the screen by an optical sensor. At any particular arbitrary distance the separation between diffraction dots can easily be measured with photosensitive detector. The separation is inversely proportional to the distance between the two successive nodes. It is infact a grating element or period. This grating element will be used to determine the sound wavelength, velocity, density, refractive index and compressibility of the liquid and liquid mixtures. The value of grating element corresponds to change in refractive index, density or concentration of the liquid which in turn is the measure of extent of adulteration in liquids.

4. Results and discussion

The position "h" of diffracted beam has been observed for pure liquids like petrol, kerosene, ethyl alcohol, carbon tetrachloride, benzene, water etc. which is tabulated in Table-1. The percentage adulteration in liquid mixture has been studied for petrol-kerosene, ethyl alcohol-carbon tetrachloride, benzene-carbon tetrachloride and water- ethyl alcohol which are tabulated in Table-2, 3, 4 and 5 respectively. The observations have been taken with sodium light (589 nm) source. The distance "h" between first order diffraction dot and central dot has been measured using Photosensitive Detector (PSD). The values of "h" are tabulated in the respective tables. Refractive index and the sound velocity for various compositions of the

Table 1—Reference values of the Refractive index, density, velocity and sound wave length of the liquid used

Liquid sample (L)	Refractive Index (n)	Velocity V (m/s)	Dots separation h (mm)	Sound wavelength Λ (nm)
Ethyl Alcohol	1.3229	1122	20.990	5.61
Water	1.3480	1473	15.995	7.37
Petrol	1.4138	980	24.041	4.90
Kerosene	1.4345	1170	20.000	5.89
CCl_4	1.4418	812	20.015	4.060
Benzene	1.4820	1024	23.008	5.12

mixture have been computed by using equation (5). The graphs plotted between wave velocity (V) and percentage composition for different samples are given in Fig. 3 for mixtures mentioned in Tables -2 to 5. The graphs in Fig. 4 have been plotted between percentage compositions (PC) versus dot separation (h). It showed a linear relationship which approves efficiency and sensitivity of the system against mole fraction of mixture of binary liquids. The different slopes indicate the device operation of various mixtures. Thus for the percentage adulteration studies in binary liquid mixtures, the sound velocity and the refractive index of pure liquids are not needed. Instead of this, 'dot' separation is needed which can be determined easily by using PSD (position sensitive detector). PSD is installed for direct beam position relative to which the diffraction dot position can be determined and hence the separation between the two dots can be calculated. Theoretically, it can be verified by using Richardson's[18] equation for density, velocity and refractive index stated for pure liquids and for this purpose one can develop an automatic computer programme to find adulteration as per the needs of the user in daily life.

Table 2—Kerosene concentration in Petrol Frequency 2MHz; wavelength of light source (λ) = 5890X 10^{-8} cm

% of Adulterated kerosene	Sound wavelength Λ (m)X10^{-4}	Dots separation h (m)	Refractive Index n (exp.)	Refractive Index n (cal.)	Velocity V(m/s)
0	4.908	0.0024	1.4130	1.41318	980
25	5.355	0.0022	1.4199	1.4190	1071
50	5.479	0.00215	1.4248	1.4242	1096
75	5.610	0.0021	1.4296	1.4293	1122
100	5.090	0.0020	1.4345	1.4345	1178

Table 3—Ethyl Alcohol concentration in Carbon tetrachloride Frequency 2MHz; wavelength of light source (λ) = 5890X 10^{-8} cm

% of Adulterated Ethyl Alcohol	Sound wavelength Λ (m)X10^{-4}	Dots separation h (m)	Refractive Index n (exp)	Refractive Index n (Cal.)	Velocity V(m/s)
0	3.993	0.00295	1.3540	1.3540	799
25	4.284	0.00275	1.3739	1.3755	857
50	4.620	0.00255	1.3704	1.4040	924
75	5.013	0.00235	1.4238	1.4185	1003
100	5.479	0.00215	1.4400	1.4400	1096

Table 4—Benzene concentration in Carbon tetrachloride Frequency 2MHz; wavelength of light source (λ) = 5890X 10^{-8} cm

% of Adulterated Benzene	Sound wavelength Λ (m)X10^{-4}	Dots separation h (m)	Refractive Index n (exp)	Refractive Index n (Cal.)	Velocity V(m/s)
0	4.062	0.0029	1.4418	1.4418	812
25	4.363	0.0027	1.4520	1.4521	873
50	4.712	0.0025	1.4649	1.4623	942
75	5.122	0.0023	1.4747	1.4723	994
100	5.890	0.0020	1.4828	1.4828	1024

Table 5—Water concentration in ethyl alcohol Frequency 2MHz; wavelength of light source (λ) = 5890X 10^{-8} cm

% of Adulterated water	Sound wavelength Λ (m)×10^{-4}	Dots separation h (m)	Refractive Index n (exp)	Refractive Index n (Cal.)	Velocity V(m/s)
0	5.610	0.0021	1.3488	1.3488	1122
25	6.544	0.0018	1.3439	1.34235	1273
50	6.929	0.0017	1.3418	1.33585	1386
75	7.139	0.0016	1.3320	1.32998	1428
100	7.363	0.0016	1.3229	1.3229	1473

The variation in the velocity of sound waves with increase in percentage of adulteration of petrol by kerosene is as shown in Fig. 3. From the figure it is evident that the velocity of sound waves increases with increase in adulteration by kerosene. The velocity for the solution with 100% concentration of kerosene was measured to be 1178 m/s. Similarly the variation in dot separation with increase in the percentage of adulteration of petrol by kerosene is as shown in Fig. 4. From the figure it is evident that the dot separation decreases with increase in adulteration by kerosene. The dot separation for the solution with 100% concentration of kerosene was measured to be 0.0020 m.

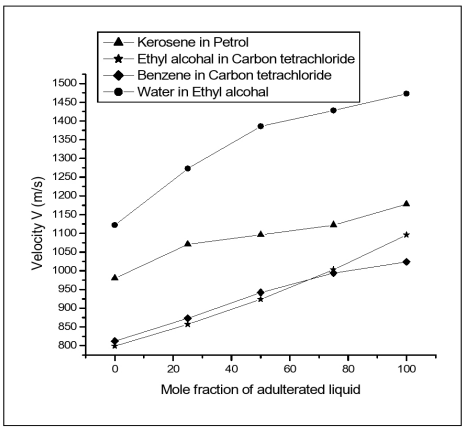

Figure 3—Change in light velocity with the increase in mole fraction of adulterated liquid

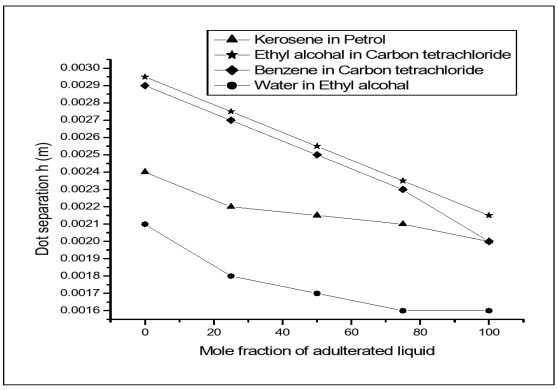

Figure 4—Change in dot separation with the increase in mole fraction of adulterated liquid

The variation in the velocity of sound waves with increase in the percentage of adulteration of carbon tetrachloride by ethyl alcohol is as shown in Figure 3. From figure it is clear that the velocity of sound waves increases with increase in adulteration by ethyl alcohol. The velocity for the solution with 100% concentration of ethyl alcohol was measured to be 1096 m/s. Similarly the variation in dot separation with increase in the percentage of adulteration of carbon tetrachloride by ethyl alcohol is as shown in Fig. 4 which shows that the dot separation decreases with increase in adulteration by

ethyl alcohol. The dot separation for the solution with 100% concentration of ethyl alcohol was measured to be 0.00215 m.

The variation in the velocity of sound waves with increase in the percentage of adulteration of carbon tetrachloride by benzene is as shown in Fig. 3. From the figure it is evident that the velocity of sound waves increases with increase in adulteration by benzene. The velocity for the solution with 100% concentration of benzene was measured to be 1024 m/s. Similarly the variation in dot separation with increase in the percentage of adulteration of carbon tetrachloride by benzene is as shown in Fig. 4. From the figure it is evident that the dot separation decreases with increase in adulteration by benzene. The dot separation for the solution with 100% concentration of benzene was measured to be 0.0020 m.

The variation in the velocity of sound waves with increase in the percentage of adulteration of ethyl alcohol by water is as shown in Fig. 3. From the figure it is evident that the velocity of sound waves increases with increase in adulteration by water. The velocity for the solution with 100% water was measured to be 1473 m/s. Similarly the variation in dot separation with increase in the percentage of adulteration of ethyl alcohol by water is as shown in Fig. 4. From the figure it is evident that the dot separation decreases with increase in adulteration by water. The dot separation for the solution with 100% was measured to be 0.0016 m.

Conclusion

The development of an ultrasonic technique is very useful in determining adulteration in liquid samples. It is very efficient and sensitive technique. For adulteration studies, sound velocity and the refractive index of pure liquids are not needed instead of this dot separation is needed which can be determined easily by using PSD (position sensitive detector). This technique is quick and economical and is found to be useful for carrying out investigations for diagnosing adulteration in liquid mixtures in daily life.

Acknowledgements

The authors are grateful to State University Grants Commission, Bhopal for the financial support. Authors are also grateful to Prof. V.P.Bhatnagar, Head, Department Of Physics Delhi College of Engineering for providing necessary facilities to design the ultrasonic cell and to the Department Of Physics, Dr. H.S.Gour University, Sagar for supporting the experimental facility.

References

1 A. Taksande and C. Hariharan, Synchronous fluorescence method to check adulteration of petrol and diesel by kerosene, Spectroscopy Lett.3, 345 (2006).
2 D. Patra, Distinguishing motor oils at higher concentration range by evaluating total fluorescence quantum yield as a novel sensing tool, Sens. Act. B 192:2, 632 (2008).
3 M. A. Al-Ghouti, Y. S. Al-Degs, M. Amer, Determination of motor gasoline adulteration using FTIR spectroscopy and multivariate calibration, Talanta , In press (2008).
4 C.R Rao, L.C S. Reddy, C.A.R. C. Prabhu, Study of adulteration in oils & fats by an ultrasonic method, Current Science 9 (1980) 19.
5 N.P. Singh, J.S. Singh, Study of the adulteration of oils & fats by ultrasonic method, Current science 49(1980)185-187.
6 B.V.G. Rao, S.B. Agrawal, V.P. Bhatnagar, An ultrasonic method to find the liquid fuel adulteration, Indian J. Acous. Soc. Ind. 9 (1981) 19
7 V. P. Bhatnagar& Rao, B.V.G., Diffraction of light by two overlapping Ultra-sonic waves traveling at right angles J. Pure Appl. Ultrasonic 5 (1983) 63- 65.
8 S. Mohan, V.K.Vaidyan, K.V. Kurian, Detection & estimation of adulteration in petrol using an ultrasonic method, presented in International Congress on Ultrasonic (ICU), held at National Physical Laboratory Delhi, India (1990).
9 S.S.Bhatti, W.Singh, Studies of ultrasonic velocity in petrol, Acoustic letters 8 (1985) 105-108.
10 Y.Makdisi, A.A Zaidi, & K.S. Bhatia Laser Refractometry of liquids with a diffractive grating optics communication 72 (1989) 148-152.
11 R. Sukhdev, "Fiber optic sensor for determining adulteration of petrol & diesel by kerosene, Science Direct: Sensors and Actuators B: Chemical 55 (2002) 212-216.
12 L. M. Bali, A. Srivastava, R. K. Shukla, A. Srivastava, Optical sensor for determining adulteration in a liquid sample, Opt. Eng. 38 (1999) 1715- 1721.
13 S. J. Sharma, S. Rajgopalan, Ultrasonics velocity studies in petrol – kerosene mixtures at low concentrations, J. Pure App. Ultrasonics 15 (1993) 124-128.
14 R. Sh. Yadav, K. V. Murthy, D. Mishra, B. Baral, Estimation of petrols and diesel adulteration with kerosene and assessment of useful of selected automobile fuel quality test parameters, International Journal of Environmental Science & Technology 1 (2005) 253-255.
15 HEI Ghandoor, E. Hegazi, I. Nasser, G.M. Bechery, Opt. Laser Technol. 35(2003) 361-367.
16 Huter & Bolt, SONICS, John Wiley & Sons, Newyork, 1955.
17 F. Docchio, S. Corini, M. Perini, R. S. Kasana, IEEE Trans Instrum Meas 44 (1995) 68-70.
18 Richardson,E.G., Ultrasonic Physics (Elsevier publishing comp. Amesterdum), 1952,178.

J. Pure Appl. Ultrason. 33 (2011) pp. 8-15

A comparative study of prediction of flaw response and flaw detection in polycrystalline materials

K.S. APRAMEYA[1], R.S. ANAND[2], B.K. MISHRA[3] and S. AHMED[4]

[1]Department of Electrical Engg,University BDT College of Engg, Davangere, [2]Department of Electrical Engg, Indian Institute of Technology, Roorkee

[3]Department of Mechanical and Industrial Engg, Indian Institute of Technology,Roorkee

[4]Senior Scientist/Engineer, Naval Surface Warfare Center, Maryland,USA.

Email: aprameya_ks@yahoo.co.in

The aim of this paper is to perform a comparative study of flaw response with the grain noise signal in an ultrasonic pulse echo simulation. This is one of the analytical methods to determine the flaw response. The flaw response is predicted using the approximation techniques like Kirchoff approximation, Born approximation and modified Born approximation. The grain noise signal generated in addition to flaw response is modelled analytically. By comparing the results of predicted flaw response and grain noise signal, the possibility of flaw detection can be estimated. Here the flaw considered for study is a spherical void and the material selected for study is a polycrystalline metal. Firstly, the comparison is made for 1MHz circular transducer and secondly the study is performed for different center frequencies of transducer.

Keywords: spherical void, pulse echo simulation, scattering amplitude, grain noise signal, predicted flaw response.

Introduction

Testing of material or a component or a product is an integral and the most important constituent of the quality assurance programme of any industry. Unlike destructive testing, non destructive testing (NDT), as the name suggests, does not impair the product or component being tested in any manner[1]. Besides that with this specific procedure the serviceability of materials or components is not impaired by the testing process. Additionally, testing during the manufacturing processes is also facilitated by NDT procedures which are needed to increase the reliability of products in service and maintenance of systems to avoid premature failure of the products.

A variety of NDT methods are followed in the industries. The choice of the specific method depends on many factors including availability, accessibility and suitability based on analysis and past experience. Ultrasonic testing (UT) is one of the most widely used methods of non destructive testing and evaluation of industrial materials and components[6]. This testing method has applications to polymers, plastics, composites and ceramics. Prime uses of ultrasonic testing are the detection and characterization of internal flaws and wall thickness measurements. In recent years, ultrasonic testing has been employed to determine physical properties, elastic constants and microstructure including grain size, phases etc.

In this paper, an analytical study is carried out to predict the flaw response in polycrystalline metals in an ultrasonic pulse echo simulation. In a polycrystalline metal, there are numerous discrete grains and each grain having a regular crystalline atomic structure[8]. When an ultrasonic wave propagates through such a polycrystalline aggregate, it is attenuated due to scattering at the grain boundaries[9,10]. The energy scattered by a flaw when subjected to an incident wave field and received by a transducer (flaw response) depends on the size, shape and material properties of the flaw. Here the flaw considered is a spherical void.

The prediction of flaw response is determined by assuming that the incident ultrasonic beam is modelled by well known Multi Gaussian Beam (MGB) approach[4]. The significant advantage of MGB model is that it can easily treat transmission and reflection at multiple curved interfaces and propagation through complex media such as anisotropic solids[4]. The flaw response is related to scattering amplitude and particle velocity due to passage of ultrasonic wave. The scattering amplitude is different for different types of scatterers[3]. The scattering amplitude can be determined by different approximation techniques like Kirchoff approximation, Born approximation, modified Born approximation[3,6]. In this paper, the flaw response is predicted using all these approximation techniques. Here, both the near field and far field responses can be determined. The flaw response is determined for homogeneous isotropic case and then by assuming the material to be microscopically inhomogeneous. In addition to this, in an ultrasonic inspection system, the

grain noise signals tend to mask the signals from small and subtle defects[9]. Hence, these predicted flaw responses are compared with the grain noise signal so that possibility of flaw detection can be made and the results thus obtained are compared. In this study, a circular transducer of 1MHz is considered and further the results are compared for different center frequencies of transducer. The particle velocity due to passage of ultrasonic wave is same for all the approximation techniques and is determined by differentiating velocity potential[5].

2. Theory

Consider a pulse echo simulation as shown in Fig. 1. Let the flaw be a spherical void of radius *b*, at a distance Z_F from the contact circular transducer.

2.1 Determination of Received Voltage $V_R(\omega)$

The voltage received at the transducer is simulated by considering the flaw at different locations. For pulse echo set up, the voltage received at the transducer[3], for small flaws is:

$$V_R(\omega) = \beta(\omega)[-\frac{2\pi}{ikS_T}][\hat{V}(\omega)]^2 A(\omega) \qquad (1)$$

The notations for different symbols are given in the reference[5]. The scattering amplitude $A(\omega)$ is different for different geometries. Here, the scattering amplitude is considered from Kirchoff approximation, Born approximation and modified Born approximation.

Obtaining the exact scattering amplitudes normally requires solving an appropriate boundary value problem. However at high frequencies, by making some strong assumptions about the scattering process we can obtain explicit approximate expressions for the scattering amplitude for volumetric and crack like flaw cases. This high frequency approximation is called the Kirchoff approximation. The scattering amplitude $A(\omega)$ is derived for the case of ellipsoidal void[6] and with suitable modifications it can be applied for spherical void.

Explicit scattering expression can be obtained for volumetric flaws or inclusions whose material properties do not differ substantially from that of the surrounding host material by assuming that the incident wave is only slightly affected by the presence of the flaw. This weak scattering approximation is called Born approximation in recognition of its close relationship to the method used by Born for potential scattering problems.

The limitation of Kirchoff approximation is that it can be applied for strongly scattering flaws whereas the Born approximation can be used to predict the response due to weak scattering flaws. However with some modifications[7] Born approximation can be used to predict response for both strong and weak flaws. Hence, this approximation method is called modified Born approximation. It can be demonstrated that the Born approximation works well at very low frequencies and for very weak scatterers only. For the more prevalent types of inclusions that might be found in NDT tests, the Born approximation generally predicts incorrect scattering amplitudes and an incorrect time delay between responses from the front and back flaw surfaces. The drawbacks of Born approximation can be eliminated and scattering results can be improved for inclusions in isotropic solids with suitable modifications[7]. This modification on Born approximation is called doubly distorted (DD) Born approximation which has been developed recently. However, as observed by Schemerr et al.[7] even this doubly distorted Born approximation has

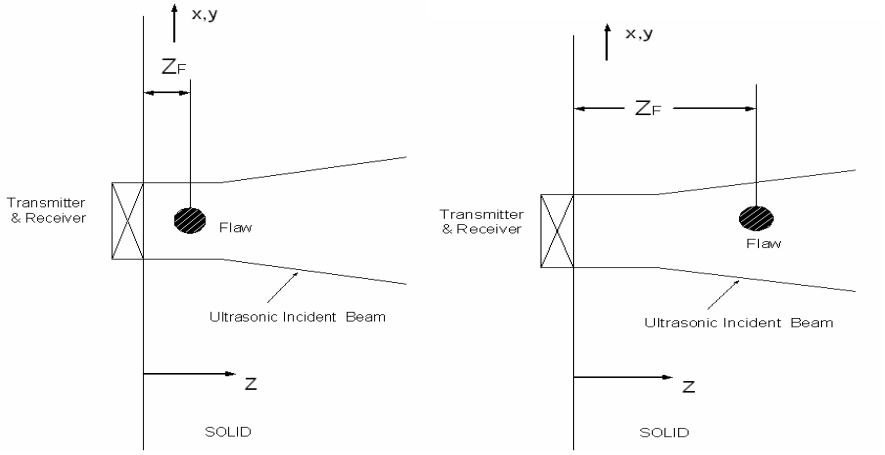

Fig. 1—Pulse Echo Simulation (a) Flaw located in near field (b) Flaw located in far field

inherent errors. Although it predicts the correct time delay between responses from front and back flaw surfaces it predicts the wrong arrival time of the leading edge response. Hence, in the case of strong scatterers (the properties of the flaw differ significantly from the host material) the accuracy of the predicted scattering amplitude is reduced. Thus the DD Born approximation is modified again by Schmerr et al. [7]. As proposed by Schmerr et al. [7], the modification on DD Born approximation involves modifications on amplitude and phase. With this modification, it can be applied for both weak and strong scatterers .

Thus, the expressions for scattering amplitude $A(\omega)$ for a spherical void using Kirchoff approximation, Born approximation and modified Born approximation are respectively given by Eqn.2-4[3, 5, 7].

$$A(\omega) = -\frac{b}{2}\exp(-ikb)\left[\exp(-ikb) - \frac{\sin(kb)}{kb}\right] \tag{2}$$

$$A(e_i;-e_s) = A(\omega) = -R_p b \times \left[\frac{\sin(2kb) - 2kb\cos(2kb)}{2kb}\right] \tag{3}$$

$$A(e_i;-e_i) = A(\omega) = -\frac{f(e_i;-e_i)}{4} b \times \left[\frac{\sin(2kb) - 2kb\cos(2kb)}{2kb}\right] \tag{4}$$

2.2 Determination of Particle Velocity due to Passage of Ultrasonic Wave for Different Flaw Locations

The calculation of particle velocity is given in the reference [5] where the prediction of flaw response is determined using Born approximation. Here it is presented briefly. For different flaw locations, the received voltage at the transducer is a function of *z*. The particle velocity due to passage of the ultrasonic wave [4] is given by

$$\vec{v} = -\nabla\phi \tag{5}$$

where ϕ is the velocity potential ϕ is a function of two variables z and r [4]. It can be shown that the particle velocity is given by

$$\vec{v}(\omega) = \sum_{n=1}^{10} \frac{A_n \exp(ikz)}{1 + \frac{izB_n}{z_R}\left(1 - \frac{B_n}{kz_R\left(1 + \frac{izB_n}{z_R}\right)}\right)} \tag{6}$$

Hence, the normalized particle velocity $\hat{V}(\omega)$ given by $\frac{\vec{v}(\omega)}{v_0}$ can be determined. Here, v_0 is the velocity on the surface of the transducer. This normalized particle velocity is same for all the approximation techniques. Thus substituting Eqn.6 in Eqn.1 and corresponding scattering amplitude expressions in Eqn.1, the received voltage at the transducer using Kirchoff approximation, Born approximation and modified Born approximation can be determined.

In Eqn.2-4 and Eqn.6, *k* is the wave number. For homogeneous isotropic medium it is a real quantity and for the microscopically inhomogeneous medium, the wave number is a complex quantity, where real part depends on the phase velocity dispersion and imaginary part accounts for ultrasonic attenuation due to grain scattering. Thus the flaw response is determined by considering the effect of ultrasonic attenuation due to scattering [10]. Here, these *k* values are computed by using Unified Theory of Stanke and Kino[2].

2.3 Modelling of grain noise signal

The modeling of grain noise signal is briefly explained. The possibility of detection of a flaw of a given size involves the determination of the back scattered power and the average grain noise spectra [8-10]. The average grain noise spectra is given by

$$\langle N(\omega)\rangle = \left[\left\langle \delta\Gamma(\omega)\delta\Gamma^*(\omega)\right\rangle\right]^{\frac{1}{2}} = \frac{\beta}{2a^2\sqrt{\pi}} \times \sqrt{\Omega} \times \left[\frac{\left\langle \delta C_{3333}\delta C_{3333}\right\rangle^{\frac{1}{2}}}{k^{\frac{1}{2}} C^0_{3333}} \cdot \frac{x^{3/2}}{(1+x^2)}\right] \tag{7}$$

A back scatter coefficient may be defined as

$$\eta = \frac{d^{1/2}\left\langle \delta C_{3333}\delta C_{3333}\right\rangle^{1/2}}{C^0_{3333}} \cdot \frac{x}{(1+x^2)} \tag{8}$$

The back scatter coefficient η has the dimension of $\sqrt{length}$ .Using Eqn.8, $\langle N(\omega)\rangle$ may be written as

$$\langle N(\omega)\rangle = \left\{\frac{\beta}{2a^2\sqrt{\pi}}\sqrt{\Omega}\right\}.\eta \tag{9}$$

By taking $\Omega = \pi a^2 D$ in Eqn. 9 when analyzing the likelihood of detection of a volumetric defect. We find that $\langle N(\omega) \rangle$ is given by,

$$\langle N(\omega) \rangle = \frac{\beta}{2a} \sqrt{D}.\eta \qquad (10)$$

It is observed from Eqn.10 that the grain noise signal is a function of frequency. The back scatter coefficient depends on the material properties. The material properties of the chosen material iron are C_{11} = 2.16 $\times 10^{11}$ N/m^2, C_{12} = 1.45×10^{11} N/m^2, C_{44} = 1.29×10^{11} N/m^2 and ρ = 7.86×10^3 kg/m^3. This grain noise signal is compared with the predicted flaw response determined using the approximation techniques when the material is microscopically inhomogeneous to ascertain the possibility of flaw detection. Further this study is performed for different center frequencies of transducer.

Results and Discussions

A circular transducer of diameter 20*mm* with a center frequency of 1MHz is considered. For ultrasonic wave propagating in the steel medium with velocity of 5.9 $mm/\mu S$, the length of near field corresponds to 16.94*mm*. The time domain response is obtained by taking Inverse Discrete Fourier Transform (IDFT). The flaw response in frequency domain is considered as Discrete Fourier Transform (DFT) coefficients here. The number of points considered for DFT and IDFT are 1024. To obtain the flaw response a Matlab program is written.

3.1 Predicted flaw response

The flaw response is predicted using Born approximation[5]. For illustration, the results of predicted flaw response using modified Born approximation are shown in Fig. 2 and Fig. 3, when the distance from flaw to transducer *z* is 10 *mm,* for radius of void being 2.5 *mm*. Fig. 2 shows the response for the homogeneous isotropic case and Fig. 3 shows the response for microscopically inhomogeneous case. Similarly the results are obtained from Kirchoff and Born approximation techniques.

From Fig. 2 and Fig. 3 it is observed that the amplitude of flaw response obtained in frequency and time domain is reduced considerably for the microscopically inhomogeneous case since the effect of ultrasonic attenuation and phase velocity dispersion due to grain scattering is considered in the calculations.

3.2 Grain noise signal

Using Eqn.10, the RMS value of the grain noise is determined for a flaw of given size and shape. The flaw considered in this case is a spherical void. The back scatter coefficient is determined using the material properties. The grain noise signal is considered in the frequency domain and its variation is shown in Fig. 4 for a flaw of radius 2 *mm*.

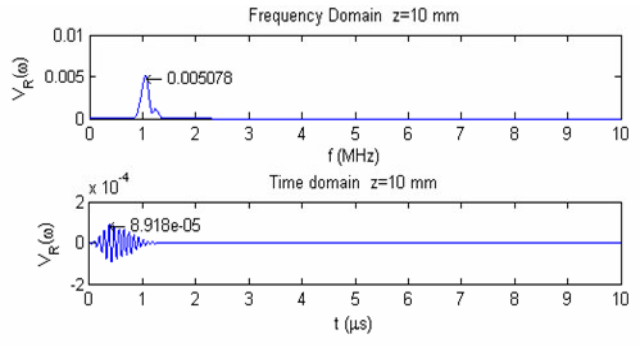

Fig. 2—Predicted flaw response for z = 10 *mm* for homogeneous isotropic case

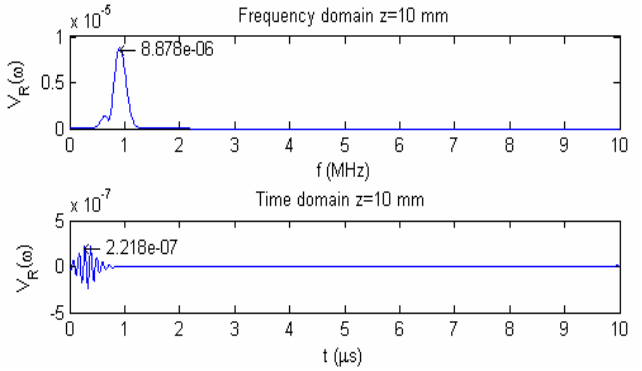

Fig. 3—Predicted flaw response for microscopically inhomogeneous case for z = 10 *mm*

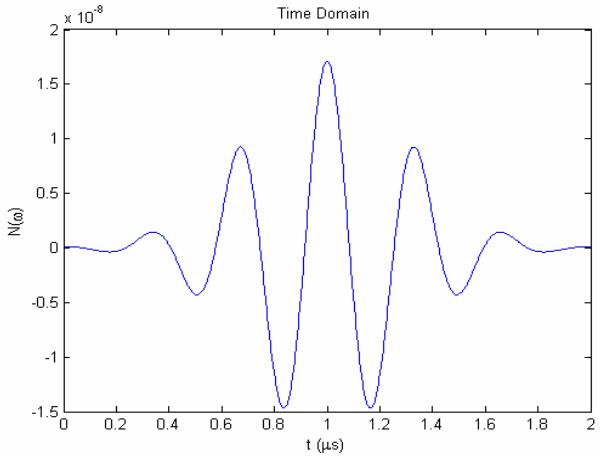

Fig. 4—Grain noise signal in frequency domain

Fig 5 shows the time domain response of this grain noise signal.

3.3 Comparison of grain noise signal and predicted flaw response

To determine the possibility of flaw detection, the amplitude of predicted flaw response in frequency domain is compared with that of the grain noise signal. The expression for far field scattering amplitude depends on the approximation technique used. The scattering amplitude is determined by Kirchoff approximation, Born approximation and modified Born approximation. In all these techniques, it is assumed that the flaw is small.

The Tables T1-T3 list the amplitude of predicted flaw response obtained from these three approximation techniques and grain noise signal for different values of distance z and for varying radius of inclusion. Table-1 shows the case for z = 10 *mm*. Table-2 shows the results for z = 14 *mm* while Table-3 shows the same for z = 20 *mm*. These values are for the center frequency of transducer 1 MHz. The graphical plot of these results is shown in Fig. 6.

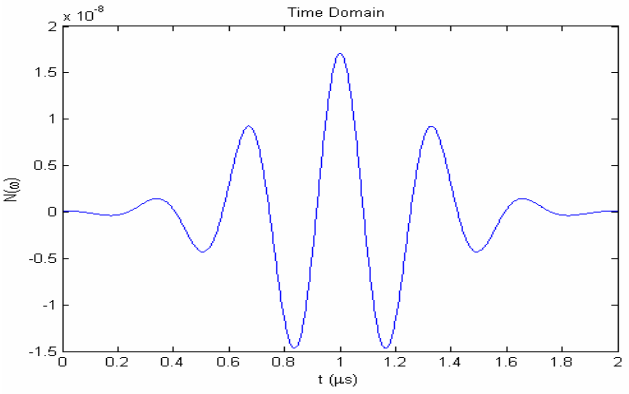

Fig. 5—Grain noise signal in time domain

In the Tables T1-T3 and also in Fig. 6, KA, BA and MBA stand for the predicted flaw response determined using Kirchoff, Born and modified Born approximation methods, respectively. GNS is grain noise signal.

Fig. 6 shows the variation of grain noise signal and predicted flaw response obtained by the three approximation methods versus radius of flaw for different values of z Here, the centre frequency of the transducer is 1MHz. In Fig. 6, PFS stands for predicted flaw response. From Fig. 6 (a) it is clear that the predicted flaw response is more than the grain noise signal when *z* is 10 *mm* and flaw of more than 0.5 *mm* can be detected by using any of these three methods. Further, the amplitude of flaw response obtained in Kirchoff method is more than that of Born and modified Born method for the same value of flaw radius. Also, the amplitude of flaw response obtained in modified Born method is slightly more than that of Born method.

When the distance *z* is 14 *mm*, from Fig. 6 (b), it is clear that the flaw of radius more than 1.5 *mm* can be

T-1 Amplitude of flaw response and grain noise signal (z = 10 *mm*)

Approximation Technique	Predicted flaw response for radius of flaw (*b*) equal to				
	0.25 *mm*	0.5 *mm*	1*mm*	2.5 *mm*	5 *mm*
KA	1.355E-06	2.238 E-06	5.568 E-06	3.032E-05	0.0001372
BA	1.73E-07	1.251 E-06	6.593 E-06	1.538 E-05	2.611 E-05
MBA	1.74E-07	1.268 E-06	6.735 E-06	1.633 E-05	3.262 E-05
GNS	1.606E-06	2.271E-06	3.211 E-06	5.078 E-06	7.181 E-06

T-2 Amplitude of flaw response and grain noise signal (z = 14 *mm*)

Approximation Technique	Predicted flaw response for radius of flaw (b) equal to				
	0.25 *mm*	0.5 *mm*	1 *mm*	2.5 *mm*	5 *mm*
KA	2.31E-07	1 E-06	2.234 E-06	1.249E-05	5.635E-05
BA	2.76E-08	5 E-07	2.638 E-06	6.104 E-06	1.033 E-05
MBA	2.81E-08	5.035 E-07	2.692 E-06	6.36 E-06	1.33 E-05
GNS	1.606E-06	2.271E-06	3.211 E-06	5.078 E-06	7.181 E-06

T-3 Amplitude of flaw response and grain noise signal (z = 20 *mm*)

Approximation Technique	Predicted flaw response for radius of flaw (*b*) equal to				
	0.25 *mm*	0.5 *mm*	1 *mm*	2.5 *mm*	5 *mm*
KA	1.12E-07	3.678 E-06	8.71E-07	5.002E-06	2.249E-05
BA	1.25E-08	2 E-07	1.026 E-06	2.329 E-06	4E-06
MBA	1.314E-08	2 E-07	1.047 E-06	1.2473 E-06	5.253E-06
GNS	1.606E-06	2.271E-06	3.211 E-06	5.078 E-06	7.181 E-06

detected by these methods. It is observed that amplitude of flaw response obtained in Kirchoff method is once again more than that of Born and modified Born methods.

Similarly when the distance z is 20 *mm*, as seen from Fig. 6 (c), it is clear that the flaw of radius of more than 2.5 *mm* can be detected in Kirchoff method whereas it goes undetected in Born and modified Born methods. In this case, the grain noise signal is more than that of the predicted flaw response as observed in Born and modified Born methods. However, the amplitude of predicted flaw response obtained in modified Born method is slightly more than that of Born method for radius of flaw more than 4 *mm*.

Further, as the distance z is increased, the amplitude of flaw response is decreased, as can be seen from Table 1-.3 and Fig. 6.

3.4 Predicted flaw response and grain noise signal for different center frequencies of transducer

The above study of comparing the predicted flaw response with the grain noise signal is performed for different center frequencies of transducer. The different center frequencies considered for study are 2MHz, 3MHz and 5MHz. The results of comparison of predicted flaw response with grain noise signal using Kirchoff approximation is shown in Fig. 7, when f = 2MHz. Similarly, the method of comparison of predicted flaw response with grain noise signal is carried out for f = 3MHz and 5 MHz. Since the variation of the amplitude of flaw response is very small particularly for z values being greater than 25 *mm*, the summary of results obtained using Kirchoff approximation method is given in Table T-4. In a similar manner, the results obtained using Born and modified Born approximation techniques are listed in the tables T5 and T6 respectively.

In the case of Kirchoff approximation (Fig. 7), it is found that for center frequency of transducer to be 2MHz, the flaw of radius of more than 0.5 *mm* can be detected when z is within 10 *mm*. The flaw of radius more than 2 *mm* can be detected when z is within the limit of 25 *m.* Similarly, the flaw of radius more than 3.5 *mm* can be detected if z is in the limit of 35 *mm*. For higher values of z (more than 35 *mm*), the flaws cannot be detected for this centre frequency of the transducer. But when the center frequency of transducer is 3MHz and 5MHz, it is found that the flaw of size more than 0.5 *mm* can be detected when z is within the limit of 10 *mm* and for higher values of z

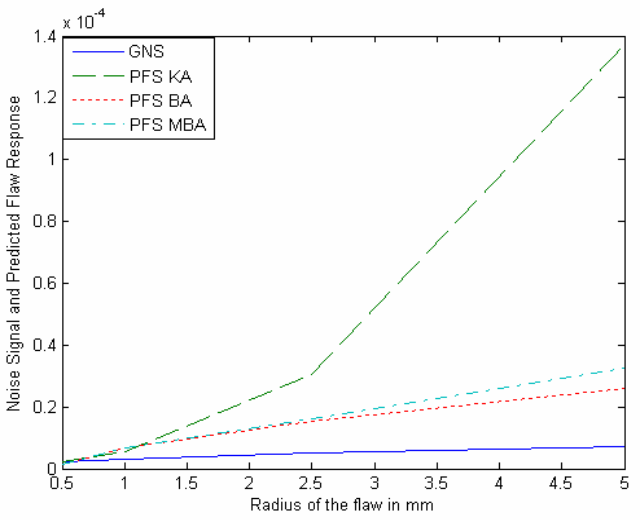

(a)

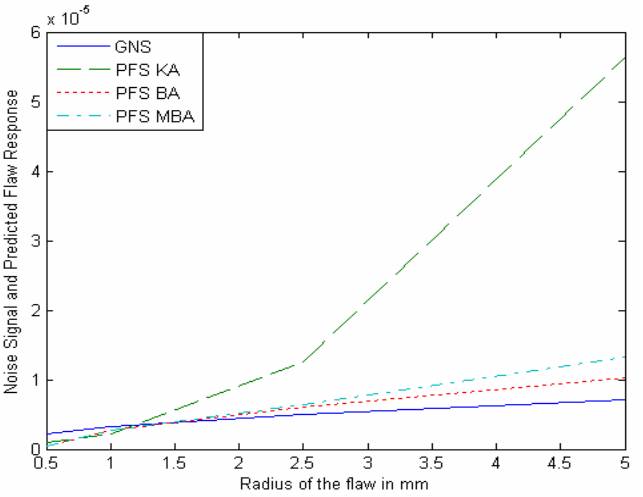

(b)

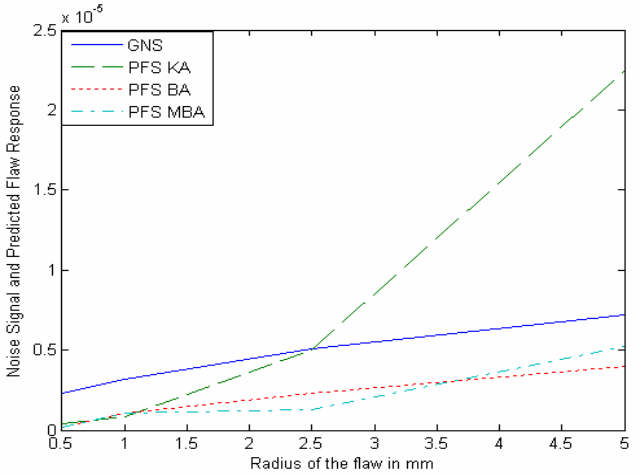

(c)

Fig. 6—Variation of grain noise signal and predicted flaw response determined using approximation techniques versus radius of flaw for (a) z = 10 *mm* (b) z = 14 *mm* (c) z = 20 *mm*

T-4 Summary of results obtained using Kirchoff approximation method

T- 4 (a) f = 2MHz

b in *mm*	0.5	1	2	3	4	5
GNS	0.06E-05	0.064E-05	0.067E-05	0.071E-05	0.075E-05	0.12E-05
PFS z = 10 *mm*	0.07E-04	0.18E-04	0.41E-04	0.78E-04	1.19E-04	1.79E-04
PFS, z = 25 *mm*	0.012E-07	0.031E-06	0.071E-04	0.192E-04	0.372E-04	0.592E-04
PFS, z = 35 *mm*	0.011E-07	0.014E-07	0.051E-04	0.69E-04	0.181E-04	0.21E-04

T-4 (b) f = 3MHz

b in *mm*	0.5	1	2	3	4	5
GNS	0.021E-04	0.025E-04	0.029E-04	0.032E-04	0.041E-04	0.051E-04
PFS z = 10 *mm*	0.15E-03	0.249E-03	0.567E-03	1.312E-03	1.912E-03	3.349E-03
PFS, z = 25 *mm*	0.12E-08	0.14E-08	0.241E-08	0.281E-08	0.361E-08	0.412E-08
PFS, z = 30 *mm*	0.09E-09	0.094E-09	0.21E-09	0.31E-09	0.414E-09	0.421E-09

T-4 (c) f =5MHz

b in *mm*	0.5	1	2	3	4	5
GNS	0.025E-03	0.026E-03	0.031E-03	0.036E-03	0.044E-03	0.054E-03
PFS z = 10 *mm*	0.167E-03	0.371E-03	0.614E-03	1.514E-03	2.31E-03	3.391E-03
PFS, z = 30 *mm*	0.14E-08	0.156E-08	0.245E-08	0.286E-08	0.371E-08	0.514E-08
PFS, z = 50 *mm*	0.094E-09	0.098E-09	0.261E-09	0.361E-09	0.614E-09	0.814E-09

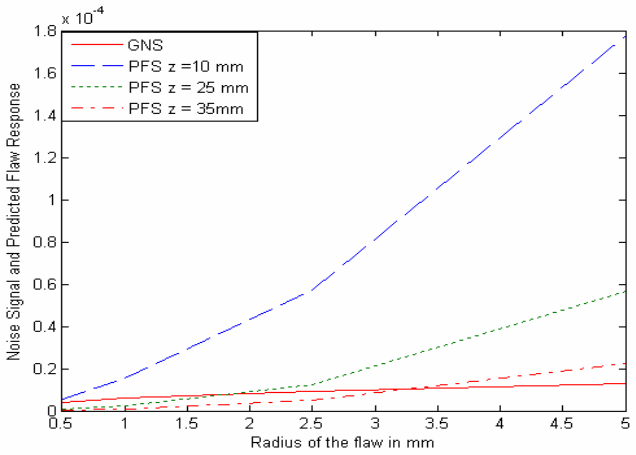

Fig.7—Comparison of flaw response and grain noise signal using Kirchoff approximation for f= 2MHz

it goes undetected. Similarly when the results of predicted flaw response of Born and modified Born approximation are compared with the grain noise signal for center frequency of transducer to be 2MHz, 3MHz and 5MHz (Tables T-5 and T-6), it is observed that that only flaws of more than 0.5 *mm* can be detected when z is upto the range of 10 *mm* and for higher values of z the noise signal exceeds the flaw response and hence the flaws become undetectable.

Thus, it can be concluded that the accuracy of detectability of a flaw by a specified modelling technique depends on the size of the flaw. Further, as mentioned earlier smaller flaws which goes undetected at lower frequency of the transducer can be detected at higher center frequency of transducer.

Conclusions

In this paper an analytical method is explained to determine the flaw response using different approximation techniques and modelling of grain noise signal is briefly summarized. The results of comparison of predicted flaw response determined from these three approximation techniques with the grain noise signal reveals that flaw of radius more than 3.5 *mm* can be detected even when the distance from flaw to transducer is in the range of 35 mm, when the center frequency of transducer is 2MHz using Kirchoff approximation whereas it goes undetected in Born and modified Born methods. Similarly the results are explained for other center frequencies of the transducer. It can be concluded that if the grain noise signal is more than the predicted flaw response, then the flaw may not be detected from the received signal without the use of complex signal processing methodology. Also, in otherwords it can be mentioned that accuracy of flaw detection depends on the modeling techniques used and also on the wavelength of ultrasound.

Acknowledgements

The authors are grateful to the department of Electrical Engineering of Indian Institute of Technology, Roorkee and the sponsorship of QIP program (AICTE New Delhi) to K.S.Aprameya is gratefully acknowledged.

T-5 Summary of results obtained using Born approximation method

T-5 (a) f = 2MHz

b in *mm*	0.5	1	1.5	2	3	4
GNS	0.039E-05	0.042E-05	0.047E-05	0.914E-05	1.51E-05	1.21E-05
PFS z = 10 *mm*	0.691E-05	1.312E-05	2.12E-05	2.417E-05	5.214E-05	6.6E-05
PFS, z = 25 *mm*	0.041E-07	0.047E-07	0.051E-07	0.056E-07	0.011E-05	0.019E-05
PFS, z = 35 *mm*	0.35E-07	0.031E-07	0.036E-07	0.039E-07	0.047E-07	0.054E-07

T-5 (b) f = 3MHz

b in *mm*	0.5	1	1.5	2	3	4
GNS	0.012E-04	0.015E-04	0.019E-04	0.025E-04	0.031E-04	0.044E-05
PFS z = 10 *mm*	0.34E-04	0.41E-04	0.714E-04	1.112E-04	1.619E-04	2.412E-04
PFS, z = 25 *mm*	0.052E-07	0.054E-07	0.061E-07	0.065E-07	0.076E-07	0.085E-07
PFS, z = 35 *mm*	0.041E-07	0.0414E-07	0.041E-07	0.051E-07	0.061E-07	0.067E-07

T-5 (c) f =5MHz

b in *mm*	0.5	1	1.5	2	3	4
GNS	0.014E-03	0.0148E-03	0.0149E-07	0.023E-03	0.027E-03	0.044E-03
PFS z = 10 *mm*	0.12E-03	0.241E-03	0.421E-03	0.571E-03	1.212E-03	1.791E-03
PFS, z = 30 *mm*	0.0671E-07	0.0674E-07	0.0681E-07	0.0714E-07	0.0758E-07	0.081E-07
PFS, z = 50 *mm*	0.0514E-07	0.0517E-07	0.0519E-07	0.0612E-07	0.0617E-07	0.0691E-07

T- 6 Summary of results obtained using modified Born approximation method

T-6 (a) f = 2MHz

b in *mm*	0.5	1	1.5	2	3	4.5
GNS	0.0591E-04	0.0614E-04	0.0712E-04	0.0814E-04	0.0871E-04	0.151E-04
PFS z = 10 *mm*	0.081E-04	0.167E-04	0.221E-04	0.224E-04	0.391E-04	1.013E-04
PFS, z = 25 *mm*	0.042E-07	0.044E-07	0.045E-07	0.048E-07	0.061E-04	0.021E-04
PFS, z = 35 *mm*	0.036E-07	0.037E-07	0.039E-07	0.041E-07	0.0435E-07	0.0441E-07

T-6 (b) f = 3MHz

b in *mm*	0.5	1	1.5	2	3	4.5
GNS	0.112E-04	0.119E-04	0.121E-04	0.141E-04	0.241E-04	0.312E-04
PFS z = 10 *mm*	0.318E-04	0.618E-04	1.014E-04	1.494E-04	2.484E-04	4.487E-04
PFS, z = 25 *mm*	0.044E-07	0.0451E-07	0.0461E-07	0.0462E-07	0.0481E-07	0.053E-07
PFS, z = 35 *mm*	0.0381E-07	0.0391E-07	0.042E-07	0.044E-07	0.0461E-07	0.051E-07

T-6 (c) f =5MHz

b in *mm*	0.5	1	1.5	2	3	4.5
GNS	0.0241E-03	0.0243E-03	0.0245E-03	0.0247E-03	0.0312E-03	0.0319E-03
PFS z = 10 *mm*	0.125E-03	0.451E-03	0.621E-03	0.751E-03	1.514E-03	4.312E-03
PFS, z = 30 *mm*	0.045E-07	0.046E-07	0.049E-07	0.049E-07	0.053E-07	0.0548E-07
PFS, z = 50 *mm*	0.038E-07	0.039E-07	0.0417E-07	0.0412E-07	0.0417E=-7	0.054E-07

References

1 C. J. Hellier, Handbook of nondestructive evaluation, *McGraw-Hill Book Company*, New York, 2001.

2 F. E. Stanke and G.S. Kino, A unified theory for elastic wave propagation in polycrystalline materials", *J. Acoust. Soc.Am*, 75(3) (1984) 665-681.

3 H. J. Kim, S.J. Song and L.W. Schmerr, An ultrasonic measurement model using a multi-Gaussian beam model for a rectangular transducer, *Ultrasonics* , 44, (2006) 969-974.

4 J. J.Wen and M.A.Breazeale, A diffraction field expressed as the superposition of Gaussian beams, *J. Acoust. Soc.Am*, 83 (5), (1988) 1752-1756.

5 K.S.Aprameya,R.S.Anand,B.K.Mishra and S.Ahmed, Prediction of flaw response in polycrystalline metals in an ultrasonic pulse echo simulation using Born approximation, *Journal of NDT and E*, 24(3) (2009) 289-300.

6 L. W. Schmerr Jr, Fundamentals of ultrasonic nondestructive evaluation – A modeling approach, Plenum Press, New York, 1998.

7 R. Huang, L.W. Schmerr and A. Sedov, Improving the Born approximation for the scattering of ultrasound in elastic solids, *Ultrasonics* , 44, (2006) 981-984.

8 S. Ahmed and R.B. Thompson, Propagation of elastic waves in equiaxed stainless-steel polycrystals with aligned [001] axes, *J. Acoust. Soc.Am* , 99(4) (1996) 2086-2096.

9 S. Ahmed and R.B. Thompson, Effect of preferred grain orientation and elongation on ultrasonic wave propagation in stainless steel, *Review of progress in QNDE*, 11B, edited by D.O. Thompson and D.E. Chimenti,(1992) 1999-2006.

10 S. Ahmed and R.B. Thompson, Influence of columnar microstructure on ultrasonic backscattering, *Review of progress in QNDE*, 14, edited by D.O. Thompson and D.E. Chimenti, (1995) 1617-1624.

J. Pure Appl. Ultrason. 33 (2011) pp. 16-20

Effect of potassium halides on the equilibrium of aqueous t-butanol system at 30°C - II

P. SUBRAMANYAM NAIDU and K. RAVINDRA PRASAD.

S.V.U. P.G. Centre, KAVALI-524201 (AP) INDIA.

Email : psnaidujb@yahoo.co.in

Ultrasonic velocity and density have been measured experimentally at 30^0C in t-butanol + water system at low concentrations. To this aqueous t-butanol system, small quantities of potassium halides, KCl, KBr and KI have been added and the measurements repeated. From the velocity peaks and compressibility minima, the effect of potassium halides on the clathrate structures of aqueous t-butanol system has been studied. Also by computing apparent molar volumes and apparent molar compressibilities, ion-solvent, solute-solvent interactions are estimated in the total system.

Keywords : Potassium halides, ultrasonic velocity, apparent molar volumes, compressibility, solute-solvent interactions.

Introduction

It is well known that the aqueous solutions of alcohols at low concentrations exhibit a peak in the velocity and minimum in the compressibility at a particular concentration called critical concentration. This peak is attributed to the formation of clathrate structure. Many electrolytes show effect on this equilibrium formation which speaks about the ion-solvent/ solute-solvent interactions. 't-butanol – water' is such a system which has been studied in the direction of the effect of electrolytes on it by many workers[1-6]. To have a systematic study, in our earlier paper[7], the effect of sodium halides (NaCl, NaBr and NaI) has been studied on the equilibrium of the aqueous t-butanol system. As a continuation of the study, in the present investigation, an attempt has been made to study the effect of potassium halides-KCl, KBr and KI. From the velocity peaks and compressibility minima and also from the derived parameters, apparent molar volumes and apparent molar compressibilities, solute-solvent and ion-solvent interactions are estimated. Finally, a comparison is made between the effects of sodium and potassium halides.

Experimental

Ultrasonic velocity has been measured using a standard variable path single crystal interferometer working at 2MHz with an accuracy of ± 0.05%. Density has been measured employing a double stem pyknometer, the accuracy being 2 parts in 10^5. For standardizing the system, triply distilled water is used. The details are presented elsewhere[8].

Results And Discussion

Ultrasonic velocity and density have been measured experimentally first in t-butanol – water system at low concentration of t-butanol and then by adding small quantities of potassium halides KCl, KBr and KI and are presented in Table 1. In the pure t-butanol – water system velocity peak at a concentration has been observed which is attributed to clathrate formation of TBA $(H_2O)_{21.}$ As the peak concentrations of t-butanol for all molarities of the three electrolytes are less than the critical concentration observed for pure aqueous system, it may be said that the effect of all the three potassium halides (KCl, KBr and KI) is very little on the clathrate structure equilibrium $TBO(H_2O)_{21}$. Also nearly at the same concentration, compressibility minimum is observed. Figs. 1 and 2 portray the variation of peak velocity and compressibility minimum concentrations with the molarities of electrolytes respectively. From figures it may be noticed that the peak concentration increased except for KBr where it is almost flat. Similar behavior is observed in the case of compressibility minimum (Fig. 2). In Fig. 1 the order is KI, KCl and KBr while in Fig. 2 it is KCl, KBr and KI.

To ascertain more information about the nature of interactions, apparent molar volumes and apparent molar compressibilities have been computed in all the three halide systems at 30°C using the standard relations explained elswhere[9]. Mostly all the apparent molar volumes are negative while both positive and negative values are observed in the case of apparent molar compressibilities. By fitting the apparent molar volumes (Φ_v) and molar compressibilities

Table 1—Ultrasonic velocity and density for different molarities at 30 ^{0}C.

System 1: t-butanol + water + KCl

Molarity of KCl →	0.0000	0.0134	0.0335	0.0669	0.1334	0.3311
Mole fraction of t-butanol				Velocity (m s^{-1})		
0.0262	1585.6	1581.1	1589.8	1573.9	1579.0	1581.7
0.0321	1598.2	1597.2	1600.0	1585.5	1593.2	1595.9
0.0346	1604.2	1605.0	1603.9	1591.7	1599.5	1602.1
0.0371	1608.7	1613.3	1607.7	1598.2	1604.7	1607.1
0.0410	1610.2	1617.3	1611.9	1607.2	1613.2	1615.3
0.0423	1608.5	1614.5	1612.2	1609.9	1616.4	1618.5
0.0436	1606.4	1611.2	1611.3	1612.0	1619.3	1621.1
0.0449	1604.5	1608.6	1610.1	1612.7	1621.9	1623.2
0.0465	1601.8	1605.2	1608.5	1611.6	1621.7	1624.2
0.0488	1596.8	1598.9	1605.6	1607.6	1615.4	1619.9
0.0504	1593.6	1594.6	1603.8	1604.9	1609.6	1615.8
Mole fraction of t-butanol				Density x10^3 (kg m^{-3})		
0.0262	0.97977	0.98136	0.98277	0.98566	0.99437	1.00749
0.0321	0.97687	0.97891	0.98048	0.98399	0.99014	1.00338
0.0346	0.97588	0.97786	0.97958	0.98285	0.98891	1.00202
0.0371	0.97454	0.97650	0.97835	0.98155	0.98747	1.00046
0.0410	0.97253	0.97433	0.97623	0.97949	0.98486	0.99777
0.0423	0.97213	0.97372	0.97536	0.97868	0.98412	0.99710
0.0436	0.97152	0.97298	0.97487	0.97823	0.98322	0.99608
0.0449	0.97073	0.97245	0.97434	0.97743	0.98226	0.99555
0.0465	0.96994	0.97171	0.97348	0.97637	0.98135	0.99429
0.0488	0.96882	0.97026	0.97203	0.97476	0.98023	0.99283
0.0504	0.96808	0.96926	0.97103	0.97374	0.97894	0.99174

System 2: t-butanol + water + KBr

Molarity of KBr →	0.0000	0.0084	0.0210	0.0419	0.0837	0.2082
Mole fraction of t-butanol				Velocity (m s^{-1})		
0.0262	1585.6	1584.8	1583.4	1582.3	1579.5	1575.5
0.0290	1591.5	1590.0	1588.4	1586.7	1584.1	1580.4
0.0321	1598.2	1596.4	1593.9	1591.8	1589.4	1586.2
0.0346	1604.2	1602.4	1599.0	1596.5	1594.0	1591.5
0.0371	1608.7	1606.5	1604.0	1600.4	1598.6	1596.8
0.0391	1610.7	1608.8	1607.3	1603.1	1602.1	1600.3
0.0410	1610.2	1609.4	1609.1	1604.4	1605.8	1602.6
0.0423	1608.5	1608.9	1610.0	1605.0	1607.7	1603.8
0.0436	1606.4	1607.9	1610.7	1605.3	1608.5	1604.5
0.0449	1604.5	1606.2	1610.4	1604.2	1607.8	1603.6
0.0480	1598.8	1600.9	1607.0	1601.6	1604.6	1600.2
0.0504	1593.6	1596.2	1603.4	1600.5	1602.1	1598.4
Mole fraction of t-butanol				Density x10^3 (kg m^{-3})		
0.0262	0.97977	0.98094	0.98320	0.98757	0.99231	1.00848
0.0290	0.97839	0.97970	0.98216	0.98608	0.99067	1.00689
0.0321	0.97687	0.97847	0.98088	0.98478	0.98886	1.00550
0.0346	0.97588	0.97736	0.97979	0.98337	0.98729	1.00416
0.0371	0.97454	0.97619	0.97842	0.98200	0.98568	1.00308
0.0391	0.97348	0.97511	0.97724	0.98068	0.98429	1.00197
0.0410	0.97253	0.97406	0.97632	0.97926	0.98316	1.00112
0.0423	0.97213	0.97343	0.97557	0.97849	0.98234	1.00045
0.0436	0.97152	0.97269	0.97486	0.97766	0.98172	0.99958
0.0449	0.97073	0.97211	0.97416	0.97680	0.98105	0.99868
0.0480	0.96921	0.97036	0.97249	0.97528	0.97921	0.99558
0.0504	0.96808	0.96905	0.97151	0.97419	0.97808	0.99330

(Contd.)

Table 1—Ultrasonic velocity and density for different molarities at 30 ^{0}C *(Contd.)*.

System 3: t-butanol + water + KI

Molarity of KI →	0.0000	0.0060	0.0150	0.0301	0.0600	0.1494
Mole fraction of t-butanol				Velocity (m s^{-1})		
0.0262	1585.6	1590.7	1590.0	1580.9	1578.2	1565.4
0.0290	1591.1	1597.7	1594.5	1588.5	1585.3	1574.0
0.0321	1598.2	1604.5	1599.1	1596.0	1591.5	1582.8
0.0346	1604.2	1608.5	1602.1	1600.9	1595.5	1589.3
0.0371	1608.7	1613.2	1605.0	1604.9	1599.5	1593.7
0.0391	1610.6	1617.2	1606.2	1607.9	1602.2	1595.9
0.0410	1610.2	1619.8	1607.5	1610.3	1603.6	1597.7
0.0423	1608.2	1616.9	1608.2	1611.8	1604.3	1599.1
0.0436	1606.4	1611.3	1607.3	1612.7	1605.0	1599.9
0.0449	1604.5	1605.9	1605.8	1611.1	1605.6	1600.8
0.0480	1598.9	1598.1	1602.3	1606.8	1601.5	1600.7
0.0504	1593.6	1594.8	1600.5	1603.7	1598.1	1598.7
Mole fraction of t-butanol				Density x10^3 (kg m^{-3})		
0.0262	0.97977	0.98170	0.98286	0.98609	0.99086	1.00618
0.0290	0.97817	0.97952	0.98115	0.98412	0.98873	1.00416
0.0321	0.97687	0.97812	0.97963	0.98255	0.98698	1.00226
0.0346	0.97588	0.97697	0.97855	0.98135	0.98573	1.00112
0.0371	0.97454	0.97552	0.97711	0.98029	0.98479	1.00027
0.0391	0.97329	0.97438	0.97654	0.97952	0.98385	0.99955
0.0410	0.97253	0.97353	0.97565	0.97883	0.98306	0.99941
0.0423	0.97213	0.97294	0.97505	0.97830	0.98259	0.99908
0.0436	0.97152	0.97257	0.97474	0.97768	0.98193	0.99877
0.0449	0.97073	0.97186	0.97423	0.97730	0.98132	0.99826
0.0480	0.96889	0.97025	0.97323	0.97648	0.98087	0.99732
0.0504	0.96808	0.96919	0.97260	0.97598	0.98116	0.99700

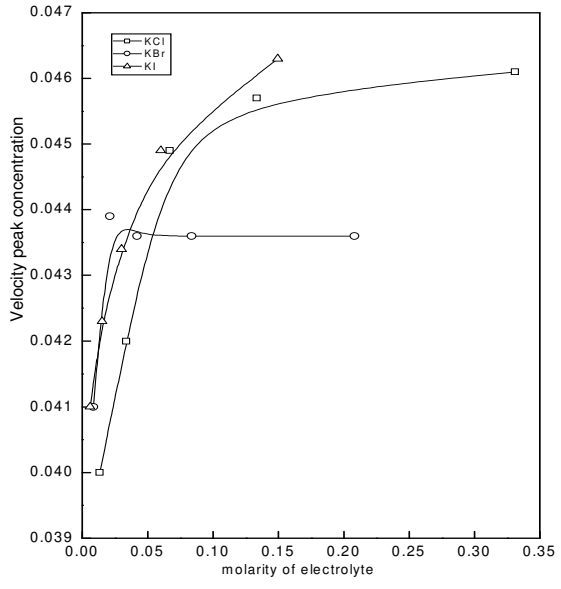

Fig.1

Fig. 1—Variation of peak velocity concertration with molarity of electrolyte.

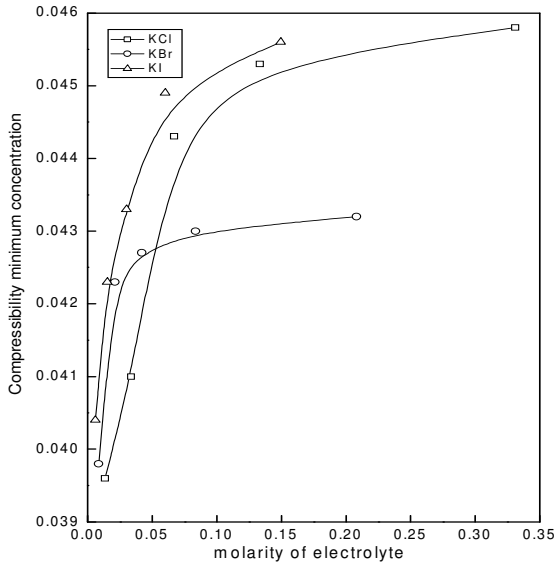

Fig.2

Fig. 2—Variation of compressibility minimum concertration with molarity of electrolyte.

(Φ_k) linearly to the square root of molarities of electrolytes ($\Phi_k = \Phi_k^o + S_k\sqrt{C}$ and $\Phi_k = \Phi_k^o + S_k\sqrt{C}$), the partial molar volumes (Φ_v^0) and partial molar compressibilities (Φ_k^0) obtained are shown in Table 2 along with S_v and S_k. Φ_v^0 values are all negative and S_v are positive for all the three electrolyte systems while Φ_k^0 are mostly negative for KCl and KI systems but positive and negative for KBr system. With increase in the mole fraction of t-butanol, the values of S_v decrease up to a concentration 0.045 and thereafter increase for all the three systems indicating that the clathrate of aqueous butanol is not very much changed (affected) by the addition of small quantities of potassium halides. As Φ_k^0 are negative, electrostrictive and hydrophobic interactions are noticed effectively/strongly in KCl and KI while for KBr, either reactions are not that strong. From S_v values, ion-solvent interactions are not shown out. From viscosity studies also, solute –solvent interactions are suggested [8].

The results of t-butanol aqueous system studied by other workers in various electrolytes need the attention here for comparison of our work. From viscometric studies of various electrolytes in aqueous

Table 2—Limiting values of apparent molar volume and apparent molar compressibility along with slopes in t- butanol + water + KCl, KBr and KI systems at 30 ^{0}C.

Mole fraction of t-butanol	Φ_V^0	S_v	Φ_K^0 (x10^{-8})	S_k (x10^{-8})
			t-butanol+water+KCl	
0.0262	-37.01	44.10	0.42	-1.56
0.0321	-74.08	128.94	-0.54	0.64
0.0346	-72.31	127.68	-0.80	1.30
0.0371	-73.48	130.74	-1.69	3.27
0.0410	-64.84	117.14	-2.54	4.69
0.0423	-46.39	82.42	-2.36	3.97
0.0436	-43.08	76.24	-2.22	3.32
0.0449	-58.91	110.78	-2.28	3.19
0.0465	-59.73	116.68	-2.22	2.89
0.0488	-37.36	71.43	-1.92	2.15
0.0504	-20.08	38.91	-1.62	1.55
			t-butanol+water+KBr	
0.0262	-47.49	44.03	-3.16	-3.11
0.0290	-65.48	97.10	-0.44	-8.53
0.0321	-94.28	176.43	0.20	-8.19
0.0346	-80.32	149.93	2.73	-12.35
0.0371	-91.78	184.00	2.98	-13.27
0.0391	-85.62	173.86	0.70	-8.45
0.0410	-75.02	149.23	-5.66	5.14
0.0423	-47.06	82.68	-11.53	17.76
0.0436	-33.80	50.03	-18.47	32.94
0.0449	-51.79	101.00	-22.81	43.08
0.0480	-34.00	65.80	-26.75	50.47
0.0504	-26.47	50.42	-31.43	58.49
			t-butanol+water+KI	
0.0262	-126.73	358.81	-5.26	1.67
0.0290	-59.05	151.47	-5.39	1.69
0.0321	-40.20	110.18	-4.61	1.46
0.0346	-18.49	47.84	-2.82	0.91
0.0371	-5.29	-12.10	-2.52	0.82
0.0391	-42.31	81.90	-3.85	1.23
0.0410	-27.39	25.60	-5.67	1.77
0.0423	0.86	-63.95	-5.57	1.65
0.0436	-33.33	44.03	-4.13	1.09
0.0449	-54.36	96.85	-2.52	0.49
0.0480	-114.90	236.34	-2.19	0.25
0.0504	-96.59	142.60	-3.79	0.68

t-butanol[10], conductometric studies of tetra alkyl ammonium bromide in aqueous t-butanol[5] and a study of transfer of electrolytes in t-butanol + water system[6], solute-solvent interactions are suggested. In our earlier paper[7] also, i.e study of the effect of sodium halides on aqueous t-butanol system, solute- solvent interactions are suggested. In sodium halides, strong hydrophobic and electrostrictive interactions are noticed in NaBr and NaI systems. In NaCl and NaBr systems, weak solute-solvent interactions are indicated.

In the present study also i.e in the potassium halides, strong hydrophobic and electrostrictive interactions are observed in KCl and KI. Compared to sodium halides, solute-solvent interactions appear to be stronger in potassium halide systems. The different hydrations of both the alkali elements i.e sodium and potassium also appear to play an important role in determining the degree of interaction.

Acknowledgements

The authors are thankful to Prof. Y. C. Ratnakaram, Professor of Physics for his interest and initiation in this work. One of the authors (PSN) is grateful to the UGC for awarding him Faculty Development Programme Fellowship for two years.

References

1 Lara, Jaime and Desnoyers, Jacques E., Isentropic compressibilities of alcohol-water mixtures at 250C, J. Solution Chem., 10 (1981) 465.

2 Iwasaki, Kenji and Fujjiyama, Tsunetake., Light scattering study of clathrate hydrate formation in binary mixtures of tert-butyl alcohol and water, J. Phy. Chem 81 (1977) 1908.

3 Iwasaki, Kenji and Fujjiyama, Tsunetake., Light scattering study of clathrate hydrate formation in binary mixtures of tert-butyl alcohol and water, 2. Temparature effect, J. Amer. Chem. Soc., 83 (1979) 463.

4 Siva Prasad, V., Siva Kumar, K.V., Rajgopal, E. and Manohar Murthy, N., Ultrasonic behaviour of ternary mixtures containing water, dimethyl sulphoxide and t-butanol at 298.15K, J. Pure Appl. Ultrason., 26 (2004) 684.

5 Ansari, A.A., Ansri, M., Patel R.B. and Topiwala, K.A., conductometric studies of associationbehaviour of tetra alkyl ammonium bromide in t-butanol-water mixtures, Bull. Elec. Chem., 21 (2005) 253.

6 Patil, K.J., Mehta, G.R and Salpekar, A., Apparent molar compressibilities of transfer of electrolytes from water to aqueous t-butanol solutions, Indian J. Chem., 29A (1990) 784.

7 Subramanyam Naidu, P. and Ravindra Prasad, K., Effect of alkali halides on the equilibrium of aqueous t-butanol system at 30° C at low concentrations-An ultrasonic study, J. Pure Appl. Ultrason., 30 (2008) 131.

8 Subramanyam Naidu, P., P.hD. Thesis submitted to Sri venkateswara University, Tirupati (2006).

9 Naidu, P.S. and Ravindra Prasad, K., Ultrasonic velocity and allied parameters in solutions of cypermethrin with xylene and ethanol, Indian J. Pure & Appl. Phys. 42 (2004) 512.

10 Kipkemboi, P.K. and Easteal, A.J., Viscometric studies for some 1:1 electrolytes in water + t-butyl alcohol and water + tert-butylamine mixtures at 298.15K, Indian J. Chem., 41A (2002) 1139.

J. Pure Appl. Ultrason. 33 (2011) pp. 21-25

Acoustical studies of molecular interaction in ternary liquid mixture of cresols with benzaldehyde and tetrachloromethane solutions at 303, 308 and 313K

R. PALANI[1] and S. KALAVATHY[2]

[1]Department of Physics, D.D.E., Annamalai University, Annamalainagar–608 002, India.
[2]Department of Physics, Sri Chandrasekarendra Saraswathi Viswa Mahavidyalaya, Enathur, Kanchipuram – 631 561
Email: palani_physics06@yahoo.co.in

Ultrasonic velocity (U), density (ρ) and viscosity (η) for the ternary liquid mixtures of benzaldehyde + tetrachloromethane + o-cresol, benzaldehyde + tetrachloromethane + m-cresol and benzaldehyde + tetrachloromethane + p-cresol have been measured as a function of the composition at 303, 308 and 313K. The experimental data have been used to calculate some excess acoustical parameters, such as adiabatic compressibility (β^E), free length (L_f^E) and free volume (V_f^E). The results are discussed and interpretered in terms of specific interaction predominated by hydrogen bonding.

Keywords: Ultrasonic velocity, adiabatic compressibility, free length (L_f^E), free volume (V_f^E), hydrogen bonding.

Introduction

Ultrasonic measurements are extensively used to study the molecular interaction in pure liquids and liquid mixtures. When two liquid mixtures are mixed together the resulting changes in physical and acoustical properties can be considered as a sum of several contributions due to free volume change, change in energy, change in molecular orientations and steric hindrances. The mixing of different compounds gives rise to solutions that generally do not behave as ideal solutions. The deviation from ideality is expressed by many acoustical variables particularly by excess or residual extensive properties[1]. Excess acoustical properties of mixtures are useful in the study of molecular interactions and arrangements. Acoustical properties derived from the measurement of ultrasonic velocity, density and viscosity for binary mixtures are useful in understanding the nature and type of intermolecular interactions between the component molecules[2]. The study of the solution properties of the liquid mixtures finds applications in industrial and technological process[3].

The carbonyl group is a part of several biologically important molecules such as proteins, lipids and harmones[4]. Phenols are widely used for phonograph records, wood preservatives and selective weed killing. Cresols constitute one of the most important groups of aromatic organic compounds, which occur in three isomeric forms. They find extensive use in various fields as disinfectants, organic intermediates, textile scouring agents, herbicides, surfactants and in the production of few phenolic resins, salicyladehyde, cummarin etc., Both ortho- and para-cresols are used as end product in azo dye[5]. Many researchers[6] have studied the ultrasonic properties of cresols in different organic solvents. Moreover, literature survey indicates that no physico-chemical studies on these systems have been reported. Therefore, the study of intermolecular interactions in these systems will be interesting owing to their applications. Keeping these important aspects in view, the measurements on ultrasonic velocity, density and viscosity and their related excess thermodynamical and transport parameters for mixed solvent systems of benzaldehyde and tetrachloromethane with o-cresol, m-cresol and p-cresol at 303, 308 and 313K have been undertaken. The variations of excess parameters have been used to explain the nature and extent of intermolecular interaction in these mixtures.

Materials and Methods

All the chemicals used in this present research are analytical reagent (AR) and spectroscopic reagent (SR) grades of minimum assay of 99.9% obtained from E-Merck, Germany and SdFine chemicals, India, which were used as such without further purification. The purities of the above chemicals were checked by density determination at 303, 308 and 313K ± 0.1K. which showed an accuracy of $\pm 1 \times 10^{-4}$ gcm^{-3} with the reported values[4, 7-9]. The ternary liquid mixtures of different known compositions were prepared in stopper measuring flasks. The density, viscosity and ultrasonic velocity were measured as a function of composition of the ternary liquid mixture at 303, 308 and 313K.

The substitutes phenols such as o-cresol, m-cresol and p-cresol were added to a binary mixtures of benzaldehyde and tetrachloromethane. For this purpose, binaries with fixed mole ratios X1/X2 ≅ 3:1 were prepared by volume. The density was determined using a specific gravity bottle by relative measurement method. The weight of the sample was measured using electronic digital balance with an accuracy of ± 0.1 mg. An Ostwald's viscometer (10 ml) was used for the viscosity measurement. Efflux time was determined using a digital chronometer to within ±0.01s. An ultrasonic interferometer having the frequency of 3 MHz with an overall accuracy of ± 0.1% has been used for velocity measurement. An electronic digitally operated constant temperature bath has been used to circulate water through the double walled measuring cell made up of steel containing the experimental solution at the desired temperature. The accuracy in the temperature measurement is ± 0.1 K.

Theory and Calculation

Various acoustical parameters are calculated from the measured data such as

$$\text{Adiabatic Compressibility } \beta = \frac{1}{U^2\rho} \quad (1)$$

$$\text{Intermolecular free length } L_f = K\sqrt{\beta} \quad (2)$$

where K is a temperature dependent constant. Its values are 631×10^{-6}, 636×10^{-6} and 642×10^{-6} respectively at 303, 308 and 313K.

$$\text{Free volume } V_f = \left(\frac{M_{eff}U}{k\eta}\right)^{3/2} \quad (3)$$

where M_{eff} is the effective molecular weight ($M_{eff}=\Sigma m_i x_i$, in which m_i and x_i are the molecular weight and the molefraction of the individual constituents respectively). k is a temperature independent constant which is equal to 4.28×10^9 for all liquids.

Excess values of the above parameters can be determined using

$$A^E = A_{exp} - A_{id} \quad (4)$$

where $A_{id} = \sum A_i X_i, A_i$, A_i is any acoustical parameters and X_i the molefraction of the liquid component.

Results And Discussion

The experimental values of density (ρ), viscosity (η) and ultrasonic velocity (U) of pure liquids and for the ternary liquid systems at 303, 308 and 313K are given in Tables 1-2. Further, the variation of excess adiabatic compressibility, excess free length and excess free volume of benzaldehyde and tetrachloromethane solvent with mole fraction of cresols at 303, 308 and 313K are shown in Figs. 1-3 and the curves are drawn using least square fitting.

The excess properties are found to be more sensitive towards intermolecular interaction between the component molecules of liquid mixtures. The sign and extent of deviation of excess properties depend on the strength of interaction between unlike molecules[10].

The values of β^E (Fig.1) are negative and it is decreases with increasing the concentration of X_3 in all systems studied. Fort *et.al.*[11] found that the negative value of excess adiabatic compressibility indicated greater interaction between the components of the mixtures. Positive values in excess properties is mainly due to the existence of dispersive forces. The negative value of β^E is associated with a structure making tendency while a positive value is taken to indicate the structure breaking tendency due to hetero-molecular interaction between the component molecules of the mixture. In the present investigation

Table 1—Values of density (ρ), viscosity (η) and ultrasonic velocity (U) of pure liquids at 303, 308 and 313K

Organic liquids		ρ/ (kg m^{-3})			η/(×10^{-3} Nsm^{-2})			U/(m.s^{-1})		
		303K	308K	313K	303K	308K	313K	303K	308K	313K
Benzaldehyde	Exp. value	1055.3	1032.2	1027.0	1.3997	1.3855	1.3774	1451.7	1442.4	1434.6
	Literature value	1049.0		–	–		–	1464.0[4]	–	–
Tetrachloromethane	Exp. value	1561.9	1546.9	1531.4	0.8679	0.8521	0.7919	899.6	889.6	864.6
	Literature value	1574.8[7]		–	–	–	–	907.0[7]	–	–
o-cresol	Exp. value	1044.3	1041.7	1039.6	8.1797	8.0413	7.1458	1526.4	1521.6	1507.2
	Literature value	1048.7[8]		–	8.6430[11]	–	–	1525.0		–
m-cresol	Exp. value	1027.0	1023.6	1020.9	4.5482	3.7896	2.3430	1431.2	1424.4	1421.8
	Literature value	1030.6[9]		–	–	–	–			–
P-cresol	Exp. value	1016.4	1013.4	1011.4	3.8887	2.5679	2.3936	1400.4	1370.2	1350.5
	Literature value	1026.4[9]		–	–	–	–			–

Table-2 Values of density (ρ), viscosity (η) and ultrasonic velocity (U) at 303, 308 and 313K for

Molefraction (X_3)	ρ/ (kg m^{-3})			η/($\times 10^{-3}$ Nsm^{-2})			U/($m.s^{-1}$)		
	303K	308K	313K	303K	308K	313K	303K	308K	313K
System-I : benzaldehyde (X_1) + tetrachloromethane (X_2) + o-cresol (X_3) [(X_1)/ (X_2)=3:1]									
0	1410.5	1388.1	1371.1	1.2585	1.2354	1.2214	1176.4	1161.2	1159.1
0.02	1408.4	1374.1	1364.7	1.3280	1.2946	1.2715	1182.2	1174.1	1167.2
0.04	1390.5	1368.7	1352.8	1.3821	1.3481	1.3375	1191.4	1184.3	1170.3
0.06	1384.1	1361.9	1324.7	1.4800	1.4186	1.3943	1197.9	1189.1	1175.8
0.08	1374.1	1345.5	1310.5	1.5248	1.4586	1.4494	1208.6	1194.2	1189.3
0.10	1369.1	1321.9	1296.8	1.5712	1.5186	1.4927	1227.1	1218.7	1201.8
System-II : benzaldehyde (X_1) + tetrachloromethane (X_2) + m-cresol (X_3)									
0	1410.5	1388.1	1371.1	1.2585	1.2354	1.2214	1176.4	1161.2	1159.1
0.02	1397.2	1366.3	1358.3	1.3110	1.2842	1.2475	1179.2	1165.8	1163.2
0.04	1382.8	1351.7	1349.2	1.3658	1.3290	1.2611	1185.6	1169.1	1164.9
0.06	1373.1	1349.1	1314.1	1.3947	1.3557	1.2851	1192.3	1174.4	1172.1
0.08	1369.9	1326.9	1301.4	1.4589	1.3989	1.3183	1203.9	1183.2	1179.1
0.10	1355.6	1319.4	1284.2	1.4918	1.4403	1.3403	1216.3	1199.4	1197.0
System-III : benzaldehyde (X_1) + tetrachloromethane (X_2) + p-cresol (X_3)									
0	1410.5	1388.1	1371.1	1.2585	1.2354	1.2214	1176.4	1161.2	1159.1
0.02	1395.1	1361.8	1354.7	1.3032	1.2673	1.2456	1178.3	1164.6	1161.0
0.04	1380.3	1348.7	1344.2	1.3343	1.2941	1.2598	1181.1	1168.5	1163.2
0.06	1361.8	1346.6	1312.1	1.3922	1.3204	1.2934	1184.9	1173.2	1168.4
0.08	1354.9	1321.1	1299.2	1.4389	1.3493	1.3132	1192.9	1182.2	1172.3
0.10	1349.3	1311.2	1274.9	1.4905	1.3675	1.3365	1203.4	1196.2	1192.1

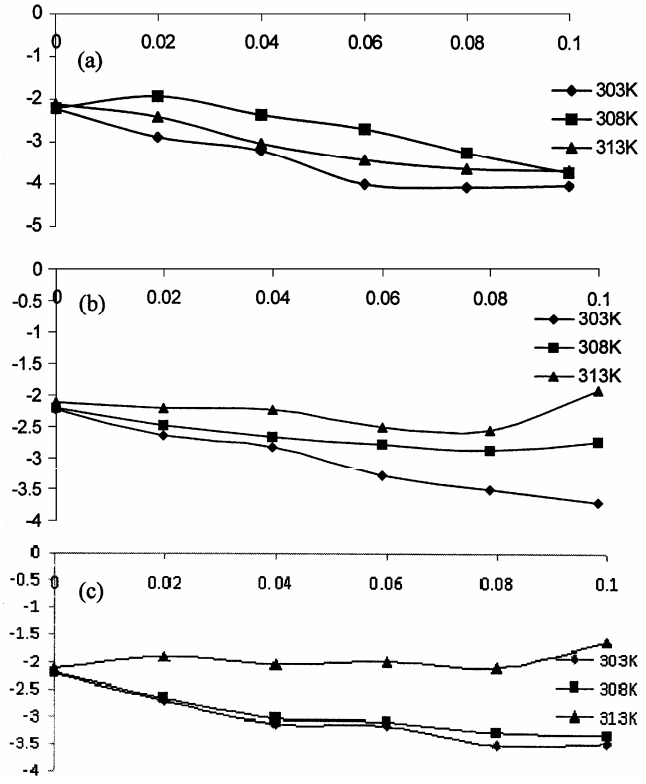

Fig.1—Variation of excess adiabatic compressibility (β^E) of benzaldehyde and tetrachloromethane solvent with mole fraction of cresols (X_3) at 303, 308 and 313K

the negative β^E values for ternary mixtures may be attributed to the formation of hydrogen bond between hydrogen atom of cresols and carbonyl oxygen atom of benzaldehyde[12].

From the Fig.2, it is observed that the values of L_f^E are negative over the entire molefraction range of X_3 as well as with the raising of temperature. According to Kannappan *et al.,*[13] negative value of L_f^E indicates that sound waves cover longer distances due to decrease in intermolecular free length ascribing the dominant nature of hydrogen bond interaction between unlike molecules.

Fort *et al.,*[11] indicated that the positive excess values of free length should be attributed to the dispersive forces and negative excess values should be due to charge transfer and hydrogen bond formation. In the present study the negative contribution of L_f^E in all the systems which prevails the existence of greater interaction.

The excess free volume values (Fig.3) for all the three systems are found to be negative. Further, these values are decreases with increasing the molefraction of X_3, but it found to increases with the raising of temperature. These variations can be explained in terms of molecular interaction, structural effect and interstitial accommodation along with changes in

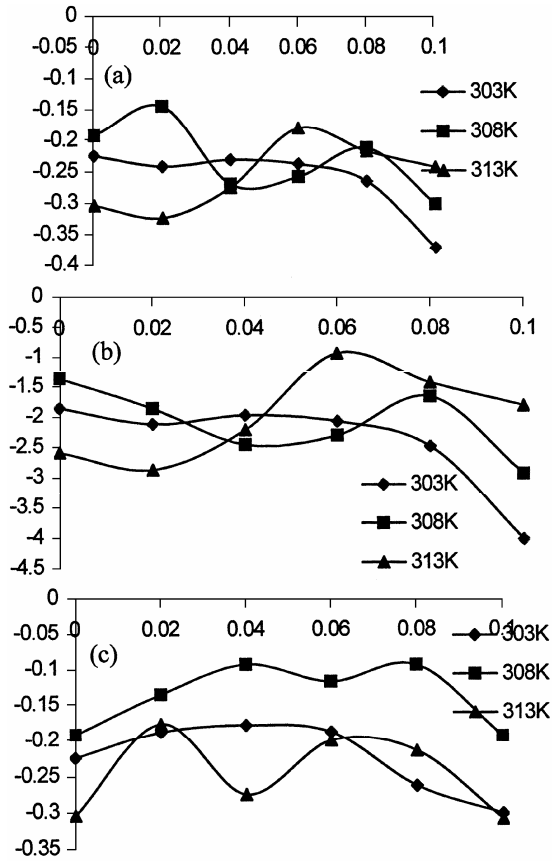

Fig.2—Variation of excess free length (L_f^E) of benzaldehyde and tetrachloromethane solvent with mole fraction of cresols (X_3) at 303, 308 and 313K

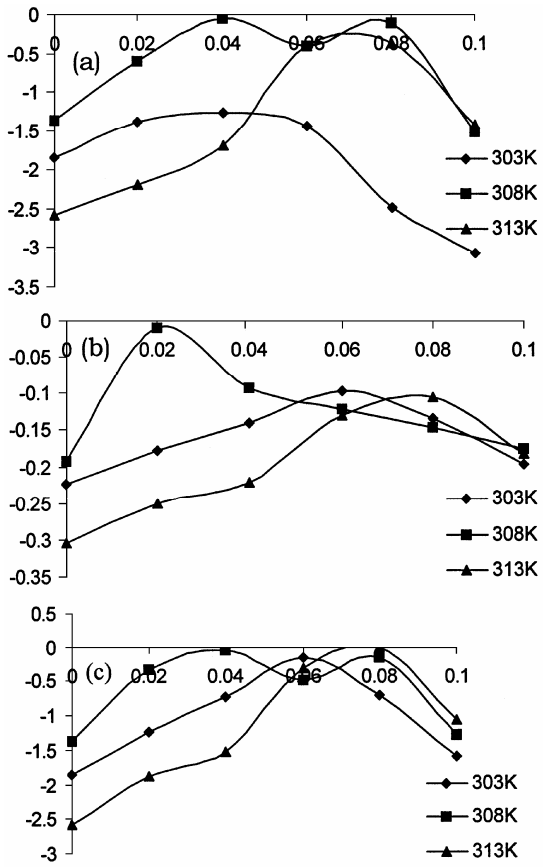

Fig.3—Variation of excess free volume (V_f^E) of benzaldehyde and tetrachloromethane solvent with mole fraction of cresols (X_3) at 303, 308 and 313K

free volume. The sign of V_f^E depends upon the relative strength between the contractive forces and expansive forces.

The factors responsible for volume contraction are

(a) Specific interaction between component molecules.

(b) Interstitial accommodation of molecules of one component into the vacant spaces of molecules of the other components. This occurs preferentially when the size difference between the component molecules is large or when large gaps are available in structural network of molecules.

(c) Weak physical forces, such as dipole-dipole or dipole-induced dipole interactions or Van der Waal's forces.

The factors that cause expansion in volume are the following:

(a) dispersion force,

(b) steric hindrance of component molecules,

(c) unfavorable geometric fitting, electrostatic repulsion, etc

The negative part of V_f^E curves of the system asserts that the combined effect of the factors responsible for volume contraction outweigh the combined effect of the factors causing volume expansion and vice-versa[14]. Adgaonker *et al.,*[15] showed positive value of V_f^E, indicate the existence of weak molecular interaction in the liquid mixtures. Fort *et al.,*[11] noticed that negative excess free volume tends to decrease as the strength of the interaction between the unlike molecules are increases. However, in the present investigation the observed behaviour of V_f^E shows the strength of molecular interaction is stronger with the increasing of molefraction X_3, but it found to be lesser with raising of temperature. The magnitude of V_f^E values follows the sequence: p-cresol > m-cresol > o-cresol.

Conclusion

Ultrasonic method is a powerful tool for characterising the physico-chemical properties and existence of molecular interaction in the mixtures. Excess ultrasonic properties of ternary liquid mixtures of cresols in benzaldehyde and tetrachloromethane at

303, 308 and 313K are considered to be a reflecting agent of magnitudeof polarity and size of the molecules in the interaction. The result of excess properties reveal that the strong molecular interaction exists in the mixtures which may be due to the dominance of hydrogen bonding and charge transfer between the mixing components. From the magnitude of V_f^E, it can be concluded that the strength of molecular interaction is in order : o-cresol > m-cresol > p-cresol. The strength of interaction tends to weaker with rising of temperature which may due to the presence of weak inter molecular forces and thermal dispersion forces.

References

1 Sastry N.V. Valan M.K. Thermodynamics of acrylic ester organic solvent mixtures, viscosities of alkyl acrylates-1-alcohol binary mixtures at 298.15 and 308.15K. Int. J. Thermophys. 1997; 18 1387-1403

2 Gupta M. Vibhum I Shukla J.P. Ultrasonic velocity, viscosity and excess properties of binary mixtures of tetrahydrofuran with 1-propanol and 2-propanol. Fluid phase equlibria 2006; 244 26-32

3 Ali A. Nain A.K. Study of molecular interactions in non-aqueous binary liquid mixtures through ultrasonic measurements J. Appl Pure Ultrason. 2000; 22 40467

4 Azhagiri S. Jayakumar S. Padmanaban R. Gunasekaran S. Srinivasan S. Acoustic and thermodynamic properties of binary liquid mixtures of benzaldehyde in hexane and cyclohexane. J. Sol. Chem. 2009; 38 441-448

5 Ranganayakulu S.V. Sreenivasa Reddy C. Linga Reddy D. Ultrasonic studies of the binary mixtures of ethyl acetate and cresols applications of Kosower and Demroth treatments. Material Chem. and Phys. 2005; 90 213-220

6 Prasad N. Evaluation of excess internal pressure and free volume of binary mixtures of carbontetra-chloride. Acoustica 1991; 74 171

7 Rajasekar P. Venkateswaralu R. Kallura S. Reddy Excess volumes, isioentropic compressibilities and viscosities of binary mixtures containing cyclohexane. Can. J. Chem. 1990; 68 363

8 Praveen, S. Ultrasonic velocity, density, viscosity and their excess parameters of the binary mixtures of tetrahydrofuran with methanol and o-cresol at varying temperature. Appl. Acoustics, 2009; 70 507-513.

9 Narayani Prasad Roy R.P.K. Ultrasonic study of binary solution of cresol isomers in cyclohexane. J. Pure. & Appl.Ultrason. 2007; 29 116-124

10 Mahan Y. Liew C.N. Mather A.E. Viscosities and excess properties of aqueous solutions of ethanolamines from 25 to 80°. J. Sol. Chem., 2002; 31 743-756

11 Fort R.J. Moore W.R. Adiabatic compressibilities in binary liquid mixtures. Trans. Farad. Soc., 1965; 61 2102-2110

12 Anuradha Sinha and Mahendra Nath Roy Studies of viscous antagonism, excess molar volume and isentropic compressibility in aqueous mixed solvent systems at different temperatures. Phys. and Chem. of liq., 2006; 44 303-314

13 Kannappan AN. and Palani R. Studies on molecular interaction in ternary liquid mixtures by ultrasonic velocity measurements. Indian J. Pure & Appl. Phys. 1996; 70B 59-65

14 Saleh M.A Akhtar S. Shamsuddin Ahmed M. Uddin M.H. Excess molar volumes and thermal expansivities in aqueous solutions of DMSO, THF and 1,4-dioxane. Physics and Chemistry of liquids 2002; 40 621-635

15 Adgaonkar, C.S. and Agnihotri Theoretical evaluations of ultrasonic velocity in binary liquid mixtures. Ultrasonics 1989; 27 248-259.

Journal of Pure and Applied Ultrasonics

VOLUME 33 NUMBER 2 APRIL - JUNE- 2011

CONTENTS

Website : www.ultrasonicsindia.com

A Publication of — Ultrasonics Society of India

Information for authors

1. Type of Contribution

JOURNAL OF PURE AND APPLIED ULTRASONICS welcomes original research papers and articles related to the subject of ultrasonics. The contributions may be in the areas of physical ultrasonics, medical ultrasonics, ultrasonic non-destructive evaluation including NDT, high power ultrasonics, underwater acoustics, ultrasonic transducers, transducer materials & devices and any other related topic. These may fall into one of the following categories.

ResearchPapers **-** These should be on original research work contributing to scientific developments. They should be written with a wide readership in mind and should emphasize the significance of the work.

Reviews Articles **-** Includes critical reviews and survey articles.

Research and Technical notes **-** These should be short descriptions of new techniques, applications, instruments and components.

Letters to the editor **-** Letters will be published on points arising out of published articles and papers and on questions of opinion.

Miscellaneous **-** Miscellaneous contributions such as conference reports, Ph.D. thesis reviews and news items are also accepted. Recommended lengths of contributions are: Research papers 2000-4000 words, reviews articles 2000-5000 words; conference reports 500-1500 words; news items, research and technical notes up to 1000 words.

2. Manuscripts

Manuscripts should be typed on one side of the paper in double spacing with 25 mm margins on all side of A4 size paper. A soft copy of the manuscript in MS WORD for text and MS EXCEL for illustrations and a PDF file thereof may be sent by e-mail or CD/DVD. Colour images should be formatted as JPEG files. Figures submitted in colour would be published in colour. Colour should be avoided unless it is required in order to convey a message or serve a purpose in the image.

Title **-** Titles should be short and indicate the nature of the contribution. About 5 keywords may be given after the abstract.

Abstract **-** An abstract of 100-200 words should be provided on the title page of paper and review article. This should describe the full scope of the contribution and include the principal conclusions.

Mathematics **-** Mathematical expressions should be arranged to occupy the minimum number of lines consistent with clarity e.g., $(x^2+y^2)/(x-y)^{1/2}$

References **-** References should be indicated in the text by its number only. The reference number should be given as superscript. The corresponding reference shall contain the following information in order; names and initials of author(s)in bold, full title of the work, journal or book title in italic, volume number in bold, the year of publication in brackets and the page number. As example: Vasanth B.K., Palanichamy P., Jayakumar T. and Sankar B.N., Assessment of residual stresses in a carbon steel weld pad using critically refracted longitudinal (L_{CR}) waves, *J. Pure Appl. Ultrason*., 28 (2006) 66-72.

Units and Abbreviations **-** Authors should use SI units wherever possible.

3. Reprints

One copy of the issue in which the paper is published is sent to the author free of charges.

J. Pure Appl. Ultrason. 33 (2011) pp. 29-32

Ultrasonic analysis of stability and structural properties of biocompatible magnetic fluids

V. VELUSAMY[1] and L. PALANIAPPAN

[1]Department of Physics, Paavai College of Engineering, Pachal, Tamilnadu-637 018.
Department of Physics (DDE), Annamalai University, Annamalainagar-608 001.

E.mail:veluphysics@yahoo.com

Ultrasound has become a powerful tool in predicting the behaviour of liquid molecules in various environments. Magnetic fluid is a colloidal suspension of magnetic particles in a carrier liquid, stabilized by a surfactant. For biomedical purposes, magnetic particles must be coated with biocompatible substances that ensure their stability, biodegradability and non-toxicity in a physiological medium. The stability and structural properties of some magnetic fluids have been studied by using ultrasonic method. Observed effects are analyzed in the light of the existing studies of magnetic fluids.

Keywords: Ultrasonic velocity, ferrofluid, structural stability

Introduction

A magnetic fluid, also known as a ferrofluid (FF), is a colloidal suspension of single domain magnetic particles with typical dimensions of about 10nm, dispersed in a liquid carrier[1-3]. Magnetic nanoparticles in aqueous magnetic fluid have been used for diagnostic and therapeutic applications in biomedicine[4,5]. They have controllable sizes ranging from a few nanometers up to tens of nanometers. This means that they can get close to a biological entity of interest. Indeed, they can be coated with biological molecules to make them interact with or bind to a biological entity also this coating ensure that their stability, biodegradability and non-toxicity in a physiological medium. For biomedical application, it is very important to know the stability and structural properties of biocompatible magnetic fluids. The behaviour of ultrasonic wave propagation through magnetic fluids, in the presence of magnetic field is relatively unexplored area. Jozefczak et al[6,7] reported that ultrasonic wave absorption coefficient is an effective parameter to determine the stability of the ferrofluid structure subjected to an external magnetic field. Many workers [8-12] have used only Continuous Wave (CW) method for the measurement of ultrasonic velocity in ferrofluids. Chung[13] concluded that CW method proved to be well–suited for studying the velocity changes due to a magnetic field. On this basis, the present study is aimed at measuring the ultrasonic wave velocity of some water based ferrofluids for different field strengths using CW method and the attempt is made to determine the stability of ferrofluids based on the ultrasound velocity.

Experimental Details

Ferrofluids synthesized in the pilot laboratory at Engineering Physics, Department of Annamalai University and tested at the ferrofluids laboratory at Pondicherry have been used for the analysis. Three magnetic fluids based on water were used in this work, obtained by a controlled chemical co-precipitation approach as described in detail by Kim et al[14]. They are FF-I(Water + Magnetite + Oleic acid), FF-II (Water + Magnetite + Sodium Oleate), FF-III(Water + Magnetite + Starch). For FF-I, the particles used was magnetite, the surfactant was oleic acid and the carrier liquid was water, whereas in FF-II & FF-III only the surfactant was different, which are sodium oleate and starch respectively. All the chemicals required for sample preparation were purchased from S.D fine chemicals and Aldrich chemicals. The average diameter of the magnetic grains as obtained from VSM measurement was 23 nm.

The density of the ferrofluid was measured by relative density method with an accuracy of ± 0.1 kgm^{-3}. The ultrasonic sound velocity in the fluids was measured by using the CW ultrasonic interferometer working at 2 MHz frequency. It has an overall accuracy of ± 0.1 ms^{-1}. The sound velocity in the fluid under various external fields up to 0.5 Tesla in parallel orientations were measured by accordingly placing the cell in between the pole pieces of a strong

electromagnet. Each measurement was made 35 minutes after the application of magnetic field as the system needed some time to set Equilibrium[15].

Results And Discussion

The values of density and sound velocity for the ferrofluid samples under parallel and perpendicular field conditions at 303K are given in the Table 1. On referring the respective Figures (1, 2 & 3), sound velocity is found to increase with increasing field for all the three ferrofluids under both parallel and perpendicular conditions.

The perusal of Table reveals that the increasing of magnetic field up to 0.5T leads to increase the sound velocity by 33.9 ms^{-1}, 17.9 ms^{-1}, and 7.3 ms^{-1} under parallel field with respect to FF-I to FF-III. Similarly, the increased velocities observed under perpendicular field are 6.5ms^{-1}, 4.5ms^{-1}, and 5.3ms^{-1}. On comparing these values, it is observed that the parallel field is more effective than the perpendicular field. It is to be noted that the externally applied magnetic field causes an ordering of the magnetic moments of the particles, giving rise to a magnetization of the sample as a whole on a microscopic scale. This leads to the observed increase in sound velocity. Further it is observed that increasing the strength of the external magnetic field shows an increasing trend in sound velocity but non-linearly. This non-linear increase in sound velocity suggests the existence of interactions in the system taken. Palaniappan et al.[16] reported that Grain-field interactions are more favoured in the

Table 1—Density & Ultrasound velocity values of various ferrofluids measured under parallel and perpendicular magnetic field at 303K.

Magnetic field (T)	Density (kg m^{-3})	Ultrasound velocity(ms^{-1}) under parallel field	Ultrasound velocity(ms^{-1}) under perpendicular field
	water + magnetite + oleic acid		
0.0	1168.7	1462.6	1462.6
0.1	1168.7	1466.2	1463.1
0.2	1168.7	1470.9	1463.9
0.3	1168.7	1476.6	1465.2
0.4	1168.7	1484.9	1467.2
0.5	1168.7	1496.5	1469.1
	water + magnetite + sodium oleate		
0.0	1166.7	1473.3	1473.3
0.1	1166.7	1475.9	1473.8
0.2	1166.7	1478.6	1474.5
0.3	1166.7	1482.1	1475.2
0.4	1166.7	1486.3	1476.2
0.5	1166.7	1491.2	1477.8
	water + magnetite + starch		
0.0	1160.2	1452.2	1452.2
0.1	1160.2	1452.5	1452.8
0.2	1160.2	1453.1	1453.7
0.3	1160.2	1454.5	1454.7
0.4	1160.2	1457.3	1456.0
0.5	1160.2	1459.5	1457.5

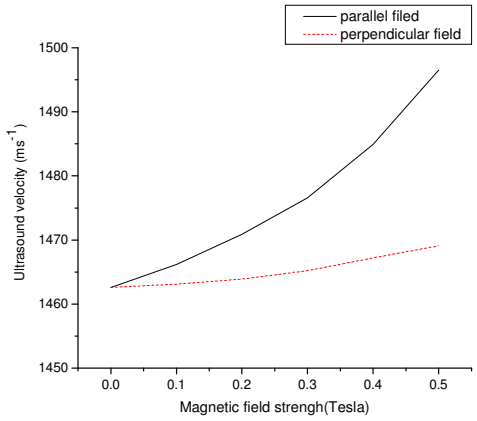

Fig. 1—Magnetic field strength vs Ultrasound velocity for FF-I

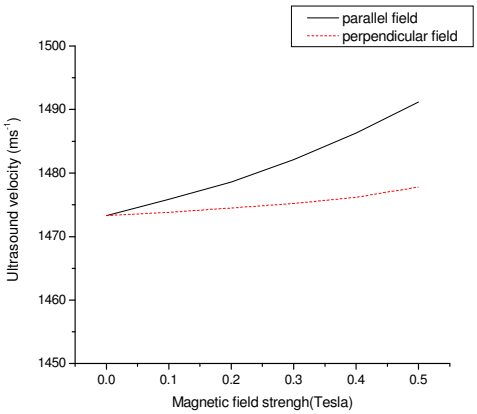

Fig. 2—Magnetic field strength vs Ultrasound velocity for FF-II

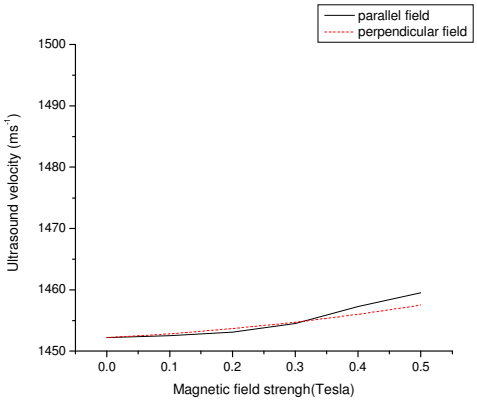

Fig. 3—Magnetic field strength vs Ultrasound velocity for FF-III

parallel field whereas grain-grain interaction is in perpendicular field. Thus the effect of magnetic field on the ferrofluid is expected to align the magnetic particles, which is only change in the layer and not in bulk, so that the bulk density remains the same.

The non-linear variation in the sound velocity (Fig1 to Fig 3) indicates that there is an appreciable degree of interactions in the medium[17-19] for which the only possibility is the effect of external field, as the system is identical in all other aspects. Thus the existence of grain-field type interactions is evident in the system but there were no agglomeration or flocculation as there were no sudden changes in the trend of the sound velocity. The visual observation of the sample also reveals no precipitation/sedimentation.

The increase of sound velocity of a medium may be attributing to two chances as (i) an elevation in the pressure of the medium and (ii) the increase in compactness of the medium or the reduction in free space between the components. In the present case, pressure and frequency are fixed, so it is only the compactness that enhances the sound velocity. Compactness in turn, may be due to the increase in the number of component molecules or the development of size of the components. The same fluid is used throughout the experiment and hence no chance for the change in the number of components is possible.

The application of external magnetic field may collect all the magnetic particles in the medium and make the component size to develop. However, the surfactant coated over the particles will restrict the agglomeration and hence the size. If the size of the component develops, more energy will be needed to overcome the inertial effects[20] and here it is provided in the form of magnetic energy. Thus the effect of external magnetic field increases the size of the components in the medium and at the same time drastically reorient the particles in the system. Hence the sound velocity increases whereas the density remains the same. However, the fluid is found to remain as magnetic fluid. It is due to the surfactant, which protects the nanoparticles from excess carrier.

From Fig.1 to Fig.3, it is observed that there exist specific changes (increase) in the ultrasound wave velocity as a function of the magnetic field strength under parallel and perpendicular field for the three magnetic fluids. The fluid-III shows small changes in the ultrasonic velocity whereas in the fluid- I & II, the maximum of changes of the ultrasonic velocity is observed. Under the effect of an external magnetic field, the particles of the ferrofluid aggregate and chain-clusters appear to arrange along the direction of the field. These observed results have shown that the field has little effect on the FF-III, in another way it tells that FF-III had a good structural stability even in a strong magnetic field. Jozefczak et al[6] reported the stability of biocomopatible coating on nanoparticle in ferrofluids can be measured based on the ultrasonic absorption coefficients.

Conclusion

On the basis of behavior of the ultrasonic velocity as a function of external magnetic field, the structure of the biocompatible ferrofluid (water +magnetite +starch) is very stable for up to the external field strength of 0.5 T compare to the remaining fluids. This result supported to explore the possibilities of starch coated magnetic fluid for the potential applications of medicine.

References

1 Papell, S.S., U.S.Patent no 3, 215 (1965) 572.

2 Rosensweig, R.E. and Kaiser, R., NTIS Rep.No.NASW-1219 (1967).

3 Rosensweig, R.E.,Ferrohydrodynamics Cambridge Univ.Press. Cambridge, London (1985) ; republished by Dover.Publ.Inc., New York (1997).

4 Pankhurst, Q.A., Connolly, J., Jones, S.K. and Dobson, J., Application of Magnetic Nanoparticles inbiomedicine, *J.Phys.D.Appl. Phys.* 36 (2003) R167.

5 Scherer, C. and Figueiredo Neto, A.M., Ferrofluids: properties and Applications, *Brazilian Journal of Phys.* 35 (2005) 3A.

6 Jozefczak, A. et al., Effects of biocompatible coating of nanoparticles on acoustic- property of the magnetic fluid, *J.Magn. Magn. Mater*. 290-291 (2005) 265-268.

7 Jozefczak, A. and Skumiel, A., Acoustic and magnetic properties of a dense commercial magnetic fluid, *Czechoslovak Journal of Phys*. 54 (2004) D 647- D650.

8 Mehta, R.V. and Patel, J.M., Velocity anisotropy of ultrasound in magnetic fluids, *J.Magn. Magn. Mater.* 65 (1987) 204-206.

9 Shrivastava, R., Vaidya, S.P., Patel, J.M. and Mehta, R.V., Ultrasonic velocity anisotropy of Magnetic fluids, *J.Colloid and Int. Sci.* 124 (1988) 248-251.

10 Chung, D.Y., Hung, H.Z. and Lin, J.X., Ultrasonic properties of magnetic fluids, *J.Magn. Magn. Mater.* 39 (1983) 111-112.

11 Chung, D.Y., Hung, H.Z. and Lin, J.X., Magnetic effects on the ultrasonic velocity and attenuation in magnetic fluids, *J.Magn.Magn. Mater.* 65 (1987) 231-234.

12 Vaidya, S.P. and Mehta, R.V., Temperature dependence of the ultrasonic velocity on magnetic fluids subjected to an external field, *J.Magn.Magn. Mater.* 39 (1983) 82-84.

13 Chung, D.Y. and Isler, W.E., Ultrasonic velocity anisotropy in ferrofluids under the influence of a magnetic fluid, *J.Appl. Phys.* 49(3) (1978) 1809-1814.

14 Kim, D.K., Zhang, Y., Kehri, J., Klason, T., Bjelke, B. and Muhammed, M.,Charaterization and MRI study of surfactant-coated superpara magnetic nanoparticles administered into the rat brain, *J.Magn. Magn. Mater.* 225 (2001) 256-261.

15 Jozefczak, A., The time dependence of the changes of ultrasonic wave velocity in ferrofluid under parallel magnetic field, *J.Magn. Magn. Mater*. 256 (2003) 267-270.

16 Samuel Ebinezer, B. and Palaniappan, L., Effect of field strength in the velocity anisotropy of ferrofluids, *Journal of Physical Sci*. 18(2) (2007) 1-13.

17 Reddy, K.C., Subrahmanyam, S.V. and Bhimsenachar, J., Thermodynamics of binary Liquid mixtures containing cyclohexane Part-1. *J.Phys. Soc. Of .Jpn*. 19 (1964) 559-566.

18 Kannappan, V. and Vinayagam, S.C., Ultrasonic Investigation of ion-solvent Interactions in Aqueous and non-aqueous Solutions of transfer and inner transfer of metal ions, *Indian J. Pure Appl. Phys*. 45(3) (2007) 143-150.

19 Kannappan, V. and Gandhi, I.N.,Ultrasonic Studies on charge transfer complexes of certain Aldehyde with benzylamine and Cyclohexylamine as donors in 1-hexane at 303K, *Indian J. Pure Appl. Phys.* 45(3) (2007) 221-225.

20 Palaniappan, L. and Nithyanandam, S., Molecular interaction studies of fructose in aqueous amylase solution, *Acta Ciencia Indica*, 37(3) (2006) 387-392.

J. Pure Appl. Ultrason. 33 (2011) pp. 33-38

A Novel Method to Distinguish Positional Isomers of Propyl Alcohol By Ultrasonic Studies.

Srirangan Govindarajan, Venu Kannappan[1], M.D.Naresh, M.Muthukrishnan, V. Arumugam*, A. Rajaram, and B. Lokanadam.

Central Leather Research Institute, Adyar, Chennai- 600 020. INDIA.
[1]Post graduate & Research Department of Chemistry (Rtd), Presidency College, Chennai-600 005. INDIA.
Email: gs1559@gmail.com

Ultrasonic velocities (u), and densities (ρ) were measured in aqueous and n-hexane solutions of 1-propanol and 2-propanol (positional isomers) at various concentrations and in the temperature range 20-40°C. Acoustical parameters such as adiabatic compressibility (β), intermolecular free length (L_f), available volume (V_a) and characteristic impedance (Z) were calculated to differentiate these position isomers. There is significant difference in the acoustical and thermodynamic parameters of the two alcohols in aqueous and hexane solutions in the temperature range investigated.

Keywords: Acoustical and thermodynamic parameters, positional isomers.

Introduction

Propyl alcohol is the simplest alcohol that exhibits position isomerism and exists as 1-propanol (n-propanol) and 2-propanol (iso-propanol). They can be distinguished by physical and chemical methods[1,2]. The two isomers belong to different class of alcohols and therefore they differ in the chemical properties. The physical methods used to distinguish the isomeric alcohols include spectroscopic techniques like IR, NMR and UV visible spectral methods[3,4]. The positional isomers are structurally different and hence the molecular interactions should be different in n-propyl and iso-propyl alcohol. Ultrasonic is an emerging field to analyse molecular interactions in binary and ternary liquid mixtures[5]. Further, it is a non-destructive, precise and quick method.

Acoustical parameters like adiabatic compressibility (β), intermolecular free length (L_f), available volume (V_a), free volume (V_f), and characteristic impedance (Z), can be computed from measured values of ultrasonic velocities and densities. It is also possible to calculate the stability constants of even weak charge transfer complexes from ultrasonic velocities[6]. These parameters also throw light on the molecular interactions, which are orientation dependent. In this paper, we report the ultrasonic velocities, densities of these two compounds at various concentrations in non-polar medium like hexane and polar solvent like water at different temperatures and different trends are observed in the case of the two positional isomers.

*Life Member:- Ultrasonics society of India.

Experimental details

2.a Materials

Hexane (SRL, extra pure, Analar, boiling point 66-70°C), propan-1-ol (Merck, boiling point 96-99°C) and propan-2-ol (Merck, boiling point 81-83°C) were distilled and used. Triple distilled water was used. Freshly prepared aqueous and hexane solutions of the two alcohols were used in all the measurements.

2.b Methods

Ultrasonic velocity measurements (accuracy ± 0.01%) were made in an ultrasonic interferometer at a frequency of 2 MHz. The temperature was maintained constant using thermostatic water bath (Pharmacia) having an accuracy of ± 0.1°C. An analytical balance with an accuracy of ± 0.01 mg. was employed for mass measurements. Density measurements were carried out for all the solutions in pyknometer. The various derived acoustical parameters were calculated using Microsoft® Excel and plotted using Microcal® Origin plotting software. The equations used in the computation of acoustical and thermodynamic parameters are given elsewhere [7].

Results and discussions

Alcohols are hydroxy derivates used as protic solvents for organic compounds. Among the alcohols, propyl alcohol is the simplest alcohol which exhibits positional isomerism. Positional isomers can be distinguished by chemical methods and spectroscopic techniques. Positional isomers have different physical and chemical properties as they are structurally different and their spatial orientations are different.

Table 1—Densities (kgm^{-3}) of Iso-Propyl Alcohol and n-Propyl Alcohol at various concentrations and at different temperatures in water and in n-hexane

Conc. (%)	Temperature (°C) 20	25	30	35	40	Temperature (°C) 20	25	30	35	40
	Iso-Propyl Alcohol + Water					**Iso-Propyl Alcohol + Hexane**				
0	998.23	997.07	995.67	994.06	992.24	660.63	657.35	654.54	649.91	647.04
2	991.07	989.56	987.85	985.99	983.96	664.56	662.02	660.77	659.71	656.72
4	988.65	986.57	984.40	982.16	979.85	665.58	664.35	664.13	661.88	658.58
6	986.19	984.65	982.87	980.85	978.49	658.94	658.32	656.89	656.39	653.69
8	985.57	984.72	983.50	981.92	979.99	667.50	666.82	664.35	664.85	662.11
10	982.05	980.90	979.31	977.43	975.26	664.35	662.29	660.03	658.74	658.12
12	978.59	977.04	975.12	973.00	970.55	670.37	669.25	666.46	662.89	658.95
14	975.89	974.25	972.28	970.06	967.51	675.42	672.50	668.26	668.25	668.08
16	973.42	971.80	969.86	967.60	965.05	680.31	674.62	671.29	667.78	664.82
18	971.22	969.15	966.84	964.19	961.35	673.90	673.08	673.67	671.21	671.75
20	968.43	966.17	963.66	960.96	957.98	688.36	681.95	676.20	672.71	669.88
	n-Propyl Alcohol + water					**n-Propyl Alcohol + Hexane**				
0	998.23	997.07	995.67	994.06	992.24	660.63	657.35	654.54	649.91	647.04
2	990.75	989.55	988.16	986.60	984.89	667.97	659.55	658.13	654.82	651.73
4	988.73	986.96	985.11	983.18	981.19	667.69	664.43	661.72	658.66	655.34
6	986.05	984.84	983.30	981.62	979.69	675.25	665.41	661.26	657.74	654.55
8	985.54	984.67	983.50	982.08	980.40	678.37	671.76	671.59	668.33	664.79
10	982.44	981.14	979.60	977.86	975.94	678.74	677.27	674.45	665.66	661.92
12	979.31	977.62	975.75	973.68	971.41	680.96	672.48	669.39	666.86	663.19
14	976.32	974.88	973.19	971.17	968.91	685.32	682.51	680.02	676.58	673.16
16	973.42	972.43	971.03	969.22	967.03	681.67	679.03	678.52	673.92	670.43
18	971.22	969.97	968.28	966.31	963.90	689.89	682.01	679.28	675.69	671.34
20	968.33	966.89	965.11	962.99	960.53	689.67	685.74	684.89	683.41	680.11

The structural differences in the positional isomers can influence the type of molecular interactions and the interaction of solvent molecules. Recently, ultrasound has been widely used to asses the intermolecular attractions between the components in binary and ternary liquid mixtures[8]. It should be possible to distinguish the positional isomers of alcohols by ultrasonic method. The trend in acoustical parameters is different for the two isomers and hence we have differentiated 1-propanol and 2-propanol by ultrasonic method.

Ultrasonic velocities, densities are measured for various concentrations of n-propanol and iso-propanol in aqueous and hexane solutions at 20-40°C. The values of density are presented in Table 1. Plots of ultrasonic velocity against concentration for aqueous and hexane solutions of the two positional isomers at 30 and 40°C are given in Fig. 1, indicate that the ultrasound behaviour in the two alcohols depends on structure of the alcohols, solvent and temperature. It is found that in non-polar hexane solvent the ultrasonic velocity does not change significantly with concentration at the two temperatures investigated.

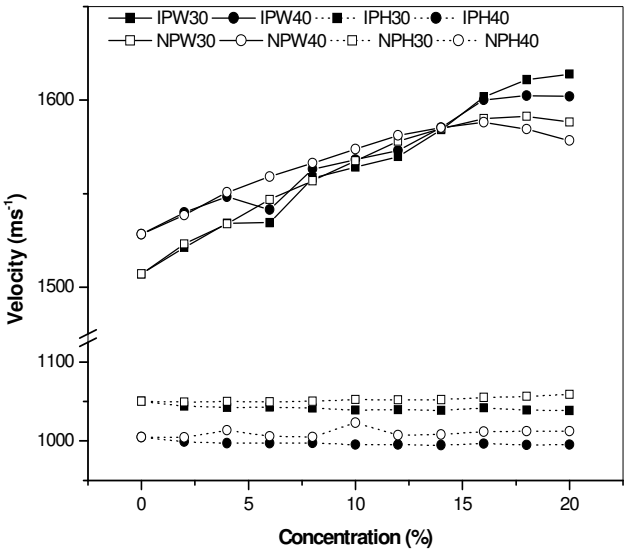

Fig. 1—Plots of ultrasonic velocity vs. percentage of n-propanol and iso-propanol in water and hexane at different temperatures. {In this and the following figures the first two alphabets of the legend indicate the type of isomer –ip for isopropanol and np for n-propanol; the third alphabet the solvant –'h' for hexane and 'w' for water and the last two digits the temperature in °C]

Further, 1-propanol has higher ultrasonic velocity than 2-propanol at any concentration in this solvent. But in the case of aqueous solutions the trend in ultrasonic velocity is same for both the positional isomers but reverse trend is observed at concentrations above 15%. At higher concentration, iso- propanol has higher velocity than that of n- propanol at the same temperature. These observations indicate that the intermolecular attractions are similar in hexane solutions of the two positional isomers. In aqueous solutions also the intermolecular attractions are almost similar for the isomeric alcohols at low concentrations. But, at higher concentrations the ultrasonic velocity decreases in the case of n-propanol suggesting that 1-propanol molecules are hydrated to a greater extent than 2-propanol at concentrations above 15%. Thus, the positional isomers differ in the variation of ultrasonic velocity in aqueous solutions at moderate concentration.

Adiabatic compressibility (β) is another parameter used in the study of molecular interactions in binary and ternary liquid mixtures[9]. Solvation studies can be made from the β values. In the present investigation, β values are calculated from the ultrasonic velocities and densities at different temperatures in hexane and water are given in Table 2. The β values do not change significantly with concentration in hexane solutions except for slight decrease at high concentration. This may be due to smaller β values of pure propyl alcohols than hexane. The molecular interactions between propyl alcohols and water molecules are much stronger than those between the alcohol molecules and hexane molecules. This is indicated by the decrease in β values with increase in concentration in aqueous solutions at the three temperatures investigated. However, the change is not uniform and the trend is different for the positional isomers. In the case of n-propanol, at very low concentration the β value decreases with increase in temperature while reverse trend is observed for this positional isomers above 15% concentration. It may be mentioned here that in the case of iso-propanol water system compressibility factor decreases with increase in temperature at very low concentrations and the behaviour is similar to aqueous solution of 1-propanol. However, above 15% concentration, the change in β values with temperature is not

Table 2—Adiabatic compressibility ($\beta/10^{-10}$ ms^2 kg^{-1}) of Iso-Propyl Alcohol and n-Propyl Alcohol at various concentrations and at different temperatures in water and in n-hexane

Conc.	**Temperature (°C)**					**Temperature (°C)**				
(%).	20	25	30	35	40	20	25	30	35	40
	Iso-Propyl Alcohol + Water					**Iso-Propyl Alcohol + Hexane**				
0	4.555	4.491	4.422	4.363	4.314	12.473	13.095	13.852	14.600	15.306
2	4.496	4.432	4.374	4.329	4.285	12.513	13.178	13.882	14.522	15.258
4	4.421	4.366	4.316	4.284	4.257	12.512	13.143	13.860	14.533	15.274
6	4.400	4.355	4.321	4.304	4.301	12.669	13.281	14.005	14.703	15.386
8	4.265	4.248	4.186	4.186	4.176	12.512	13.131	13.878	14.488	15.181
10	4.234	4.223	4.174	4.176	4.170	12.621	13.244	14.031	14.708	15.339
12	4.201	4.198	4.162	4.166	4.163	12.514	13.187	13.885	14.633	15.321
14	4.111	4.110	4.099	4.108	4.112	12.470	13.102	13.866	14.516	15.132
16	4.005	4.004	4.020	4.034	4.048	12.298	13.025	13.727	14.463	15.145
18	3.955	3.968	3.986	4.021	4.051	12.492	13.098	13.751	14.460	15.038
20	4.030	3.955	3.984	4.039	4.068	12.233	12.902	13.712	14.391	15.069
	n-Propyl Alcohol + water					**n-Propyl Alcohol + Hexane**				
0	4.555	4.491	4.422	4.363	4.314	12.473	13.095	13.853	14.600	15.306
2	4.508	4.426	4.362	4.327	4.290	12.367	13.092	13.802	14.515	15.210
4	4.412	4.351	4.315	4.276	4.238	12.351	13.024	13.707	14.421	14.858
6	4.348	4.290	4.250	4.226	4.199	12.214	12.949	13.732	14.440	15.103
8	4.261	4.223	4.195	4.172	4.157	12.140	12.834	13.498	14.186	14.890
10	4.201	4.174	4.155	4.144	4.137	12.055	13.018	13.381	14.176	14.434
12	4.143	4.125	4.115	4.116	4.117	12.039	12.777	13.499	14.196	14.862
14	4.098	4.086	4.092	4.095	4.107	11.948	12.596	13.280	13.944	14.615
16	4.058	4.049	4.074	4.076	4.100	12.000	12.600	13.243	13.933	14.570
18	4.034	4.069	4.078	4.101	4.132	11.790	12.503	13.190	13.851	14.531
20	4.048	4.086	4.108	4.149	4.179	11.787	12.387	13.021	13.644	14.350

Table 3—Free Length (L_f /10^{-11}m) of Iso-Propyl Alcohol and n-Propyl Alcohol at various concentrations and at different temperature in water and in n-hexane

Conc.	Temperature (°C)					Temperature (°C)				
(%)	20	25	30	35	40	20	25	30	35	40
	Iso-Propyl Alcohol + water					**Iso-Propyl Alcohol + Hexane**				
0	4.162	4.169	4.173	4.181	4.194	6.887	7.119	7.387	7.649	7.899
2	4.135	4.142	4.151	4.165	4.180	6.898	7.142	7.394	7.629	7.887
4	4.101	4.111	4.123	4.144	4.166	6.898	7.132	7.389	7.631	7.891
6	4.091	4.106	4.125	4.153	4.187	6.941	7.170	7.427	7.676	7.920
8	4.027	4.055	4.061	4.096	4.126	6.898	7.129	7.393	7.620	7.867
10	4.013	4.043	4.055	4.091	4.123	6.928	7.160	7.434	7.677	7.908
12	3.997	4.031	4.049	4.086	4.120	6.899	7.144	7.395	7.658	7.903
14	3.954	3.988	4.018	4.057	4.095	6.886	7.121	7.390	7.627	7.854
16	3.902	3.936	3.979	4.021	4.062	6.839	7.100	7.353	7.613	7.858
18	3.878	3.919	3.962	4.014	4.064	6.892	7.120	7.360	7.612	7.830
20	3.915	3.913	3.961	4.023	4.072	6.821	7.067	7.349	7.594	7.838
	n-Propyl Alcohol + water					**n-Propyl Alcohol + Hexane**				
0	4.162	4.169	4.173	4.181	4.194	6.887	7.119	7.387	7.649	7.899
2	4.141	4.139	4.145	4.164	4.182	6.858	7.119	7.373	7.627	7.874
4	4.096	4.104	4.122	4.140	4.157	6.853	7.100	7.348	7.602	7.783
6	4.066	4.075	4.091	4.115	4.138	6.815	7.080	7.354	7.607	7.847
8	4.026	4.043	4.065	4.089	4.117	6.795	7.048	7.291	7.540	7.791
10	3.997	4.019	4.045	4.075	4.107	6.771	7.098	7.260	7.537	7.671
12	3.969	3.996	4.026	4.061	4.097	6.766	7.032	7.292	7.543	7.784
14	3.948	3.977	4.014	4.051	4.092	6.741	6.982	7.232	7.475	7.719
16	3.928	3.959	4.006	4.042	4.088	6.755	6.984	7.222	7.472	7.707
18	3.917	3.968	4.008	4.054	4.104	6.696	6.956	7.208	7.450	7.697
20	3.923	3.977	4.022	4.077	4.127	6.695	6.924	7.161	7.394	7.649

uniform. If we compare the β values of 20% iso-propanol in water, β value decreases as we go from 20 to 30°C and increases above this temperature. Thus, variations in the β values with concentration and temperature are different for aqueous solutions of n- propanol and iso-propanol.

Intermolecular free length (L_f) in a liquid system is a measure of molecular association. In the case of binary mixtures, L_f values depend on the interaction between the component molecules. The positional isomers of propyl alcohol are structurally different and hence the intermolecular attraction may be different in the two alcohols. In order to compare the intermolecular attraction in the two positional isomers, intermolecular free length values are computed from the ultrasonic velocities and densities of hexane solutions and aqueous solutions of the two alcohols at different temperatures. These values are tabulated in Table 3. Analysis of the data indicate that L_f values increase with increase in temperature for a particular concentration but decreases with increase in concentration at a given temperature. This may be due to the thermal agitation and loosening of intermolecular attractions with rise in temperature and the association of molecules with increase in concentration. The data in hexane solutions cannot be used to distinguish the two positional isomers since the trend is the same for both iso-propanol and n-propanal. However, the isomeric propyl alcohols can be distinguished from L_f values in aqueous solutions. The increase in L_f values with temperature is less in aqueous solutions than in hexane solutions. This may be due to increase in solute- solvent interaction in aqueous medium. In both cases the L_f value decreases with increase in concentration, reaches minimum at about 20% and thereafter increases. Thus, the solute-solvent interaction is maximum at about 20% of the alcohol. It may be noted that the L_f value of n-propanol in water at a given temperature and concentration is slightly less than that of iso-propanol in aqueous medium. These observations suggest that in the case of n-propanol the molecules are closer than in aqueous solution of iso-propanol. This is supported by the difference in the β values of the positional isomers in aqueous solutions but not in hexane solutions. This can be illustrated diagrammatically as follows in Fig. 2 (a) & (b).

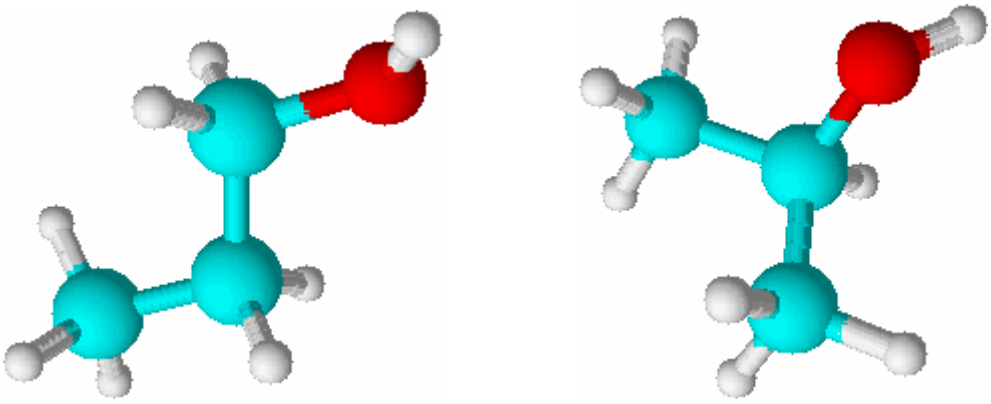

Fig. 2—Schematic representation of (a) n-propanol and (b) iso-propanol.

The difference in the orientation of molecules in n-propanol and iso-propanol can influence the available volume V_a, which can be calculated from ultrasonic velocity and density values. Fig. 3 contains plots of V_a against concentration of the alcohols at three different temperatures in hexane and aqueous solutions. In general, the V_a decreases with increase in concentration of alcohol, may be due to increase in the extent of solvation. It may be seen from the plots that there is uniform decrease in V_a values with concentration of n-propanol and iso-propanol. However, in aqueous solution the variation of V_a with concentration differs for the two isomeric alcohols. It is found that for both the isomeric alcohols the curves are steeper for the plots in aqueous medium than those for hexane solutions. This is due to the strong intermolecular hydrogen bond between the alcohol molecules and solvent molecules in aqueous medium. It is interesting to note that the values of V_a are negative for aqueous solutions of iso-propanol above 15% where as the V_a values are positive for aqueous solutions of n-propanol at any concentration. This difference in V_a values supports that the orientation of the two isomeric alcohol molecules in space are different. Actually, in aqueous medium the alcohols are not only associated among them but also associated with the solvent molecules through intermolecular hydrogen bond. It may be seen from Fig. 2(a) & (b) that the actual volume of the solvated iso-propanol molecules are larger than the solvated n-propanol molecules. Therefore, the V_a becomes negative at moderate concentration of iso-propanol alcohol in aqueous medium.

In order to establish this, free volume (V_f) values were also calculated for the four systems at different concentrations. The plots of V_f against

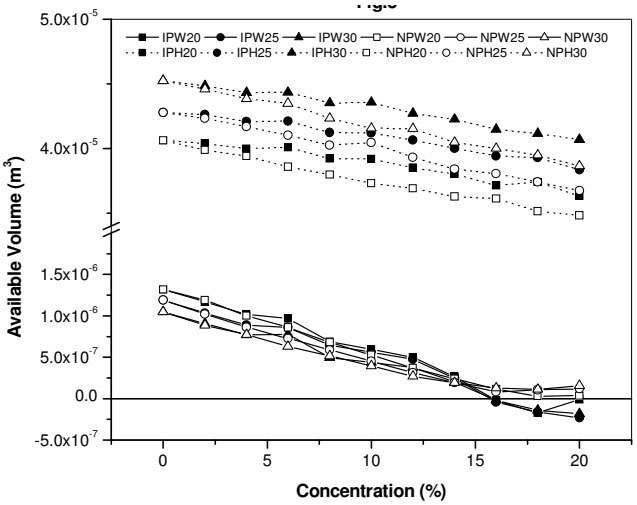

Fig. 3—Plots of available volume vs. percentage of n-propanol and iso-propanol in water and hexane at different temperatures.

concentration for the four systems are presented in Fig. 4. It is evident from these plots that the V_f decreases with increase in concentration in all the systems investigated, due to increase in the solute-solvent interaction with concentration. V_f values are much smaller in aqueous medium for both the isomeric alcohols than in hexane solution at all concentrations. This may be due to stronger solute-solvent interactions in aqueous solution. Further, the V_f value of iso- propanol in aqueous medium is less than that of n-propanol in the same medium above 10% concentration at a given temperature. The reverse trend is observed in case of hexane solution. Thus, the positional isomers of propyl alcohol can be distinguished from the trend in the V_a and V_f values as the function of concentration of the alcohols.

Characteristic impedance (Z) in a liquid system can be used to assess the molecular interaction between the components[10]. It is found that the

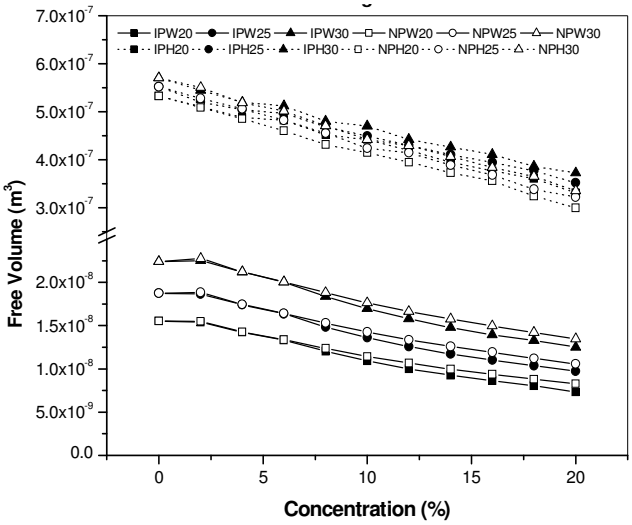

Fig. 4—Plots of free volume vs. percentage of n-propanol and iso-propanol in water and hexane at various temperatures.

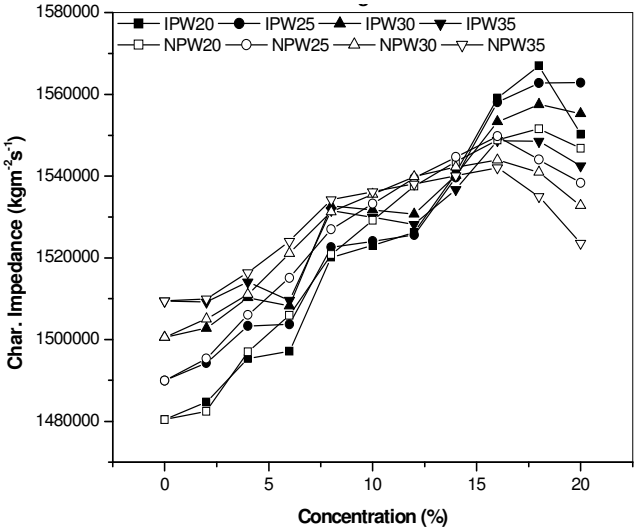

Fig. 5—Plots of Characteristic Impedance Vs. percentage of n-propanol and iso propanol in water at different temperatures.

Z values for the two alcohols at different concentrations in hexane solutions are almost constant. Plots of Z against concentration for the two alcohols in aqueous solutions at four temperatures are given in Fig. 5. It is found that in n-propanol water system the Z values increases with increase in concentration suggesting that the solute-solvent interaction increases with increase in the concentration. However, in the case of iso-propanol Z values initially decrease with increase in concentration and reach minimum at about 6% iso-propanol and there after there is uniform increase in the Z values. Thus, the interaction between iso-propanol and water is weak in very dilute solutions but become stronger at higher concentration. Thus, the two isomeric alcohols differ in the variation of Z values with concentration in aqueous solution.

Conclusions

The two isomeric propyl alcohols differ in the acoustical properties and other thermodynamic parameters. The significant difference was found in the adiabatic compressibility, available volume values of the two positional isomers in aqueous solutions at various concentrations. This difference in the acoustical parameters of the two alcohols in aqueous and hexane solutions can be used to distinguish the two positional isomers.

Acknowledgement

The authors gratefully acknowledge the Director, CLRI, Adyar, Chennai for his permission to publish this work.

References and Notes

1 John A. Monick., Alcohols: Their Chemistry, Properties and manufacture. Ireinhold Book Corporation, New York, 1968.

2 Furniss, B.S., Hannaford, A.J., Rogers, V., Smith, P.W.G., Tatchell, Vogel, A.R., Text book of Practical Organic Chemistry. Longman Group Ltd., 4th ed.; Essex: England, 1984.

3 Dip Singh Gill, Taranjit Kaur, Harkiran Kaur, Inder Mohan Joshi and Jasbir Singh., Ultrasonic velocity, permittivity, density, viscosity and proton nuclear magnetic resonance measurements of binary mixtures of benzonitrile with organic solvents J. Chem. Soc .Faraday Trans., 89 (1993) 1737.

4 Adgoanhar, C.S., Mulay, N.N., Study of someH-bond molecular complexes by dielectric measurements, Indian. J. Pure & Appl. Physics, 25 (1987) 281.

5 Jayakumar, S., "Ultrasonic studies on the molecular interactions in Certain binary and ternary mixtures" Ph.D., Thesis, 1999 University of Madras.

6 Kannappan. V., Askar.S.J., Abdul mahaboob P.A., Determination of stability Constants of charge transfer complexes of iodine mono chloride and certain ethers in solution at 303k by ultrasonic method., Indian. J. Pure & Appl. Physics, 44(2006)903-908.

7 Jayakumar, Kannappan. V., study of molecular interactions in binary liquid mixture, Indian. J. Pure & Appl. Physics, vol. 46(2008) 168-175.

8 Pandey J D., Sanguri. V., Misra.R.k., and singh A K., Acoustic method for the estimation of effective debye temperarue of binary and ternary liquid mixtures, J. pure.Appl. Ultrason. 26(2004) pp18-29.

9 Govindarajan, S., Venu Kannappan, Naresh, M.D., Venkataboopathy, K., Lokanadam, B., Ultrasonic studies on the molecular interaction of Gallic Acid in aqueous methanol and Acetone solutions and the role of Gallic Acid as Viscosity reducer., J Molecular Liquids, 107/1-3(2003) 289-316.

10 Atkins, P.W., Physical Chemistry, Oxford University Press: 5th ed.; Oxford, 1994, p 781.

J. Pure Appl. Ultrason. 33 (2011) pp. 39-42

Acoustic behaviour of terbium laurate and myristate solutions in 60/40 benzene-methanol mixture (v/v)

Kamal Kishore and S.K. Upadhyaya

Department of Chemistry, S.S.L. Jain P.G. College, Vidisha-464001, (M.P) INDIA

Email:k_81kishore@yahoo.com

The ultrasonic measurements of solutions of terbium soaps (laurate and myristate) in a mixture of 60/40 benzene-methanol (v/v) have been used to evaluate critical micellar concentration (CMC), ultrasonic velocity and various acoustic parameters at 40°C. The results confirm that there is a significant interaction between the soap and solvent molecules. The values of critical micellar concentration (CMC) for terbium laurate and myristate are in agreement with those obtained from other physical parameters. The soap molecules do not aggregate appreciably in dilute soap solution below the critical micellar concentration.

Keywords: Ultrasonic velocity, terbium soaps, acoustic parameters, CMC.

Introduction

Carboxylate of metals other than alkali metals are generally insoluble in water and are called "metallic soaps". The metallic soaps are soluble in a wide variety of pure and mixed organic solvents. These soaps have found wide applications in different industries as detergents, softeners, plasticizers, greases, lubricants, cosmetics, medicines, emulsifiers and water proofing agents. The study and understanding of acoustical properties are necessary for their application in industries. Sound velocity is purely a thermodynamic function and with the help of this technique[1], a number of other acoustic parameters of electrolyte solutions can be measured. Mehrotra et al[2, 3, 4] determined acoustical parameters of metallic soaps in mixed organic solvents. Verghese et al[5,6] studied ultrasonic behaviour of transition metal soap in liquor ammonia. Acoustical studies, compressibility behaviour and Rao formalism of lanthanide soaps solutions were carried out by Upadhyaya and Chaturvedi[7]. Rawat and coworkers[8] investigated molecular interaction and compressibility behaviour of alkaline-earth metal soaps. However studies on terbium soaps in benzene-methanol mixture have not yet been undertaken systematically.

The work reported here deals with the study of ultrasonic velocity and density of terbium laurate and myristate in a mixture of 60/40 benzene-methanol (v/v) in order to calculate various acoustical parameters at 40°C. The ultrasonic velocity of solution of these soaps increase with increasing concentration and chain-length of soaps.

Experimental

Anala R grade lauric acid, myristic acid, benzene, methanol, acetone and terbium acetate were used for the present investigation. The terbium laurate and myristate was prepared by direct metathesis of corresponding potassium soap (laurate and myristate) by pouring a slight stoichiometric excess of aqueous terbium acetate solution into clear potassium laurate and myristate dispersion at raised temperature with vigorous stirring. The precipitates were filtered off and washed with hot distilled water and acetone. After initial drying in an air oven at 50-60°C, final drying was carried out under reduced pressure. The purity of soap was checked by the elemental analysis and results were found in agreement with theoretically calculated values. The absence of hydroxyl groups was confirmed by IR spectra.

Solutions of terbium soaps were prepared by dissolving a known amount of soap in a mixture of 60/40 benzene-methanol (v/v) and kept for 2 hrs. in a thermostat at desired temperature. Ultrasonic measurements were carried out on an ultrasonic interferometer at 40°C by using a 1 MHz frequency. Water maintained at the desired temperature and controlled to ± 0.5°C by a thermostat passed through the jacket of cell before the measurement was actually made. The measured velocities have an uncertainty of ± 0.5 ms^{-1}. The densities of the solutions were determined at different temperatures with RD bottle calibrated with pure benzene.

Results and discussion

The ultrasonic velocity and various other acoustical parameters of terbium laurate and myristate were

measured at a temperature of 40°C in a mixture of 60/40 benzene-methanol (v/v) mentioned in Table 1 and Table 2. The results indicate that ultrasonic velocity and density increase with increasing soap concentration and chain length. The variation of ultrasonic velocity ν with soap concentration C depends upon the concentration derivative of density ρ and adiabatic compressibility β by the relationship.

$$\frac{d\nu}{dC} = -\frac{\nu}{2}\left[\frac{1}{\rho}\left(\frac{\partial\rho}{\partial C}\right) + \frac{1}{\beta}\left(\frac{\partial\beta}{\partial C}\right)\right] \quad (1)$$

The concentration derivative of density $\left(\frac{\partial\rho}{\partial C}\right)$ is positive, while the quantity $\left(\frac{\partial\beta}{\partial C}\right)$ is negative and since the value of $\frac{1}{\beta}\left(\frac{\partial\beta}{\partial C}\right)$ predominates over $\frac{1}{\rho}\left(\frac{\partial\rho}{\partial C}\right)$ for these soap solutions $\frac{d\nu}{dC}$ will be positive, i.e. ultrasonic velocity increases with increasing soap concentration. The variation of ultrasonic velocity ν with soap concentration C for dilute solution is given by following equation

$$\nu = \nu_0 + GC \quad (2)$$

where, ν_0 is ultrasonic velocity of pure solvent and G is Garnsey's constant[9].

The plots of ultrasonic velocity ν versus soap concentration C are characterised by an intersection of two straight lines at a definite soap concentration, which corresponds to the CMC of soap (Fig. 1). The soap form micelles at a particular concentration of soap because of balance between the attractive hydrophobic interaction of the long chain hydrocarbon tails and repulsive forces between the ionic head groups. The values of CMC decrease with increasing the chain length of the soap. The value of Garnsey's constant G obtained from the plots of ν versus C increase with increasing chain length (Table 3).

The nature of adiabatic compressibility, β and molar compressibility, W has been calculated by the following relationship.

$$\beta = \rho^{-1}\nu^{-2} \quad (3)$$

$$W = (\overline{M}/\rho)(\beta)^{-1/7} \quad (4)$$

$$\overline{M} = \frac{n_0 M_0 + nM}{n_0 + n}$$

where,

Here n_0, n, M_0, and M are the number of moles and molecular weight of solvent and solute, respectively. The behaviour of adiabatic compressibility is reverse to that of ultrasonic velocity. Increase in soap concentration and chain length cause decrease in the

Table 1—Ultrasonic velocity, compressibility and other acoustical parameters of terbium Laurate in 60/40 benzene-methanol (v/v) mixture at 40°C ± 0.5°C

S. No.	$C\times10^3$ mol dm^{-3}	ρ Kg m^{-3}	$v\times10^{-3}$ m s^{-1}	$\beta\times10^{10}$ m^2 N^{-1}	$W\times10^3$ m^3/mol (N/m^2)$^{1/7}$	$-\phi_{k\times10^5}$ m^5 N kg^{-1} mol^{-1}
1.	1.0	846.2	1.148	8.97	1.175	4.69
2.	1.5	847.0	1.167	8.67	1.180	5.17
3.	2.0	847.8	1.182	8.44	1.184	5.06
4.	2.5	848.6	1.199	8.20	1.189	5.06
5.	3.0	849.6	1.215	7.97	1.192	5.00
6.	3.5	850.2	1.230	7.77	1.196	4.87
7.	4.0	850.7	1.236	7.69	1.98	4.48
8.	4.5	851.0	1.243	7.60	1.200	4.19
9.	5.0	851.5	1.248	7.54	1.201	3.91

Table 2—Ultrasonic velocity, compressibility and other acoustical parameters of terbium myristate in 60/40 benzene-methanol (v/v) mixture at 40°C ± 0.5°C.

S. No.	$C\times10^3$ mol dm^{-3}	ρ Kg m^{-3}	$v\times10^{-3}$m s^{-1}	$\beta\times10^{10}$ m^2 N^{-1}	$W\times10^3$ m^3/mol (N/m^2)$^{1/7}$	$-\phi_{k\times10^5}$ m^5 N kg^{-1} mol^{-1}
1.	1.0	848.2	1.149	8.93	1.173	5.29
2.	1.5	849.0	1.169	8.62	1.179	5.63
3.	2.0	850.0	1.189	8.32	1.183	5.78
4.	2.5	850.8	1.208	8.05	1.189	5.73
5.	3.0	851.6	1.228	7.79	1.194	5.70
6.	3.5	852.2	1.240	7.63	1.197	5.35
7.	4.0	852.4	1.244	7.58	1.198	4.81
8.	4.5	852.7	1.248	7.53	1.200	4.40
9.	5.0	852.9	1.253	7.47	1.201	4.09

Table 3—Values of various acoustic constants for terbium laurate and myristate in a mixture of 60/40 benzene-methanol (v/v) at 40°C.

Name of the soap	$CMC\times10^3$ mol dm^{-3}	$G\times10^{-4}$ m s^{-1} mol^{-1} dm^3	$-A\times10^8$ m^2 N^{-1} mol^{-1} dm^3	$B\times10^8$ m^2 N^{-1} mol^{-2} dm^6	$-\phi_k^0\times10^5$ m^5 N kg^{-1} mol^{-1}	$S_k\times10^5$ m^5 N kg^{-1} mol^{-1}
Terbium laurate	3.40	3.22	4.44	20.00	5.58	40.04
Terbium myristate	3.20	3.86	4.36	30.03	4.80	36.03

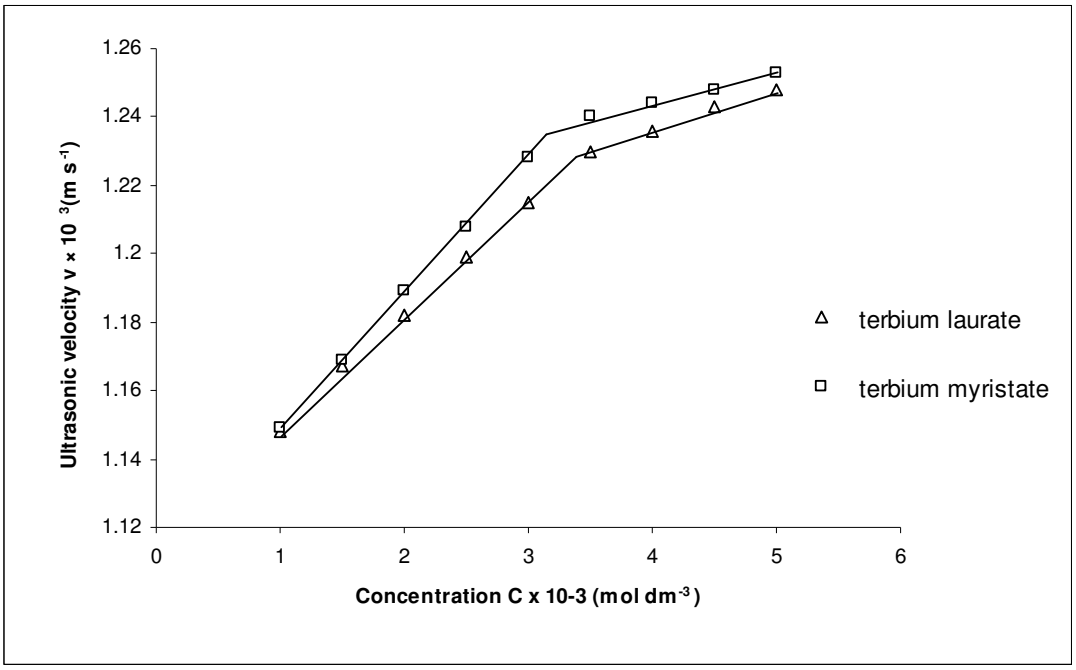

Fig. 1—Ultrasonic velocity Vs Concentration of terbium laurate and myristate in a mixture of 60/40 benzene – methanol (v/v) at 40°C

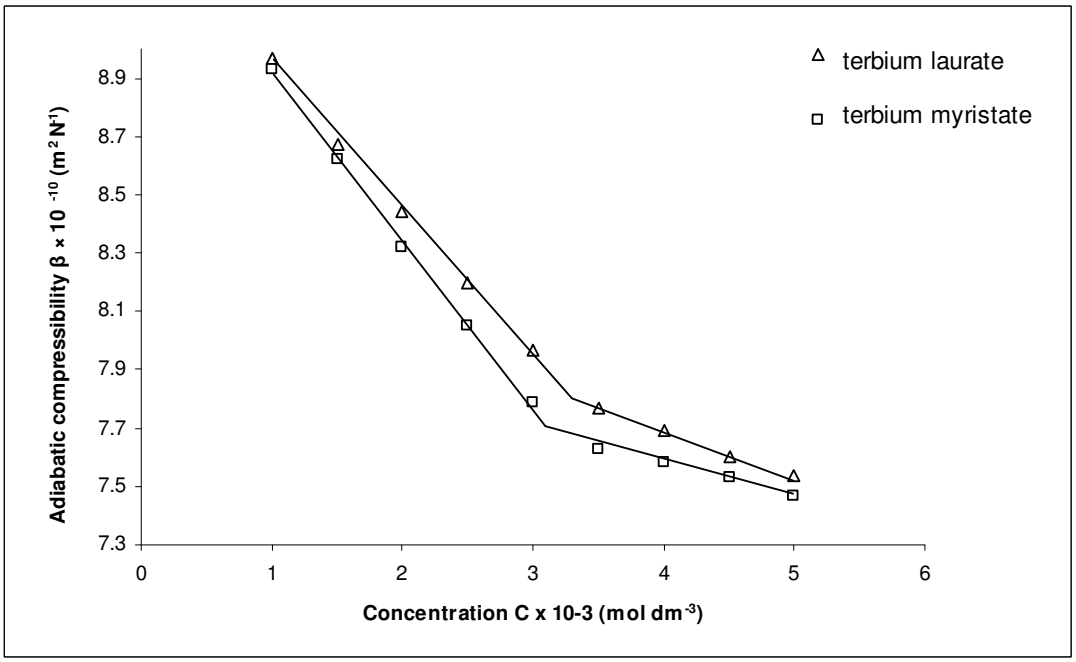

Fig. 2—Adiabatic compressibility Vs Concentration of terbium laurate and myristate in a mixture of 60/40 benzene – methanol (v/v) at 40°C

values of adiabatic compressibility (Fig. 2). The decrease in adiabatic compressibility is attributed to the fact that soap molecules in dilute solutions are considerably ionised into metal cation and fatty acid anions. These ions are surrounded by a layer of solvent molecules firmly bounded and orient towards the ions. The orientation of solvent molecules around the ions is attributed to the influence of electrostatic field of the ions and thus the internal pressure increases, this lowers the compressibility of the soap solutions.

The results of adiabatic compressibility β have also been explained in term of Bachem's relationship[10].

$$\beta = \beta_0 + AC + BC^{3/2} \qquad (5)$$

Where A and B are constants, C is molar concentration of soap solutions. β and β_0 are the adiabatic compressibilities of solutions and solvent, respectively. The values of constants have been obtained from the intercept and slope of plots of β-β_0/C vs. $\sqrt{C}$ (Table 3). The plots of β-β_0/C vs . $\sqrt{C}$ show a break at CMC.

The molar compressibility W, of terbium soaps in a mixture of 60/40 benzene-methanol (v/v) increase with increase in soap concentration and decrease with increasing chain length.

Apparent molar compressibility, ϕ_k[11] can be calculated by the relation.

$$\phi_k = \frac{1000}{C\rho_0}(\rho_0\beta - \beta_0\rho) + \frac{\beta_0 M}{\rho_0} \quad (6)$$

Here ρ_o,ρ, β_o, β, are the density, adiabatic compressibility of solvent and solutions, respectively.

The apparent molar compressibility ϕ_k is related to concentration C by Gucker's limiting law[12].

$$\phi_k = \phi_k^0 + S_k C^{1/2} \quad (7)$$

where ϕ_k^o is limiting apparent partial molar compressibility and S_k is constant. The ϕ_k vs. $\sqrt{C}$ plots are linear. ϕ_k^o and S_k have been obtained from intercept and slope of plots ϕ_k vs. $\sqrt{C}$ below the CMC. The positive value of S_k signifies a considerable soap and solvent interaction below CMC (Table 3).

Conclusion

The ultrasonic velocity throws light on evaluation of acoustical parameters of terbium laurate and myristate in a mixture of 60/40 benzene-methanol (v/v) at 40°C. The results confirm that there is a significant interaction between the soap and solvent molecules in dilute solutions[13, 14]. Data on ultrasonic velocity show that terbium laurate and myristate behave, as weak electrolyte and soap molecules do not aggregate appreciably below the CMC.

References

1 Synder W. J. and Synder J. R., Velocity of sound in binary mixtures of benzene, hexane and methanol at 0-65. deg., J. Chem. Eng. Data, 19 (1974) 270.

2 Mehrotra K. N., Gahlaut A. S. and Sharma M., Ultrasonic studies of molecular interaction in the solution of lanthanum soaps, Journal of Colloid and Interface Science, 120 (1) (1987) 110.

3 Mehrotra K. N. and Upadhyaya S.K., Ultrasonic measurements and other allied parameters of Praseodymium and Neodymium palmitates in mixed organic solvents, Colloid and Polymer Science, 267 (8) (1989) 741.

4 Mehrotra K. N. and Rawat M. K., Micellization and acoustic behaviour of manganese soaps in mixed solvents, Tenside, Surfactants, Detergents, 32 (3) (1995) 255.

5 Verghese S. P., Suleman, Prasad F. M. and Kulshrestha H., Ultrasonic studies of Vanadium palmitate in liquor ammonia, J. Ind. Coun. Chem., 24(2) (2007) 21.

6 Suleman, Verghese S. P., Prasad F. M., Ultrasonic studies of Vanadium myristate in liquor ammonia, J. Indian Chem. Soc., 85 (2008) 856.

7 Upadhyaya S. K. and Chaturvedi P. K., Acoustic studies, compressibility behaviour and rao formalism of Dysprosium soaps in 60% benzene and 40% methanol mixture (v/v), J. Ind. Coun. Chem., 24 (4) (2007) 74.

8 Rawat M. K., Sharma Y. and Kumari S., Molar interaction and compressibility behaviour of Beryllium soaps in non–aqueous medium, Asian J. Chem., 20(2) (2008)1464.

9 Garnsey R., Boe R. J., Mohoney R. and Litovitz T. A., Determination of electrolyte apparent molal compressibilities at infinite dilution using a high-precision ultrasonic velocimeter, J. Chem. Phys. 50 (1969) 5222.

10 Bachem C., The compressibility of electrolytic solution, Z Phys. A., 101 (1936) 541.

11 E'lpiner I. E., Ultrasound Physical, Chemical and Biological Effects, Consultants Bureau, Moscow pp. 371 (1964).

12 Gucker F. T., The apparent molal heat capacity, volume and compressibility of electrolytes, Chem. Rev., 13 (1933) 111.

13 Kishore K., Upadhyaya S.K. and Walia Y., Acoustic measurements and compressibility behaviour of terbium myristate in benzene-methanol mixture, Int. J. Theor. App. Sci., 1(1) (2009) 32.

14 Kishore K. and Upadhyaya S.K., Studies on Acoustic and Thermodynamic Behaviour of Terbium Laurate and Myristate in Mixed Organic Solvent, Tenside Surf. Det., 3 (2010) 184.

J. Pure Appl. Ultrason. 33 (2011) pp. 43-45

Ultrasound velocities and adiabatic compressibilities for the binary mixtures of methoxybenzene and several chlorohydrocarbons.

S.K. Choudhari, Neetu Yadav and S.S. Yadava*

Department of Chemistry, D.D.U. Gorakhpur University, Gorakhpur-273009

[1]Chemistry Department, C.M. Science College, Darbhanga-846004, Bihar.

E-mail: ssyadava1@rediffmail.com

Ultrasound velocities (u) for binary liquid mixtures of methoxybenzene with several chlorohydrocarbons viz. dichloromethane, 1,2-dichloroethane, trichloroethene and tetrachloroethene at 293.15K and 303.15K have been measured over whole concentration range. Adiabatic compressibilities (K_s) for the studied binary mixtures have been calculated from the experimental ultrasound velocity data. Ultrasound velocities increase and adiabatic compressibilities decrease with mole fraction of methoxybenzene at experimental temperature for all the systems studied. Results have been discussed in terms of molecular interactions between the components of the binary mixtures.

Keywords: Ultrasonic velocity, compressibility, methoxybenzene, chlorohydrocarbons

Introduction

There has been considerable interest in the ultrasonic studies of binary liquid mixtures [1-2]. Binary liquid mixtures with one of the components having (-O-) functional group have been studied by ultrasound velocities [3,4] measurements and by other [5,6] techniques. Ward et al[7]. have concluded, on the basis of study of chemicals viz indole, phenol and anisole (methoxybenzene), both alone and as binary mixtures that anisole has been a major component of the sex pheromone working as male attractant pheromone of the scarab beetle 'Holotrichia reynaudi' an agricultural pest. Anisole is also the sex pheromone of H. consanguinea. Raj kumar et al.[8] have studied binary mixtures of anisole with o-chlorophenol by ultrasound velocity and density measurements. However, binary mixtures of compounds containing methoxy group with aliphatic chlorocompounds have not been studied so far.

In view of the above, binary mixtures of methoxy benzene with several chloroaliphatic hydrocarbons viz. dichloromethane, 1,2-dichloroethane, trichloroethene and tetrachloroethene are studied in the present investigations by ultrasound velocity measurement. Compounds containing more than one chloro group are chosen in order to demonstrate the effect of chloro group over molecular interactions present between components of binary mixtures.

Experimental

Methoxybenzene (AR), dichloromethane (UV Spectroscopic grade), 1, 2-dichloroethane (UV Spectroscopic grade), trichloroethene (UV Spectroscopic grade), and tetrachloroethene (AR) were used in the present investigation. Compounds were puried by the method [9] described earlier and their purities were checked by densities measurements. Binary mixtures were prepared by weight. Precaution was taken to minimise evaporation losses during sample preparation. Ultrasound velocities with uncertainty of ± 0.03% of experimental liquids and their mixtures at 1 MHz were measured by ultrasonic interferometer at different temperatures 293.15K and 303.15K. The experimental ultrasound velocities for several liquids at 303.15K were compared with literature values as follows:

Ultrasound velocity (ms^{-1})

Liquids	experimental	literature value [10-11]
Dichloromethane	1053.4	1052.0
1,2-dichloroethane	1174.4	1175.0
Tetrachloroethene	1025.0	1024.2

Constant temperature up to ± 0.1K of the liquids and their mixtures were maintained by circulating water by tullu pump around the cell of interferometer from a constant temperature toluene regulated water bath. Densities needed in different calculations for the binary mixtures were evaluated from molar volumes of pure liquids and excess volume data of the binary mixtures.

Results and discussion

The experimental values of ultrasound velocities (u) with mole fractions of methoxybenzene with several chloro-aliphatic hydrocarbons viz. dichloro-methane, 1,2-dichloroethane, trichloroethene and

*Life Member:- Ultrasonics society of India.

tetrachloroethene at 293.15K and 303.15K are shown in Figures 1 and 2 respectively. The values of u_{12} are used to evaluate adiabatic compressibilities (K_s) for all the binary mixtures studied employing equation (1)

$$K_s = u^2 .\rho^{-1} \quad \ldots (1)$$

where ρ is the density of the mixtures evaluated by equation (2)

$$\rho = (x_1 M_1 + X_2 M_2)/ V_1 + V_2 + V^E) \quad \ldots (2)$$

M_1, M_2 and x_1, x_2 are molecular weights and mole fractions respectively of components 1 and 2.V_1, V_2 are molar volumes of components 1and 2 and V^E is the excess volume of binary mixtures at particular composition. The calculated values of adiabatic compressibilities (K_s) at 293.15K and 303.15K with mole fractions of methoxybenzene for all the binary mixtures studied are also given diagrammatically in Figures 3 and 4 respectively.

Perusal of Figures 1 and 2 reveals that values of u_{12} increase at both experimental temperature as mole fractions of methoxybenzene in the binary mixtures increase. It is also evident that at 303.15K, u values are lower than that at 293.15K at every composition for all the binary mixtures. Ultrasound velocity of methoxybenzene is larger than that of chlorohydrocarbons taken in present investigation. Thus increase in u_{12} values with composition of methoxybenzene is evident. Ultrasound waves are mechanical waves having high frequency. Their velocities depend inversely on the density and compressibilities of the medium in which they pass through.

It is evident from Figures 3 and 4 that adiabatic compressibilities decrease at both experimental temperatures as one moves towards higher concentration of methoxybenzene in the binary mixtures with chlorocompounds under investigation.

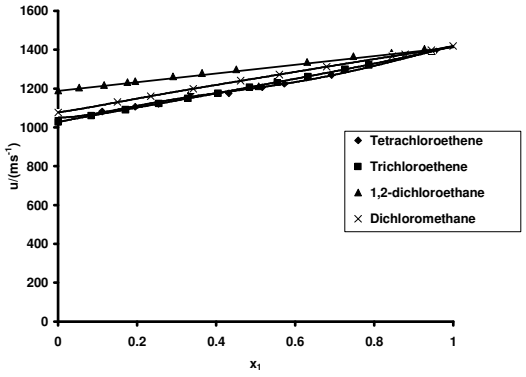

Fig. 1—Ultrasound Velocities (u_{12}) versus mole fractions (x_1) of methoxybenzene for binary mixtures of methoxybenzene + chlorohydrocarbons at 293.15K.

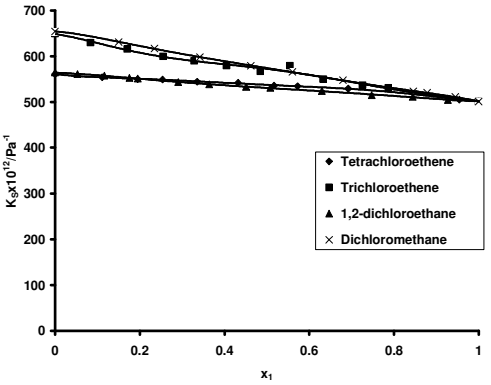

Fig. 3—Adiabatic Compressibilities (K_s) versus mole fractions (x_1) of methoxybenzene for binary mixtures of methoxybenzene + chlorohydrocarbons at 293.15K.

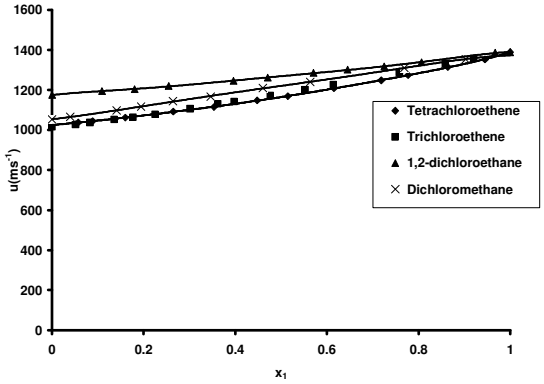

Fig. 2—Ultrasound Velocities (u_{12}) versus mole fractions (x_1) of methoxybenzene for binary mixtures of methoxybenzene + chlorohydrocarbons at 303.15K.

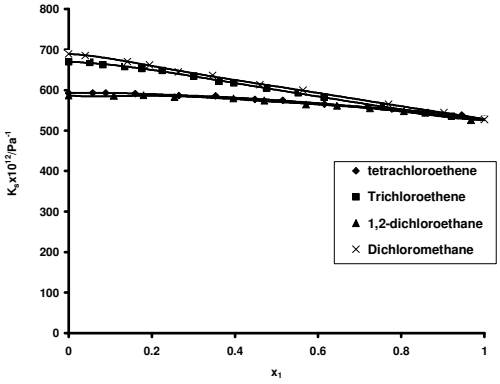

Fig. 4—Adiabatic Compressibilities (K_s) versus mole fractions (x_1) of methoxybenzene for binary mixtures of methoxybenzene + chlorohydrocarbons at 303.15K.

An observation of Figures 3 and 4 shows that K_s values for equimolar binary mixtures of methoxybenzene with chloro-hydrocarbons at both experimental temperatures are largest for the mixture with chlorohydrocarbon containing least number of chlorine atom in it and lowest for the mixture having chlorohydrocarbon with highest number of chlorine atom i.e. K_s values follow the order:

Tetrachloroethene < trichloroethene < dichloromethane

However, K_s values of equimolar mixtures of methoxybenzene + 1,2-dichloroethane are exceptionally lowest at 303.15K and larger than the values of K_s for mixture with tetrachloroethene at 293.15K.

It appears that due to interactions between unlike molecules, the binary mixtures with chloro-hydrocarbons containing lowest number of chlorine atom become more compressible rather than the mixture with chlorohydrocarbon having higher number of chlorine atoms. It is also evident that at higher temperature of 303.15K values of K_s are larger than the values at lower temperature of 293.15K for the binary mixtures of same composition. It is a well known fact that densities of liquids decrease on increase of temperature resulting larger molar volume which causes lager values of compressibility. Our observation of larger values of K_s at higher temperature for all binary systems at every composition is quite in line with the above fact.

Acknowledgements

The authors are thankful to the Head, Department of Chemistry, D.D.U. Gorakhpur University for providing necessary facilities. One of the authors (S.K. Choudhari) is also thankful to Prof. Jagan Nath for encouragement and interest in

References

1 Yadava, S.S. and Yadav A., Ultrasonic study on binary liquid mixtures between some bromoalkanes and hydrocarbons, Ultrasonics, 43(2005) 732.

2 Takagi, T., Sawada, K., Urakawa,H., Ueda, M. and Cibulka, I., Speed of sound in liquid tetrachloromethane and benzene at temperatures from 283.15 K to 333.15 K and pressures upto 30 MPa, J.Chem.Thermodyn.,36(2004) 659.

3 Pereira, S.M., Rivas,M.A., Legido,J.L. and Iglesias, T.P., Speeds of sounds, densities, isentropic compressibilities of the system (methanol + polyethylene glycol dimethyl ether 250) at temperatures from 293.15 to 333.15 K, J. Chem. Thermodyn. , 35(2003) 383.

4 George, J. and Sastry, N.V., Densities, excess molar volumes, viscosities, speeds of sounds, excess isentropic compressibilities and relative permitivities for CmH2m+1 (OCH2 CH2)n OH (m=1 or 2 or 4 and n=1) + benzene, + ethylbenzene and + cyclohexane, J.Chem. Eng. Data, 48(4) (2003) 977.

5 Pal,A. and Kumar, H., Temperature dependence of the volumetric properties of some alkoxypropanols + n-alkanol mixtures, J. Chem. Thermodyn., 36(2004)173.

6 Ali, A., Nain, A.K., Chand, D. and Lal, B., Molecular interactions in binary mixtures of anosole with benzyl chloride, chlorobenzene and nitrobenzene at 303.15 K : An ultrasonic, volumetric, viscometric and refractive index study, Indian J. Chem., 44A (2005) 511.

7 Ward, A., Moore, C., Anitha, V.,Wightman and Rogers, D. J., Identification of the sex pheromone of holotrichia reynaudi, J. Chem. Ecology, 28(2002) 515.

8 Rajkumar,X.R., Raman, K.V. and Arulraj, S.J., Isentropic compressibilities and excess volumes of binary systems of anisole with some aromatic compounds having different functional groups, J. Indian Chem. Soc.,LXII(1985) 516.

9 Nath, J. and Chaudhari, S.K., Excess volumes, dielectric constants,refractive indexes and viscosities for anisole + methyl chloride, 1,2-dichloroethane, trichloroethane, tetrachloroethane and cyclohexane, J. Chem.Eng.Data,37 (1992)387.

10 Jain,D.V.S.,North,A.M. and Pethrick, R.A., Adiabatic compressibility of binary liquid mixtures, J.Chem.Soc. Faraday Trans I, 70(1974)1292.

11 Nath, J. and Rashmi, Ultrasonic, dielectric and viscometric behaviour of binary systems: 1,4-dioxane with 1,2-dichloroethane, methylene chloride, trichlorohexane, J.Chem. Soc. Faraday Trans. I,86(20)(1990)3399.

Forthcoming Events:

1. **The 20th International Congress on Acoustics**
   Sydney, Australia
   23 - 27 August-2011

2. **International Congress on Ultrasonics, ICU 2011**
   Institute of Experimental Physics, University of Gdanks., Poland.
   05 - 08 September-2011

3. **IEEE International Ultrasonics Symposium 2011 (IUS-2011)**
   Caribe Royale, Orlando, Florida, USA
   18 - 21 October-2011

4. **National Symposium on Acoustics (NSA-2011)**
   Bundelkhand University, Jhansi-284128, Uttar Pradesh
   17 - 19 November-2011

5. **National Seminar and Exhibition on Non-Destructive Evaluation, NDE 2011**
   Chennai Chapter of the Indian Society for Non-Destructive Testing, Chennai, Tamil Nadu
   08 - 10 December-2011

6. **18th World Conference on Non-Destructive Testing**
   International Convention Center, Durban, South Africa
   16 - 20 April-2012

Condolence Message

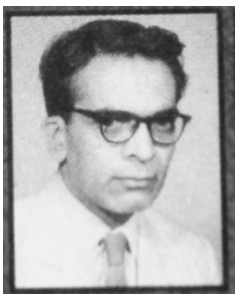

With heavy heart and profound grief we inform you that Dr M Pancholy has left for his heavenly abode on 19 June 2011. He was 95 years of age. Dr M Pancholy was the Deputy Director and Head of the Standards Division at National Physical Laboratory. He was the first Editor-in-chief of the J. Pure and Applied Ultrasonics. The Ultrasonics Society of India has constituted an award in his name as Dr M Pancholy Award. This award is given for the best oral paper presentation at the National Symposium of Ultrasonics, organized by the Society. A brief profile of Dr M Pancholy was published in the issue no.3 of vol. 30 (2008) of this journal.

On behalf of the J. of Pure and Applied Ultrasonics, we extend our deepest sympathies to the bereaved family of Dr Pancholy.

Journal of Pure and Applied Ultrasonics

VOLUME 33 NUMBER 3 JULY TO SEPT.- 2011

CONTENTS

Website : www.ultrasonicsindia.com

A Publication of — Ultrasonics Society of India

Information for authors

1. Type of Contribution

JOURNAL OF PURE AND APPLIED ULTRASONICS welcomes original research papers and articles related to the subject of ultrasonics. The contributions may be in the areas of physical ultrasonics, medical ultrasonics, ultrasonic non-destructive evaluation including NDT, high power ultrasonics, underwater acoustics, ultrasonic transducers, transducer materials & devices and any other related topic. These may fall into one of the following categories.

ResearchPapers **-** These should be on original research work contributing to scientific developments. They should be written with a wide readership in mind and should emphasize the significance of the work.

Reviews Articles **-** Includes critical reviews and survey articles.

Research and Technical notes **-** These should be short descriptions of new techniques, applications, instruments and components.

Letters to the editor **-** Letters will be published on points arising out of published articles and papers and on questions of opinion.

Miscellaneous **-** Miscellaneous contributions such as conference reports, Ph.D. thesis reviews and news items are also accepted. Recommended lengths of contributions are: Research papers 2000-4000 words, reviews articles 2000-5000 words; conference reports 500-1500 words; news items, research and technical notes up to 1000 words.

2. Manuscripts

Manuscripts should be typed on one side of the paper in double spacing with 25 mm margins on all side of A4 size paper. A soft copy of the manuscript in MS WORD for text and MS EXCEL for illustrations and a PDF file thereof may be sent by e-mail or CD/DVD. Colour images should be formatted as JPEG files. Figures submitted in colour would be published in colour. Colour should be avoided unless it is required in order to convey a message or serve a purpose in the image.

Title **-** Titles should be short and indicate the nature of the contribution. About 5 keywords may be given after the abstract.

Abstract **-** An abstract of 100-200 words should be provided on the title page of paper and review article. This should describe the full scope of the contribution and include the principal conclusions.

Mathematics **-** Mathematical expressions should be arranged to occupy the minimum number of lines consistent with clarity e.g., $(x^2+y^2)/(x-y)^{1/2}$

References **-** References should be indicated in the text by its number only. The reference number should be given as superscript. The corresponding reference shall contain the following information in order; names and initials of author(s)in bold, full title of the work, journal or book title in italic, volume number in bold, the year of publication in brackets and the page number. As example: Vasanth B.K., Palanichamy P., Jayakumar T. and Sankar B.N., Assessment of residual stresses in a carbon steel weld pad using critically refracted longitudinal (L_{CR}) waves, *J. Pure Appl. Ultrason*., 28 (2006) 66-72.

Units and Abbreviations **-** Authors should use SI units wherever possible.

3. Reprints

One copy of the issue in which the paper is published is sent to the author free of charges.

J. Pure Appl. Ultrason. 33 (2011) pp. 49-53

A novel method of ultrasonic antifouling

K. M.Swamy[1*]

Department of Applied Electronics and Instrumentation engineering,
Gandhi Institute of Engineering and Technology, Gunupur-765022, Orissa
[1]Formerly Scientist-G, CSIR
E-mail: kodavantiswamy617@gmail.com

Power ultrasound can provide the driving force for a wide range of industrial processing and other emerging applications in environmental protection and remediation. Seaweeds like algae cause fouling on the hull or other submerged ship parts. An overview of antifouling system that uses high frequency power ultrasound waves to destroy algae, therefore prevent weed and barnacle growth, is presented. Benefits of the system along with R&D gaps have been highlighted. Eventhough some versions are commercially available elsewhere in the world, still such units are yet to be developed in India.

Keywords: ultrasound, acoustic frequency, antifouling, algae.

Introduction

The present paper deals with a system and method for inhibiting growth of marine life on submerged surfaces which are exposed to seawater. More specifically it focuses on a device that can inhibit the growth of marine life using ultrasonic signals. Growth of marine organisms on submerged surfaces has long been a problem. These organisms, including barnacles, mussels, marine worms, corals, anemones, sponges, and algae, attach themselves to any exposed surface of boats, ships, docks and other submerged or partially submerged structures. When these organisms attach themselves to the hulls of ships or boats, their presence hastens the breakdown of the outer finish of the hull as well as detracting from the performance of effected vessel. Another major issue that is created by the unchecked growth of these marine organisms is that the vessels travelling significant distances unknowingly transport marine organisms from one area of the world to other areas, where the native marine life, including vital food sources, might be endangered by the introduction of new species or variety of organisms.

For boats and ships, probably the most common way of treating the build up of marine organisms, which happens quite rapidly when the vessel is moored or docked, is to have scuba divers scrape the submerged surface, such as the boat hull. Typically, this must be done every three to six weeks, and may be required even more frequently in tropical climates. Even with regular scraping, degradation of the surface of the hull make it is necessary to thoroughly clean and refinish or repaint the hull every few years. In order to accomplish this, the vessel must be removed from the water and placed in dry dock. All of these procedures can become quite expensive towards maintenance.

The scraping and refinishing procedures are often enhanced by utilizing specialized marine paints which kill or repel the organisms, or provide a surface to which the organisms have difficulty in firmly attaching. Typically, these paints contained tin or copper. However, as environmental regulations have become increasingly stringent, the use of most of these paints has been or will soon be prohibited. Such prohibition is primarily due to the harm these paints cause to the environment, particularly since their effectiveness arises from their toxicity to marine organisms.

A number of devices were fabricated and methods have been developed in the past as means for addressing the problem of the growth of marine organisms on boat hulls. Many of these devices are intended for use in conjunction with specialized marine paints, and thus, have not been required to rely entirely on their own effectiveness.

Scientific literature and patents on Ultrasonic Antifouling

The basic approach suggested would be, if the seaweed (seaweed is the generic name for under water algae) was prevented from attaching itself to the ship/boat hull in the first place, there would be no need to paint the various products on it. An alternate

physical method of antifouling is by the application of suitable frequency vibrations to the hull. Back in the 1970s, when a US Coastguard cutter was slipped for a refit, the shipyard was puzzled when they found that one area of hull was completely free of fouling. On investigation they found that it correlated to a sailor's cabin and that sailor was a hi fi enthusiast and had speakers mounted all round the cabin, including on the hull. Thus an antifouling system based on sonics was born. Sonic transducers glued on the inside of the hull designed to blast away fouling, though no-one used it long enough to ascertain its efficiency.

Acoustical shock waves are generated by electrical sparks within a gap between electrodes adjustably positioned for exposure to water adjacent to a surface immersed therein. In laboratory experiments, exposure to sound pulses (10.4 kHz) significantly increased marine antifouling for inhibiting the growth on a submerged surface[1]. Submersible ultrasonic emitter that can be integrated with scientific probes for measuring eg. dissolved oxygen, minimizes biofouling of the sensor membranes (Piedrahita and Wong 1999 in ref:1). Ultrasonic waves are also able to clean biofouled surfaces by detachment of the bacteria (Zips et al. 1990 in ref: 1).

The destruction of gas vacuoles brought about by ultrasonic irradiation has been tested in 32 ha lake over a period of 2 years. Incorporation of ultrasonification promoted close contact between cyanobacteria and their lysing Myxobacter leading to immediate and accelerated destruction of the cells[2]. Ultrasonic irradiation of 1.7 MHz and 20 kHz frequencies were applied separately to prevent cynobacteria spirulina platensis from bloom. Results indicated at both the frequencies gas vesicles in cells collapsed, but 5 min of 1.7 MHz ultrasonic irradiation every third day might be an effective and economic operation mode for practical application[3]. A study on growth inhibition of cynobacteria by ultrasonic radiation was conducted[4]. After 3 days of ultrasonification it was observed that the algal cell density and chlorophyll concentration drastically decreased. It would appear that ultrasonic radiation has considerable potential as an effective control method for cyanobacterial bloom, selectively[4] compared to other algal species. For a rapid control of blue-green algae (BGA) bloom, an ultrasonic frequency of 28 kHz, 120W was found more effective[5] than higher frequency of 100 kHz. Ultrasonic irradiation did not only collapse gas vacuoles and precipitated BGA, but may have also inflicted damage on the photosynthetic system of BGA[5]. 20 min of ultrasonic irradiation at 150 kHz and 30W, the removal rate of microcystins[6] (which are produced by bloom-forming algae) reached 70%.

Several patents on ultrasonic antifouling devices have been filed and some representative of them are presented in the foregoing.

An independent ultrasonic cleaning device for use in cleaning the hull exterior of a boat by robotic spraying was patented[7]. The device can only be used in dry dock. With a view to make surface clean, different ultrasonic frequencies were used[8]. The device moves along the hull exterior, but may be used while the hull remains in the water. While both of these devices facilitate currently-used methods of hull cleaning, neither one offers a preventive solution.

The use of an audible sound vibration to inhibit the growth of marine life on the outer surface of a submerged object is attempted[9]. This is achieved by the placement of speakers in the hull below the water line which are electrically driven to create vibrations which are thereby transmitted to the boat's hull. These vibrations, however, are in the audible frequency range, which have been found to be substantially ineffective in the inhibition of marine growth.

In order to prevent marine fouling[10] piezoelectric polymer antifouling coating method and use of application are patented[11]. They are similar in their application of a piezofilm to boat hulls. More specifically, both patents disclose the use of a piezofilm which is laminated over a significant portion of the hull's exterior surface and excited by an electrical signal applied through wires connected to the underside of the film. In this manner, virtually the entire surface of the hull can emit a uniform vibrating signal to repel marine organisms. A disadvantage of these methods, however, is that when refinishing of the outer surface of the hull is required, the piezofilm would likely be damaged or destroyed such that it would require complete replacement. Such replacement would, perhaps, be more costly and more time consuming than the periodic hull scrapings and refinishings. Another interesting work on a marine antifouling system and method for inhibiting growth of marine life on a submerged surface was patented[12]. The ultrasonic driver generates signals continually varying between 25 kHz and 60 kHz which are applied to the transducer for effective use.

Proposed Ultrasonic Antifouling system

A marine anti-fouling system has been conceived for inhibiting the growth of marine life on a submerged surface, which includes a control box and a number of transducers. The control box further includes an ultrasonic driver board, a magna-polar filter and a power source. The ultrasonic driver board generates an electrical signal having an ultrasonic frequency which continually varies between 25 KHz to 60 KHz. A portion of this continually varying electrical signal is passed through the magna-polar filter. This magna-polar filter includes a housing which contains an input piezoelectric transducer, a collector grid, and a copper loop between them. The piezoelectric transducer creates an ultrasonic signal of the same frequency as the electrical signal. Once created, the ultrasonic signal from the input piezoelectric transducer passes through the copper loop which is inductively coupled to a pair of diametrically opposed like-poled neodymium magnets. This induction causes an electromagnetic field to be generated around the copper loop. As a result of this field, the acoustic signal which passes through the loop becomes enhanced. This enhanced signal is then returned to the ultrasonic driver board where it is combined with the electrical signal varying between 25 KHz and 60 KHz. This combined signal is then electrically communicated to a number of transducers which are mounted on the submerged surface to be protected. There, the electrical signal having combined frequencies is translated from electrical energy to acoustic energy which it transmitted to the submerged surface as shown in Fig. 1 of the boat hull or other surface to be protected to inhibit the growth of marine life on the submerged surface.

The input piezoelectric transducer, copper loop and collector grid are contained within a housing, with the neodymium magnets disposed on opposite facing sides of the housing so that the north pole of each magnet is immediately adjacent the outer surface of the housing. The electrical signals entering and leaving the filter housing are transmitted along input wires and an output wire. These wires may be easily sealed into the housing wall making the filter housing water-tight. Such water-tightness is an important feature when placing the system in the hull of a boat below the waterline or in some other application where the system cannot be maintained in an entirely dry location. For boat and ship hulls, the transducers may be placed in a ring on a flat surface as shown in Fig. 2, around the interior of the hull below the waterline, with additional placements at, for example, the keel of a sailboat.

It is interesting to note that the transducer performance is not affected by water. However, it is vital that the surface to which it is to be attached is totally dry and free from grease when the epoxy is applied to the hull. The location of the transducer should be thoroughly cleaned and it should be on as flat a surface as possible in order to form an effective bond with the inside of the hull. Failure to do this will lessen the resonance and reduce the effectiveness of the system. Holding of transducer firmly in position via already fixed ring is shown in Fig. 3.

Working principle

The system then transmits the ultrasonic frequencies through the hull into the water. These ultrasonic waves cause the water around the submerged hull to vibrate and more at very high frequencies. In other words, the resonance created by

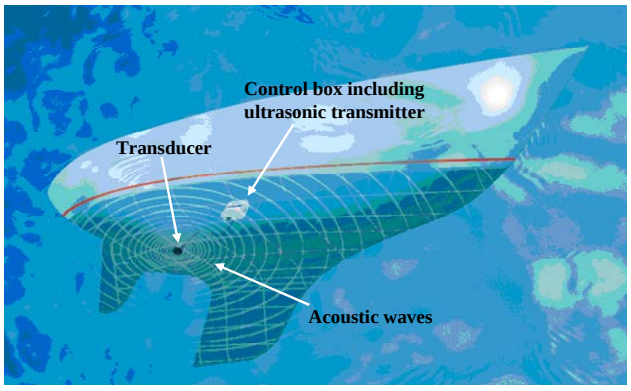

Fig. 1—Positioning of Ultrasonic transmitter and transducer to a boat hull.

Fig. 2—Positioning a ring to hold US transducer on a flat surface of boat hull.

Fig. 3—Ultrasonic transducer firmly screwed into the ring.

ultrasound forms a micro-thin layer of rapidly moving water which acts to blanket the hull and running gear, hence making it difficult for fouling organisms and algae to attach. Algae cannot survive in this environment. As a result no more algae fouling. Without the algae as a food source, barnacles, mussels, molluscs and other organisms will not attach to hull. Thus, ultrasound performs its job automatically without any toxic chemical action which could harm or endanger the marine environment. However, each transducer effectively covers at least a ten feet diameter. So the purpose of ultrasound to prevent the formation of biofilm and the growth of a sea-weed, barnacles.

Very recently ultrasonic anti-fouling for boats has been reported[13] specially to manoeuvre electronically the marine growth on boats. Further report[14] incorporates the encapsulation of the transducer as sometimes it is potentially lethal.

Commercial availability of ultrasonic systems

A new invention called Aquasonic has been developed that transmits ultrasonic vibrations through the water causing algae cells to implode and die and preventing reinfestation. Most algae are killed within 48 hours but thread algae may take a couple of weeks. There are devices for water ponds (freshwater) from 2-150 metre diameters. The device works on mains power and the transducer floats in the water. Since 1997, number of Aquasonic units (upto 2000) have been installed in The Netherlands and Belgium, mainly in freshwater water reservoirs used by market gardens . Of late many firms have started producing different types of sonic/ultrasonic frequency systems. They usually consume 20W to 80W power per unit. For large vessels/ships antifouling application use of multiple systems are suggested.

Field tests conducted using one of the systems over six months during May 2008 to Oct 2008 revealed that ultrasound has considerably reduced the infestation of barnacles and that the performance of the boat did not deteriorate significantly during the season. The ultrasonic system has proved to be effective in discouraging barnacles and other species causing marine fouling[15].

5. The Benefits of Ultrasonic antifouling:

i) Since ultrasonic antifouling device cleans the hull thoroughly, it enables the ship to maintain maximum speed. It will also keep clear all those underwater areas that are critical to the performance of a boat. i.e., speed log impellors, water intakes for engine and aircon units, props and running gear.

ii) The fuel savings will be substantial, particularly for motor boats. Pushing a heavily fouled hull through the water takes considerably more power than a clean one which has much less resistance. It can take up to 20% more fuel to push a dirty hull through the water.

iii) It will only fit once and it won't get covered by paint when painted. So one can look forward to more time on the water and less time in refit [cost effectiveness by reducing down-time] and annual maintenance. It will pay for itself in a very short time if one considers the cost of the lift in and out of the water, the cost of the antifoul and the cost of the person to apply the same.

iv) The ultrasonic device is easy to install because attaching to the hull with no skin fitting or dry docking required.

v) Environment friendly-as there are no pollutants associated with this method of preventative antifouling. It is also completely harmless to humans, marine or aquatic life.

vi) The other advantages are that antifouling coatings are not necessary.

vii) Keeps log, echo sounder and other equipment clean.

viii) Suitable for marine and freshwater and finally,

ix) The Ultrasonic antifouling system is totally effective whether it is powered by AC or DC. The unit uses very little power and will operate in exactly the same way.

R&D Gaps

(i) Acoustic devices hitherto available commercially are of analogue version technology which has

not received wide acceptability by the users as analogue uses up to 40% more power than digital systems. So a new ultrasonic antifouling system needs to be introduced that can provide the very latest digital technology.

(ii) The system developed should be capable of using an increased number of different frequencies simultaneously, which means it can destroy more species of algae. Algae develop in slightly different ways, so bombarding them with several frequencies will have a much greater effect than using fewer frequencies. Supplementing to this, digital operation produces a much clearer ultrasonic sound wave and has a much greater scale of frequency possibilities.

(iii) When the technology advances the very best thing about ultrasonic antifouling system should use a re-programmable chip that can modify the frequencies to suit the conditions. When the first GPSs were launched, they had 2 channel receivers and now multi channels are the norm. As the ultrasonic antifouling technology advances, it will be able to simply replace a chip at a nominal postage cost and continue to benefit from the most up to date system, without buying a new one every few years.

For ultrasonic antifouling device to be fully effective, position of the resonator is very important. Some keels may cause a "shadowing" effect which could reduce the effectiveness slightly on the outside of the keels. In such cases the new design should take care that extra resonator rings are fitted so that the resonator can be moved periodically so that the whole hull is exposed to the ultrasound over time.

Summary and Future trends

While this ultrasonic antifouling technology is new to the marine market, it is an established method used to prevent fouling in lakes, ponds, reservoirs and even greenhouses. However, the fact that one or more of these means has not been widely adopted indicates that they are not as effective as would be desirable to effectively eliminate the problems caused by the marine growths. Further, the apparent need to supplement these devices with anti-fouling paints leaves much to be desired. Therefore, the need still exists for an effective, economical device and method for inhibiting the growth of marine organisms which will gain wide acceptance for many marine applications if R&D gaps focused are incorporated without producing any environmentally harmful results. Undoubtedly ultrasonic antifouling unit has many benefits, can offer an environmentally friendly solution to an age old problem possibly in a cost effective way.

Acknowledgements

The author gratefully thanks D. Panda, Secretary and Dr. S.P. Panda, Chairman, Gandhi group of Institutions, Gunupur, Orissa for their constant encouragement and interest in this work.

References

1 McEnnulty, F.R., Jones, T.E. and Bax, N.J. (2001), The web-Based Rapid Response Toll Box., Web publication: http://crimp.marine. csiro.au /NIMPIS/controls.htm.

2 Lee,T.J., Nakano,K., and Matsumura,M., A novel strategy for cyanobacterial bloom control by ultrasonic irradiation, Water sci. Technol.2002;46(6-7)207-15.

3 Hao,H.,Wu,M.,Chen,Y.,Tang,J.,and Wu,Q., 'Cyanobacterial bloom control by ultrasonic irradiation at 20kHz and 1.7MHz'. J.Environ.Sci. Health 2004 Jun;39(6);1435-46.

4 Ahn,C.Y., Park,M.H., Joung,S.H., Kim,H.S., Jang,K,Y., and Oh,H,M., 'Growth inhibition of cynobacteria by ultrasonic radiation:laboratory and enclosure studies. Environ. Sci. technol.2003 Jul 1;37(13)3031-7.

5 Lee,T,J.,Nakano,K.,and Matsumara, M., 'Ultrasonic irradiation for blue-green algae bloom control', Environ.Technol.2001 April; 22(4):383-90.

6 Ma.B., Chen,y., Hao,H., Wu,M., Wang, B., Lv,H and Zhang,G., 'Influence of ultrasonic field on microcystins produced by bloom-forming algae' Colloids Sur. B Biointerfaces. 2005Mar25; 41(2-3):197-201.

7 Caduff, E. A., 'Robotic ultrasonic cleaning and spraying device for ships' hulls', U.S. Pat. No. 4,890,567. 2 Jan 1990.

8 De Witz, G.H. and Yaeger,B.W., 'Ultrasonic subsurface cleaning also uses ultrasonic frequencies' U.S. Pat. No. 4,444,146., 24April1984.

9 Piper.Sr., and Donald,R.,'Marine life growth inhibitor device,' U.S. Pat. No. 4,058,075., 15Nov1977.

10 Murphy,P.V.,and Latour,M.J., 'Preventing marine fouling' U.S. Pat. No. 4,170,185., 9 Oct,1979

11 Wooden, B.J., and Edelman, S.,'Piezoelectric polymer antifouling coating and method of use and application', U.S. Pat. No. 4,297,394.,27 Oct,1981.

12 Mc Neal.,and Patrick,G.,'Marine anti-fouling system and method', U.S. Pat. No. 5,735,226., April 7, 1998.

13 Simpson, L and Clarke, J, 'Ultrasonic Anti-Fouling Unit For Boats, pt-1', Silicon Chip online, Issue 264, 7Sept 2010.

14 Simpson, L 'Ultrasonic Anti-Fouling Unit For Boats, pt-2', Silicon Chip online, Issue 266, 22 Nov 2010.

15 Eshelby-Burnham, A report on the effectiveness of the ultrasonic antifouling system, 19 Feb, 2009.

J. Pure Appl. Ultrason. 33 (2011) pp. 54-58

Non linear elastic properties and ultrasonic attenuation in Ni-Al-Cr alloy

Giridhar Mishra[1], R.R.Yadav[1]*, Baldev Raj[2]*, T. Jayakumar[2]

[1]Physics Department, University of Allahabad, Allahabad-211002, India

[2]Indira Gandhi Centre for Atomic Research, Kalpakkam-603102, India

E-mail: giridharmishra@rediffmail.com

The single crystal higher order elastic constants of Ni-Al-Cr ternary alloy at different temperatures have been calculated with the help of interaction potential model. Ultrasonic attenuation in the ternary alloy is determined using higher order elastic constants. Other ultrasonic parameters such as Gruneisen numbers, acoustic coupling constants and acoustical anisotropy have been also calculated to discuss the ultrasonic properties of the ternary alloys. The ultrasonic wave propagation behavior at different temperatures for Ni-Al-Cr alloy have been investigated and correlated with respect to the microstructural phenomena during the wave propagation and thermal behavior of the ternary alloy. An ultrasonic mechanism has been developed to correlate the temperature dependent ultrasonic properties with the thermophysical properties particularly the thermal conductivity of the alloy. The results are compared with earlier studies of the elastic constants and are found to be in good agreement. We find that the thermal conductivity of Ni-Al-Cr alloy plays important role in the ultrasonic wave propagation behavior inside the alloy.

Keywords: ternary alloy, elastic constants, ultrasonic attenuation, thermal properties

1. Introduction

In recent years binary and ternary alloy systems received much attention due to their various useful properties[1,2]. NiAl is well known shape memory alloy having high thermal conductivity[3,4]. For higher temperature applications nickel aluminide has been considered as base material to replace nickel-based super alloys[5]. By alloying we can improve the interesting properties of NiAl. There are various features of nickel aluminides based ternary alloys[6] which make the ternary alloy very useful for various advanced applications such as in making gas turbine and aircraft engines[7,8] It is important to study the mechanical properties of alloys for applications at elevated temperatures. Our main work is focused to develop a theory for the evaluation of second and third order elastic constants (SOEC and TOEC) and ultrasonic attenuation in the alloys and to correlate it with the thermal conductivity of the alloys at high temperatures. The ultrasonic properties are well correlated to micro structural and thermophysical properties of the materials[9-12]. Measurement of ultrasonic attenuation in alloys is very useful in order to characterize the materials. Present paper is concerned with the theoretical estimations of anharmonic higher order elastic constants and ultrasonic properties of the Ni-Al-Cr alloy. The calculations have been done for the $Ni_{50.0}$-$Al_{48.0}$-$Cr_{2.0}$ ternary alloy. The ultrasonic attenuation, thermal relaxation time, ultrasonic velocity and non linearity parameters in the ternary single crystal NiAl-Cr are calculated in the temperature range 300-1000K along <100> direction.

2. Theory

The obtained expression for second and third order elastic constants at 0K using above equations are[13-15]

$$\left.\begin{aligned}
C_{11}^0 &= \frac{3}{8}\frac{e^2}{r_0^4}S_5^{(2)} + \frac{3\phi(r_1)}{br_0}\left(\frac{\sqrt{3}}{3r_0}+\frac{1}{b}\right) + \frac{2\phi(r_2)}{br_0}\left(\frac{1}{2r_0}+\frac{1}{b}\right)\\
C_{12}^0 &= C_{44}^0 = \frac{3}{8}\frac{e^2}{r_0^4}S_5^{(1,1)} + \frac{\phi(r_2)}{br_0}\left(\frac{1}{2r_0}+\frac{1}{b}\right)\\
C_{111}^0 &= -\frac{15}{8}\frac{e^2}{r_0^4}S_7^{(3)} - \frac{\phi(r_1)}{9b}\left(\frac{\sqrt{3}}{r_0^2}+\frac{3}{br_0}+\frac{\sqrt{3}}{b^2}\right) - \frac{\phi(r_2)}{2b}\left(\frac{3}{r_0^2}+\frac{6}{br_0}+\frac{4}{b^2}\right)\\
C_{112}^0 &= C_{166}^0 = -\frac{15}{8}\frac{e^2}{r_0^4}S_7^{(2,1)} - \frac{\phi(r_1)}{9b}\left(\frac{\sqrt{3}}{r_0^2}+\frac{3}{br_0}+\frac{\sqrt{3}}{b^2}\right)\\
C_{123}^0 &= C_{456}^0 = C_{144}^0 = -\frac{15}{8}\frac{e^2}{r_0^4}S_7^{(1,1,1)} - \frac{\phi(r_1)}{9b}\left(\frac{\sqrt{3}}{r_0^2}+\frac{3}{br_0}+\frac{\sqrt{3}}{b^2}\right)
\end{aligned}\right\} \quad (1)$$

where $\phi(r_1) = A\exp(-r_1/b)$, $\phi(r_2) = A\exp(-r_2/b)$, $r_1 = \sqrt{3}r_0$, $r_2 = 2r_0$ and S is the lattice sum[29]. The value of A can be obtained with the equilibrium condition and is given as:

$$A = (bZ_0e^2/r_0^2)\left[8\sqrt{3}\exp(-r_1/b) + 12\exp(-r_2/b)\right] \quad (2)$$

The elastic constants due to vibrational free energy component is given by[30]:

*Life Fellow, Ultrasonics society of India.

$$C^{Vib}_{IJK....} = a_{IJK...}T \quad (3)$$

Here

$$a_{IJK...} = l_1 k_B \left|\frac{\partial C^0_{IJK....}}{\partial r}\right|_{r=r_o} + \frac{f^{Vib}_{IJK...}}{V_0 c},$$

$$l_1 = -r_0\left[\left\{\frac{8}{3}\left(2y_1 + 2y_1^2 - y_1^3\right)\phi(r_1)\right\} + \left\{\frac{3}{2}\left(2y_2 + 2y_2^2 - y_2^3\right)\phi(r_2)\right\}\right]Y^{-1} \quad (4)$$

$$Y = \left[\left\{\frac{8}{3}\left(y_1^2 - 2y_1\right)\phi(r_1)\right\} + \left\{\frac{3}{2}\left(y_2^2 - 2y_2\right)\phi(r_2)\right\}\right] \left[\left\{\frac{8}{3}\left(y_1^2 - 2y_1\right)\phi(r_1)\right\} + \left\{2\left(y_2^2 - 2y_2\right)\phi(r_2)\right\}\right] \quad (5)$$

where $y_1=r_1/b$, $y_2=r_2/b$, k_B is the Boltzmann constant and $f^{Vib}_{IJK...}$ is the vibrational free energy per unit cell[29]. Using above expressions, the vibrational part of elastic components have been calculated by eqn.(3), whose addition to static part of elastic constants gives the elastic constants at a particular temperature.

For the evaluation of ultrasonic attenuation coefficient, we have used the phonon-phonon interaction mechanism given by Mason and Bateman[17,18]. It is more genuine theory for studying the anharmonicity of crystals as it directly involves elastic constants through non-linearity parameters D in the evaluation of ultrasonic attenuation coefficient α. The ultrasonic attenuation over frequency square $(\alpha/f^2)_{Akh}$ (Akhieser type loss) due to phonon- phonon interaction mechanism at $\omega\tau<<1$ is given in previous work[19].

3. Results and discussion

Evaluations of higher order elastic constants (SOEC and TOEC) in the temperature range 300-1000K have been done using eqns. (5) and (7). Values of SOEC and TOEC for NiAl-Cr at different temperatures are presented in Tables 1, 2. Thermal conductivity (K) data at different temperatures are taken from the literature[20]. The values of specific heat per unit volume (C_V) and thermal energy density (E_0) are evaluated using physical constant Table and Debye temperature [35] and are presented in Table 3.

The ultrasonic longitudinal and shear wave velocities are calculated using SOEC. Thermal relaxation time (τ) and Debye average velocity using eqn.(13) at different temperatures[19]. The values of longitudinal, shear wave velocities, Debye average velocity (V_D) and thermal relaxation time (τ) at different temperatures are shown in Table 4. The Gruneisen parameters are calculated using SOEC and TOEC in the temperature range 300-1000K. The values of Gruneisen parameters, acoustic coupling constants for longitudinal (D_L) and shear wave (D_S) are presented in Table 5. The ultrasonic attenuation coefficient over frequency square $(\alpha/f^2)_{Akh}$ for longitudinal and shear wave and thermoelastic loss over frequency square $(\alpha/f^2)_{Th}$ are calculated. The calculated values of attenuation for different types of losses are plotted in Figs. 1-2. The temperature dependent variation of anisotropy is shown in Fig. 3.

Applying the interaction potential model the calculated values of shear modulus $C'= (C_{11}-C_{12})/2$, C_{44} and bulk modulus $B= (C_{11}+2C_{12})/3$ are 113.49 GPa, 65.26 GPa and 107.50 GPa respectively at the room temperature. C. Jiang et.al.[9] calculated the values C′=118 GPa, C_{44}=77GPa and B=85 GPa by first principle calculations. Thus there is a good agreement between the values calculated by our

Table 1— SOEC (10^{10}N/m^2) of NiAl-Cr in the temperature range 300K to 1000K.

SOEC →T. [K]↓	C_{11}	C_{12}	C_{44}
300	25.88	3.18	6.53
400	25.98	3.18	6.71
500	26.07	3.18	6.90
600	26.17	3.18	7.09
700	26.26	3.18	7.28
800	26.36	3.17	7.46
900	26.46	3.17	7.65
1000	26.55	3.17	7.84

Table 2— TOEC (10^{10}N/m^2) of NiAl-Cr in the temperature range 300K to 1000K.

TOEC→T. [K]↓	C_{111}	C_{112}	C_{123}	C_{144}	C_{166}	C_{456}
300	-196.11	-96.51	-80.89	-59.40	-64.71	-79.06
400	-188.43	-97.12	-78.63	-49.98	-54.73	-76.19
500	-180.76	-97.74	-76.37	-40.56	-44.74	-73.23
600	-173.08	-98.34	-74.11	-31.14	-34.76	-70.45
700	-165.39	-98.96	-71.85	-21.71	-24.77	-67.58
800	-157.72	-99.57	-69.59	-12.29	-14.79	-64.72
900	-150.04	-100.19	-67.33	-2.87	-4.81	-61.85
1000	-142.36	-100.79	-65.07	-6.55	-5.18	-58.97

Table 3— Thermal Conductivity (K), density (ρ), specific heat per unit volume (C_V) and thermal energy density (E_0) of NiAl-Cr in the temperature range 300-1000K.

T [K]	K (J/s. m. K)	ρ (10^3Kg/m^3)	C_V x 10^6 (J/m^{3}K)	E_0 x 10^8 (J/m^3)
300	4.11	5.896	9.73	1.85
400	4.67	5.889	10.18	2.85
500	5.44	5.881	10.35	3.86
600	5.89	5.874	10.41	4.89
700	6.11	5.867	10.47	5.93
800	6.56	5.859	10.51	6.96
900	6.89	5.852	10.55	8.02
1000	8.99	5.845	10.54	9.07

Table 4— Ultrasonic velocities (V_L, V_S, Debye average velocity (V_D) in10^3m/s) and thermal relaxation time (τ) (in 10^{-13} Sec) in NiAl-Cr in the temperature range 300-1000K.

T[K]	V_L	V_S	V_D	τ
300	6.626	3.327	3.684	93.42
400	6.642	3.377	3.736	98.50
500	6.659	3.426	3.787	110.01
600	6.675	3.474	3.838	115.22
700	6.691	3.522	3.888	115.85
800	6.708	3.569	3.937	120.73
900	6.724	3.617	3.986	123.29
1000	6.741	3.663	4.034	122.45

Table 5— Average Grüneisen number $\langle\gamma_i^j\rangle_L$ for longitudinal wave, average square Grüneisen number $\langle(\gamma_i^j)^2\rangle_L$ and $\langle(\gamma_i^j)^2\rangle_S$ for longitudinal and shear wave and acoustic coupling constant for longitudinal (D_L) and shear (D_S) waves for NiAl-Cr from 300-1000K.

T (K)	$\langle\gamma_i^j\rangle_L$	$\langle(\gamma_i^j)^2\rangle_L$	$\langle(\gamma_i^j)^2\rangle_S$	D_L	D_S
300	1.038	4.669	2.833	36.916	25.499
400	0.866	3.187	2.312	25.472	20.806
500	0.701	2.082	1.875	16.762	16.872
600	0.543	1.302	1.515	10.589	13.634
700	0.393	0.805	1.226	6.670	11.032
800	0.249	0.552	1.002	4.741	9.015
900	0.111	0.511	0.837	4.556	7.535
1000	0.022	0.655	0.728	5.893	6.548

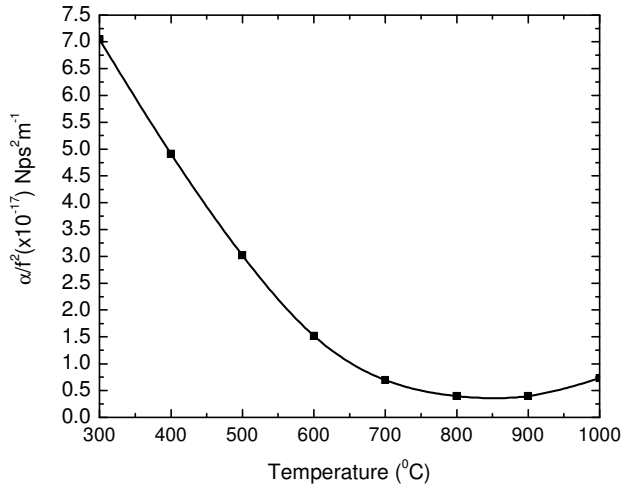

Fig. 1—Variation of ultrasonic attenuation due to thermoelastic loss $(\alpha/f^2)_{th.}$ with temperature

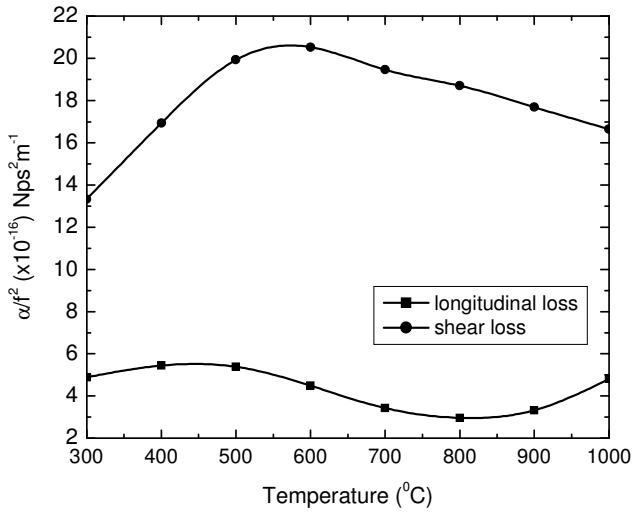

Fig. 2—Variation of ultrasonic attenuation due to phonon-phonon interaction for longitudinal and shear waves $(\alpha/f^2)_{Akh.long}$ and $(\alpha/f^2)_{Akh.shear}$ with temperature

interaction potential model approach and other workers. In the present calculations C_{111} is negative. The value of C_{111} for CsCl and Al is negative[16,22]. We can say that our theory for the calculation of the higher order elastic constants is justified. Bulk modulus of NiAl-Cr is 107.50 GPa and that is 158.5GPa for NiAl[23,24]. Thus the present alloy is more ductile at 300K due to ternary addition of Cr. The ratio $A=2C_{44}/(C_{11}-C_{12})$ is the measure of elastic anisotropy in the crystal. The temperature dependent variation of A for NiAl-Cr is shown in Fig.3. The values of A for the alloy NiAl-Cr is 0.575 while the value of A for NiAl is ≈0.33[25]. Hence by proposing that high value of anisotropy favors stability, we may say that NiAl-Cr is more stable than NiAl at room temperature. Also the value of A increases with the temperature implying the stability of the NiAl-Cr

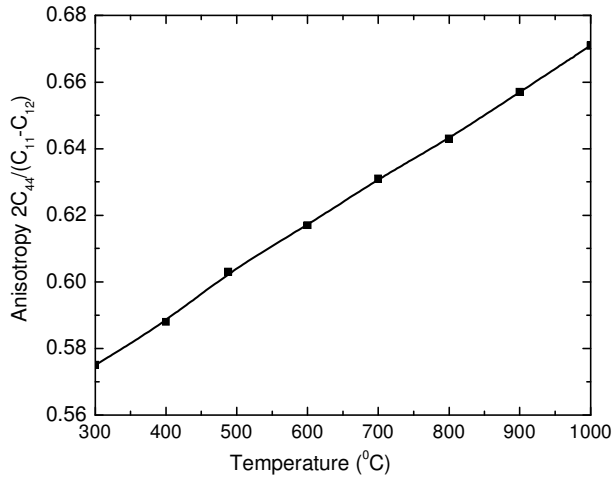

Fig. 3—Elastic anisotropy variation with temperature

alloy at higher temperatures. Hence the applicability of the ternary alloy NiAl-Cr enhances at higher temperatures. A perusal of Fig.1 shows that the ultrasonic attenuation due to thermal relaxation process decreases rapidly from 300K to 800K then it gradually increases form 800K to 1000K. Fig. 1 reveals that ultrasonic attenuation due to thermoelastic loss is mainly affected by the elastic constants through Gruneisen parameters as the bulk modulus of NiAl-Cr decreases compared to NiAl with the ternary addition[24]. The ultrasonic attenuation due to phonon-phonon interaction (Akhiezer type loss) for longitudinal wave increases slightly up to 500K then it starts decreasing up to 800K and above 800K its value increases for higher temperatures (Fig. 2). Also we can observe that the ultrasonic attenuation due to phonon-phonon interaction for shear wave increases from 300K to 600K then it starts decreasing slightly (Fig. 2). Thus the behavior of ultrasonic attenuation at 800K is very interesting for the ultrasonic attenuation due to thermal relaxation process as well as phonon-phonon interaction for longitudinal wave. The ductile to brittle transition temperature (DBTT) for the alloy NiAl-Cr is not known but on the basis of DBTT of NiAl[8] we can correlate such behavior of ultrasonic attenuation. NiAl is brittle at room temperature for both polycrystalline and single crystal forms and ductile at high temperatures. It is noteworthy that DBTT is only 625-700K in different single crystals[8]. In the case of the alloy NiAl-Cr, the ultrasonic attenuation decreases rapidly up to 800K. As in the case of NiAl there is an abrupt increase in the ductility in NiAl over a small range of temperature near DBTT, the variation of ultrasonic attenuation seems to predict the abrupt change in ductility near DBTT. Yield strength of NiAl decreases from 900K[8] and the ultrasonic attenuation in the case of NiAl increases nearly from this temperature. In similar way on the basis of the variation of ultrasonic attenuation in NiAl-Cr we can predict that yield strength decreases from 800K as the ultrasonic attenuation starts increasing above 800K. The acoustic coupling constants (D_L and D_S) contribute to the temperature variation of ultrasonic attenuation. The acoustic coupling constant depends on elastic constants through Gruneisen parameters, specific heat per unit volume and thermal energy density. In Table III one can observe that the thermal energy density increases almost linearly with temperature. So the behavior of the variation of ultrasonic attenuation is also affected by the thermal energy density. The variation of thermal conductivity with temperature (Table III) affects the ultrasonic attenuation in Ni-Al-Cr. Such type of temperature dependency of ultrasonic attenuation due to thermal relaxation process can be correlated with the behavior of temperature dependent thermal conductivity of the material as the thermal conductivity increases linearly with temperature[20].

4. Conclusions

1. The interaction potential model for evaluation of higher order elastic constants successfully explains the elastic properties of NiAl-Cr alloy justifying the results obtained from other workers.
2. The Bulk modulus decreases for NiAl-Cr as compared to NiAl. This reveals that NiAl-Cr is more ductile than NiAl.
3. The ultrasonic attenuation in NiAl-Cr is predominantly affected by phonon–phonon interaction in the temperature range 300-1000 K.
4. The variation of thermal conductivity with temperature significantly affects the elastic and ultrasonic properties of NiAl-Cr alloy.
5. The elastic anisotropy behavior shows that the stability of alloy increases at higher temperatures.

Acknowledgement:

The authors are grateful to the Department of Science and Technology, Govt. of India (DST project no. SR/S2/CMP-0069/2006) for the financial support to carryout the work.

References

1. Scudino, S., Donnadieu, P., Surreddi, K.B., Nikolowski, K., Stoica, M., and Eckert, J., Microstructure and mechanical properties of Laves phase-reinforced Fe–Zr–Cr alloys, *Intermetallics,* 17 (2009) 532.

2. Delsante, S., Raggio, R., and Borzone, G., Phase relations of the Sm–Ni–Al ternary system at 500 °C in the 40–100 at.% Al region, *Intermetallics,* 16 (2008) 1250.
3. Lazarev, N.P., Abromeit, C., Schaublin, R., and Gotthardt, R., Temperature-controlled martensitic phase transformations in a model NiAl alloy, *J. Appl. Phys.,* 100 (2006) 063520.
4. Landa, M., Novak, V., Sedlak, P., and Sittner, P., Ultrasonic characterization of Cu–Al–Ni single crystals lattice stability in the vicinity of the phase transition, Ultrasonics, 42 (2004) 519.
5. Yoon, K.E., Noebe, R.D., and Seidman, D.N., Effects of rhenium addition on the temporal evolution of the nanostructure and chemistry of a model Ni–Cr–Al superalloy. I: Experimental observations, *Acta Mater.,* 55 (2007) 1145.
6. Duan, Y., Li, J., Li, S., and Xia, J., Elasticity, band-gap bowing, and polarization of $Al_xGa_{1-x}N$ alloys, *J. Appl. Phys.,* 103 (2008) 023705.
7. Moser, M., Mayrhofer, P.H., Ross, I.M., and Rainforth, W.M., Microstructure and mechanical properties of sputtered intermetallic Al–Au coatings, *J. Appl. Phys.,*102 (2007) 023523.
8. Darolia, R., NiAl alloys for high-temperature structural applications, *J. Metals,* 43 (1991) 44.
9. Jiang, C., and Gleeson, B., Effects of Cr on the elastic properties of B2 NiAl: A first-principles study, *Scripta Materialia,* 55 (2006) 759.
10. Decremps, F., Belliard, L., Perrin, B., and Gauthier, M., Sound velocity and absorption measurements under high pressure using picosecond ultrasonics in a diamond anvil cell: Application to the stability study of AlPdMn, *Phys. Rev. Lett.,*100 (2008) 035502.
11. Pandey, D.K., Singh, D., and Yadav, R.R., Ultrasonic wave propagation in IIIrd group nitrides, *Appl. Acoust.,* 68 (2007) 766.
12. Pandey, D.K., Yadawa, P.K., and Yadav R.R., Acoustic wave propagation in Laves-phase compounds, *Mater. Lett.,* 61 (2007) 4747.
13. Brugger, K., Third-order elastic constants and the velocity of small amplitude elastic waves in homogeneously stressed media, *Phys. Rev.,*133 (1964) A1611.
14. Yadav, R.R., and Singh, D., Ultrasonic attenuation in lanthanum monochalcogenides, *J. Phys. Soc. Japan,* 70 (2001) 1825.
15. Yadav, R.R., and Pandey, D.K., Size dependent acoustical properties of bcc metal, *Acta Phys. Pol.A,* 107 (2005) 933.
16. Ghate, P.B., Third-order elastic constants of alkali halide crystals, *Phys. Rev.,* 139 (1965) A1666.
17. Mason, W.P., Physical Acoustics, Vol.III B, Academic Press, New York,1965:237.
18. Mason, W.P., and Bateman, T.B., Relation between third-order elastic moduli and the thermal attenuation of ultrasonic waves in nonconducting and metallic crystals, *J. Acoust. Soc. Am.,* 40 (1966) 852.
19. Yadav, R.R., and Singh, D., Effect of thermal conductivity on ultrasonic attenuation in praseodymium monochalcogenides, *Acoust. Phys.,* 49 (2003) 595.
20. Terada, Y., Ohkubo, K., Mohri, T., and Suzuki, T., Effects of ternary additions on thermal conductivity of NiAl, *Intermetallics,* 7 (1999) 717.
21. Gray, D.E., AIP Handbook, 3rd edition,Mc Graw Hill Co. Inc., New York, 1956.
22. Lincoln, R.C., Koliwad, K.M., and Ghate, P.B., Morse-potential evaluation of second- and third-order elastic constants of some cubic metals, *Phys. Rev.,* 157 (1967) 463.
23. Davenport, T., Zhou, L., and Trivisonno, J., Ultrasonic and atomic force studies of the martensitic transformation induced by temperature and uniaxial stress in NiAl alloys, *Phys. Rev. B,* 59 (1999) 3421.
24. Lazar, P., and Podloucky, R., *Ab initio* study of the mechanical properties of NiAl microalloyed by X=Cr,Mo,Ti,Ga, *Phys. Rev. B,* 73 (2006) 104114.
25. Pandey, D.K., Ph.D. thesis, Allahabad University, Allahabad, India (2005).

J. Pure Appl. Ultrason. 33 (2011) pp. 59-62

Miscibility studies of Acacia/Poly (vinyl pyrrolidone) and Acacia /Poly (ethylene glycol) blends in water at 30°C using ultrasonic studies

HMP. Naveen Kumar[1], K. Madhusudhana Rao[2*], M.N. Prabhakar[1], K. Chowdoji Rao[1] and M.C.S. Subha[2*]

[1]Department of Polymer Science & Tech., Sri Krishnadevaraya University, Anantapur, AP, India
[2] Department of Chemistry, Sri Krishnadevaraya University, Anantapur, A.P, India

The miscibility of Acacia (AC)/Poly (vinyl pyrrolidone) (PVP) and Acacia (AC) / Poly (ethyleneglycol) (PEG) blends in water at 30^0C were studied using ultrasonic velocity and density measurements. The results of ultrasonic velocity and the derived acoustical parameters such as adiabatic compressibility (β_{ad}) and acoustic impedance (Z) have been used to discuss the miscibility/immiscibility of the blends under study. The conclusions drawn from these results indicate that AC/PVP blends are miscible whereas AC/PEG blends are immiscible. The miscible/immiscible nature of these two blends may be attributed to the intermolecular interactions between the constituent polymers. These investigations offer an entirely new and simple approach to study the compatibility of the polymer blends, which is in general obtained by the sophisticated techniques of thermal, dynamic, mechanical and electron microscopic analysis.

Keywords: Miscibility, Acacia (AC), Poly (vinylpyrrolidone) (PVP), Poly (ethylene glycol) (PEG), density, ultrasonic velocity.

1. Introduction

The importance of polymer blending has increased in recent years, because of the preparation of new polymeric materials with desired properties, low basic cost and improved processability. Polymer blends are physical mixtures of structurally different polymers or co-polymers, which interact through secondary forces with no covalent bonding[1] that are miscible at molecular level. The basis of polymer-polymer miscibility may arise from any specific interaction, such as hydrogen bonding, dipole-dipole forces and charge transfer complexes for homo polymer mixtures[2-3]. There have been various techniques of studying the miscibility of the polymer blends[4-5]. Some of these techniques are complicated, costly and time consuming. Hence, it is desirable to identify simple, low cost and rapid techniques to study the miscibility of polymer blends. Singh and Singh[6] have suggested the use of ultrasonic velocity and viscosity measurements for investigating the polymer miscibility in solution. Rai *et al.,*[7] *and* Basavaraj *et al.*[8] have shown that the variation of ultrasonic velocity and acoustical derived parameters with blend composition is linear for miscible blends and non linear for immiscible blends. Recently, Chowdoji Rao *et al*.,[9] have used ultrasonic technique to study the miscibility of polymer blends. In order to prepare the biodegradable polymer blends by blending natural polymer with synthetic polymers, which will be useful for producing environmental pollution free materials, in the present study, Acacia is chosen as the natural polymer because of its innumerable applications. It is a genius of shrubs and trees of Gondwanian origin belonging to the sub family Mimosrideae of the papea family[10].

Structural Unit of Acacia: On the basis of the spectral studies and on the basis of the literature, Defaye and Wong *et al.,*[11] from their studies concluded that Acacia possess an internal (1-3) β-D-galactic core, with (1-6) β-D-galactopyranosyl branches and side chains of α-L-arabinofuranosyl-(1-3) α-L-arabino-furanosyl-uronic acid groups rhamnopyranosyl (1-4)-β-D-glucopyranosyl-uronic acid groups linked respectively at positions 3 and 6 of the galactosyl branch unit (see Scheme. 1)

Acacia senegal on hydrolysis yielded 27% arabinose, 44% galactose, 13% rhamnose and 14% glucuronic acid and the core was found to consists of a β-(1-3)-galactopyranose chain with branches linked through the 1,6 positions[12].

As Acacia, PVP and PEG both have been used in many applications such as pharmaceuticals, textiles, cosmetics etc., and their blends are prepared in water and their miscibility is studied by measuring physico chemical properties such as ultrasonic velocity and density and the results are presented here.

*Life member, Ultrasonic Society of India

2. Experimental

Materials and Methods

Acacia (Mol.wt. 2,50,000) from s.d. fine chemicals, Mumbai, PVP (Mol.wt 40,000) and PEG (Mol.wt. 50,000) from Himedia Laboratories, Mumbai were procured and used in the present study as supplied without any further purification.

The blends of AC/PVP and AC/PEG with 1:1 ratio of AC/PVP and AC/PEG blends over a wide range of concentrations in water have been prepared by mixing solutions of the polymers in water at 30°C. The total weight of the two components in the solution is always maintained 1.0 g/dL. Double distilled fresh water (Specific conductivity. 4×10^{-6} ohm. cm^{-1}) was used for preparing the polymer blend solutions.

The ultrasonic velocity was determined using a single crystal ultrasonic interferometer (M/s. Mittal Enterprises, New Delhi) at a frequency of 2.0 MHz with a thermostat water circulation system and the reproducibility of the velocity measurements were with in ±2.0 ms^{-1}.

The densities were measured using a specific gravity bottle of 10 ml with an accuracy of about ±0.1% Kg m^{-3}. Weight measurements in the present case were made employing a single pan electronic balance capable of measuring upto 0.5 mg.

All the above measurements were carried out with a water circulation system from a thermostat with a stability of ±0.1K maintaining a constant temperature at 30±0.05°C.

Structure of Carbohydrate Component of *Acacia senegal*

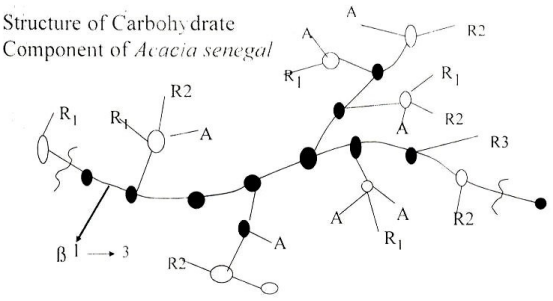

A = Arabinosyl; ● = 3-linked Gal*p* (Gla*p* attached); ❍ = 6-linked Gal*p* (Gal*p* or Glc*p*A attached), or end-group; R_1 = Rha→4 GlcA (Rha occasionally absent, or replaced by Me, or by Ara*f*); R_2 = Gal → 3 Ara; R_3 = Ara → 3 Ara → 3 Ara...

Scheme 1

3. Results and Discussion

To investigate the miscibility/immiscibility nature of these polymer blends, the authors have measured the Ultrasonic velocity and density for Acacia, PVP, PEG and different concentrations of 1:1 ratio of AC/PVP and AC/PEG blends in water at 30°C.

For further analysis of the above ultrasonic results, the derived parameters such as adiabatic compressibility (β_{ad}), acoustic impedance (Z), are calculated by using the experimentally determined ultrasonic velocity and density with the help of the following equations and the data obtained are included in Table 1.

$$\beta_{\alpha\delta} = 1/\rho v^2 \quad \ldots (1)$$

where '*v*' is the ultrasonic velocity and 'ρ' is the density. The units of 'β_{ad}' are (cm^2 dyne-1). The variation of 'β_{ad}' with concentration is widely used to reveal the molecular interactions in polymer solutions.

$$M_{12} = M_1X_1 + M_2X_2 \quad \ldots (2)$$

Table 1—Density (ρ), Ultrasonic velocity (*v*), Adiabatic compressibility (β_{ad}) and Acoustic impedance (Z) for 1:1 ratio of AC/PVP and AC/PEG blends in water at 30°C.

Conc. C (g.dl)	Density $\rho\ 10^3$ (kg/m^3)	Ultrasonic velocity *v* x 10^{-2} (m/s)	Adiabatic Compressibility β_{ad} x 10^{10} (m^2/N)	Acoustic Impedance Z x 10^3 (kg/m^2 s)
		AC/PVP		
0.1	0.99523	1502.8	4.4491	1495.63
0.2	0.99524	1510.4	4.4044	1503.21
0.4	0.99599	1520.5	4.2756	1526.26
0.6	0.99638	1521.6	4.3348	1531.00
0.8	0.99731	1525.6	4.2499	1531.87
1.0	0.99786	1514.0	4.3719	1510.76
		AC/PEG		
0.1	0.99479	1540.2	4.2375	1532.18
0.2	0.99492	1503.4	4.4469	1495.76
0.4	0.99512	1452.0	4.4614	1493.48
0.6	0.99541	1520.2	3.5200	1592.00
0.8	0.99571	1631.0	4.3675	1509.89
1.0	0.99601	1528.5	4.2974	1522.40

where 'M_1', and 'M_2' are the molecular weights and 'X_1' and 'X_2' are mole fractions of the solvent and polymer/polymer blend respectively. The units for 'β' are (cm^3/mole) (cm^2/dyne).$^{-1/7}$

$$Z = \rho v \quad \ldots (3)$$

where (Z) is the Acoustic impedance

The plots showing the typical variation of *v*, β_{ad} and Z vs. concentration of 1:1 ratio of AC/PVP and AC/PEG blend solutions are shown in Figs 1-3 and 4-6 respectively.

It was well established[13,14] that for a miscible blend ultrasonic velocity (*v*) and other parameters β_{ad} and Z vary linearly with polymer blend concentration and for an immiscible blend it varies non-linearly. In the present study, it has been observed that AC/PVP blend varies linearly (Figs 1-3) with the concentration of the blend indicating the miscible nature of the blend whereas AC/PEG blend varies non-linearly (Figs 4-6) with the composition of the blend which indicates the immiscible nature of this blend in water at 30°C. The miscibility of AC/PVP blend can be attributed to the H-bond formation between carboxylic group of AC and C=O group of PVP. But in case of AC/PEG blend it is immiscible because there is no possibility of formation of H-bonding between carboxylic groups of AC with ethylic oxygen of PEG. These conclusions are substantiated from the

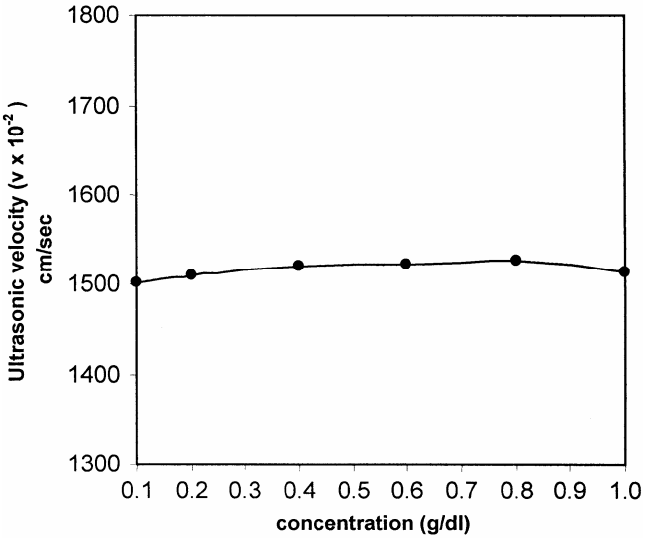

Fig. 1—Ultrasonic velocity vs 1:1 ratio of AC/PVP blends in water at 30°C

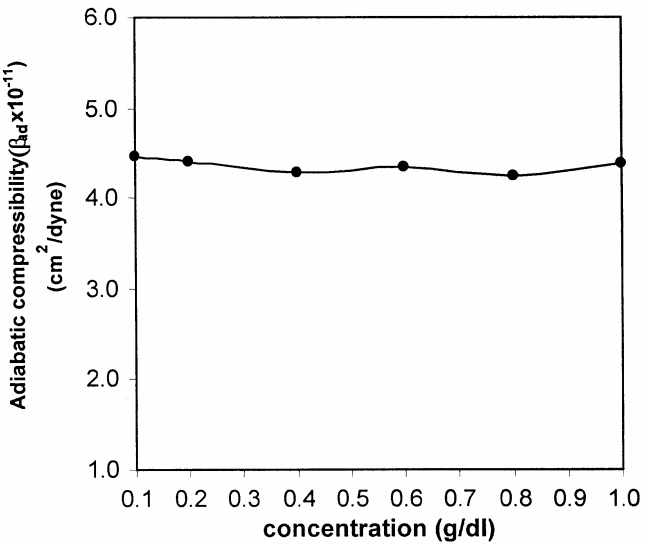

Fig. 2—Adiabatic compressibility vs 1:1 ratio of AC/PVP blends in water at 30°C

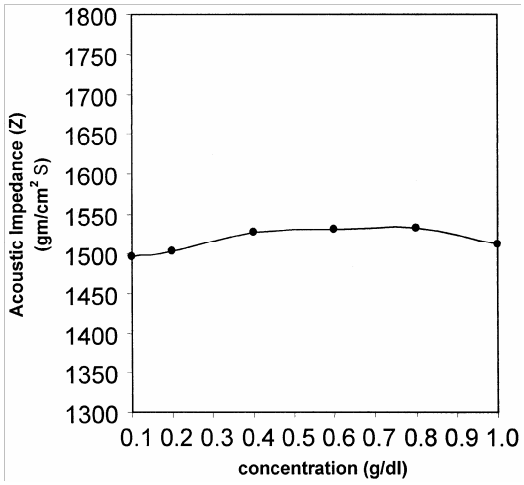

Fig. 3—Acoustic Impedance vs 1:1 ratio of AC/PVP blends in water at 30°C

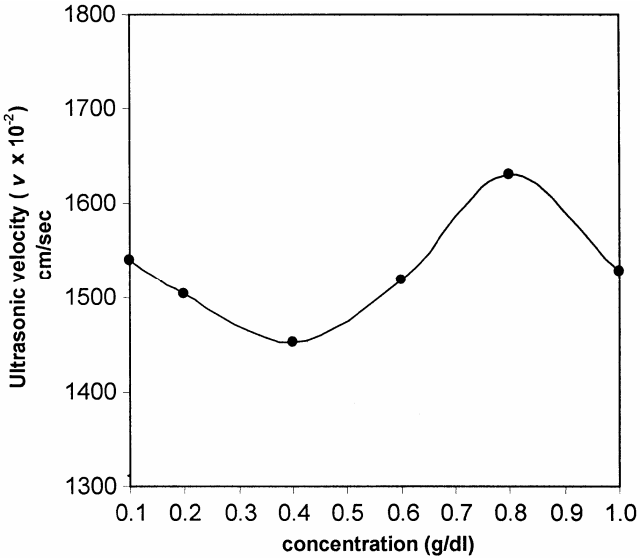

Fig. 4—Ultrasonic velocity vs 1:1 ratio of AC/PEG blends in water at 30°C

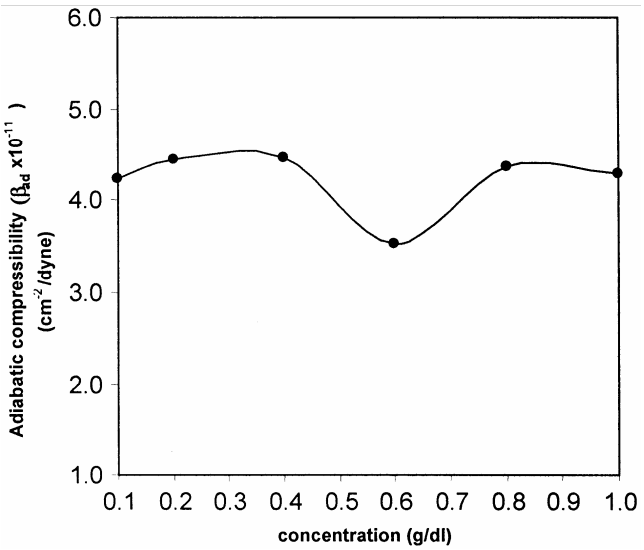

Fig. 5—Adiabatic compressibility vs 1:1 ratio of AC/PEG blends in water at 30°C

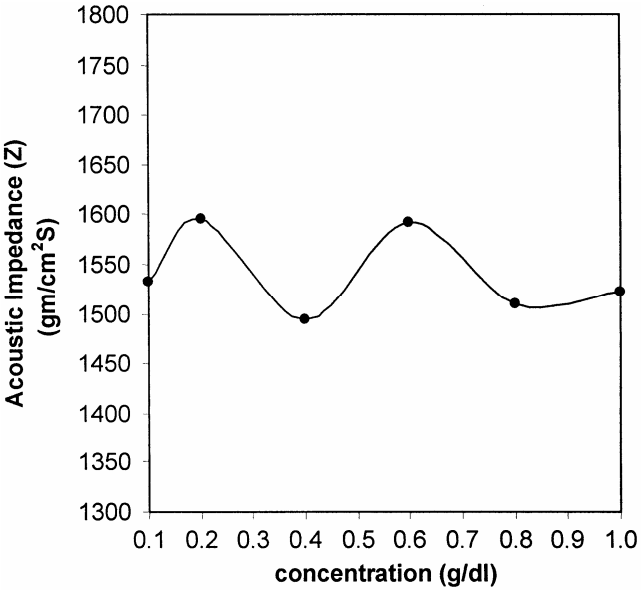

Fig. 6—Acoustic Impedance vs 1:1 ratio of AC/PEG blends in water at 30

viscosity and refractive index measurements of the above blends [15]. S.K. Rai *et al*., [7] made a similar observation from their ultrasonic velocity study of poly blend solutions.

Conclusions

Based on Ultrasonic velocity and its derived parameters it can be concluded that AC/PVP blends are miscible whereas AC/PEG blends are immiscible in water at 30°C.

Acknowledgements

One of the authors (H.M.P. Naveen Kumar) is thankful to University Grants Commission, New Delhi, India for financial support as project fellow.

References

[1] Krasue, S., Paul, S.D.R., Seymour, N.(Eds.) Polymer-Polymer compatibility in Polymer blends: New York, 1 (1978).

[2] Varenell, D.F., Coleman, M.M., FTIR. Studies of polymer blends: v. further observations on poly ester-poly (vinyl chloride) blends, *Polym. J.,* 22 (1981) 1324.

[3] Varenell, D.F., Runt J.P., and Coleman, M.M., FTIR and thermal analysis studies of blends of poly (E-caprolactone) with homo and copolymers of poly (vinylidene chloride), *Polymer.,* 24 (1983) 37.

[4] Cabanclas, J.C., Serrano, B., and Baselga, I., Development of cocontinuous morphologies in initially hetero geneous thermosets blended with poly (methyl methacylate), *Macromolecules.*, 38 (2005) 961.

[5] Crispim, E.G., Rubira, A.F., and Muniz, E.C., Solvent effects on the miscibility of poly (methyl methactrylate)/poly (vinyl acetate) blends:1 using differential scanning calorimetry and viscometry techniques, *Polym. J.,* 40 (1999) 5129.

[6] Singh Y.P., and Singh R.P., Compatability study on solutions of polymer blends by viscometric and ultrasonic techniques, *Eur.Polym.J.,* 19 (1983) 535 and Compatability studies on polyblends of PVC with chloro rubber-20 and its graft polyblends by ultrasonics, *Eur. Polym. J.,* 20 (1984) 201.

[7] Rai, S.K., Basavaraju, K.C., Jayaraju, J., and Demappa, T., Miscibility studies of xanthangum with gelatin in dilute solution, *J. Appl. Polym. Sci.,* 109 (2008) 2491.

[8] Basavaraj, K.C., Damappa, T. and Rai, S.K., Miscibility studies of poly saccharide xanthane gum and poly ethylene oxide in dilute solution, *carbohydrate polym.,* 69 (2007) 462

[9] Ashok Kumar Reddy, A.V., Venkata Prasad, C., Saraswathi, M, Naveen Kumar, H.M.P., Prabhakar, M.N., Balaji,V., Madhusudhan Rao, K., Yerriswami, B., Lakshmi Narayana Reddy, C., Mallikarjuna, B., Subha, M.C.S. and Chowdoji Rao, K. Compatibility studies of Chitosan /PEG blend in 2% aqueous Acetic acid Solutions by Ultrasonic velocity, Refractive index and Viscosity Techniques, 303.15 K, *J. Pure. Appl. Ultrason.* 31 (2009) 160.

[10] Fennema, O.R., *Food Chemistry*, Marcel Dekker, Newyork (1996).

[11] Defaye, J., and Wong.E., Stuctural studies of gum Arabic, the exudates poly saccharide from Acacia Senegal, *Carbohydrate Research.,* 150 (1986) 221.

[12] Aslam, A.M., Phillips, G.O., Sljvo, A., Snowden, M.J., and Williams, P.A., A review of recent developments on the regulatory, structural and functional aspects of gum Arabic, *Food Hydrocolloids.*, 11 (1997) 493.

[13] R.Mikkonen and A.Savlainen, *J. Appl. Polym. Sci.,* 39, (1990) 1709.

[14] M.A.Sidkey, A.M.Abd.E.I.Fattah, A.P.Yehia and N.S.Abd E.I.Ali, *J. Appl. Polym. Sci*. 43, (1991) 1441.

[15] Naveen Kumar H.M.P., Ph.D thesis, S.K. University, Anantapur, A.P.

J. Pure Appl. Ultrason. 33 (2011) pp. 63-70

Ultrasonic study and allied properties of the binary mixtures of acetophenone and NN- dimethylformamide with benzyl benzoate as common component

N. Jaya Madhuri, J. Glory, P.S. Naidu and K. Ravindra Prasad*

Department of Physics, S. V. U. P. G. Center, Kavali – 524201, Andhra Pradesh, India.
E-mail: nissi.joicy@gmail.com

Ultrasonic velocity and density have been measured in the binary mixtures of acetophenone and NN-dimethylformamide with benzyl benzoate as common component at three temperatures 30, 40 and 50°C. Adiabatic compressibility, free length, molar volume etc. have been calculated and the excess parameters of these are employed for estimating the molecular interactions in the mixed state. Mostly strong and dipole-dipole interactions are indicated in the acetophenone and dimethylformamide systems at all concentrations. In both the systems endothermic type of reactions is suggested. From a theoretical evaluation of velocities, CFT, NOMOTO and JUNJIE appear to have an edge.

Key words: ultrasonic velocity, compressibility, benzyl benzoate, molecular interactions, binary mixtures.

Introduction

Ultrasonic behaviour of several binary mixtures with benzyl benzoate as a component has been studied by us and the results have been reported already[1-6]. The present investigation aims at a study of the binary mixtures of benzyl benzoate in dimethylformamide (DMF) and acetophenone as a continuation of our previous work mentioned above. The medicinal property of benzyl benzoate has made us to study this elaborately. Benzyl benzoate is an insect repellant and used as a sterilizing agent in oily injections and as a medicine for scabies. Ultrasonic velocity and density were measured over the entire composition range in the two binary mixtures: (1) Benzyl benzoate + acetophenone and (2) Benzyl benzoate + NN- dimethylformamide at three temperatures 30, 40 and 50°C. Thermodynamic and allied parameters like adiabatic compressibility, freelength, molar volume etc., are computed and their excess parameters are used in estimating the molecular interactions in the binary state. Also theoretical evaluation of velocities has been made employing five standard theories FLT, CFT, NOMOTO, VANDEAL and JUNJIE at all temperatures. CFT, NOMOTO and JUNJIE have been found to agree well with the experiment.

Experimental

All the chemicals used in the investigation are of analar grade and are further purified by using standard techniques mentioned in literature[7]. Ultrasonic velocities in pure liquids and binary mixtures were measured using a single crystal variable path interferometer operating at 2 MHz with an accuracy of ± 0.05%. A double stem capillary type pyknometer was used for measuring density with an uncertainty of 2 parts in 10^5. An electronic single pan balance is used for weighing, the accuracy being ± 0.05 mg. Experimentally measured velocities in triply distilled water at 30° and 40°C are 1509.1 and 1530.1 ms^{-1} which agree with the values of Greenspan *et. al.*[8] in literature (1509.44 & 1529.85 ms^{-1}) with the accuracy claimed. The temperature of the liquid is maintained to within ± 0.01 K with the help of a constant temperature water bath (thermostat).

*Life Member, Ultrasonics society of India.

Theoretical aspects

The following expressions are employed in computing various thermodynamic and other allied parameters in the binary systems.

$$\text{Adiabatic Compressibility } \beta = \frac{1}{U_{exp}^2 \rho_{exp}} \quad (1)$$

$$\text{Free length } L_f = K/U_{exp}\rho_{exp}^{1/2} \quad (2)$$

The excess parameters are computed using the formula

$$A^{excess} = A^{expt} - A^{ideal} = [A^{expt} - (X_1 A_1 + X_2 A_2)] \quad (3)$$

where A is any parameter and X_1 and X_2 are the "mole fractions of components 1 and 2 respectively. For excess compressibility β^E, volume fraction Φ instead of mole fraction X is used.

The excess parameters are fitted to a 3rd order polynomial of Redlisch-Kister type.

$$A^E = X_1X_2 [A_0 + A_1 (X_1 - X_2) + A_2 (X_1 - X_2)^2 + A_3 (X_1 - X_2)^3] \quad (4)$$

For evaluating ultrasonic velocities theoretically, the following five standard expressions are used for five theories – FLT, CFT, NOMOTO, VANDEAL and JUNJIE respectively.

Velocity due to Jacobson using free lengths is given by

$$U_{FLT} = \frac{K}{L_{f\,mix}\ \rho_{mix}^{1/2}} \quad (5)$$

where K is Jacobson's constant (588 to 652 between 0 and 50°C).

Velocity due to Schaaff's theory due to Collision Factor S is given by

$$U_{CFT} = \frac{U_\infty S_{mix} B_{mix}}{V_T^M} \quad (6)$$

where U_∞ = 1600 m s^{-1}, S_{mix} and B_{mix} are Collision Factor and Available Volume respectively.

According to NOMOTO, velocity based on linearity of molar velocity is as follows.

$$U_{NOMOTO} = \left(\frac{R}{V}\right)^3 = \left[\frac{(X_A R_A + X_B R_B)}{(X_1 V_1 + X_2 V_2)}\right]^3 \quad (7)$$

where R is the molar velocity given by R = molar volume x (velocity)$^{1/3}$

According to VANDEAL'S ideal mixing,

$$U_{VANDAEL} = \frac{1}{\left[(X_1M_1 + X_2M_2)\left(\frac{X_1}{M_1U_1^2} + \frac{X_2}{M_2U_2^2}\right)\right]^{1/2}} \quad (8)$$

presents theoretical velocity.

JUNJIE calculated theoretical velocity using the formula

$$U_{JUNJIE} = \frac{\frac{X_1M_1}{\rho_1} + \frac{X_2M_2}{\rho_2}}{\left[(X_1M_1 + X_2M_2)\left(\frac{X_1M_1}{U_1^2\rho_1} + \frac{X_2M_2}{U_2^2\rho_2}\right)\right]^{1/2}} \quad (9)$$

Results and discussion

Ultrasonic velocity and density have been measured in both the binary mixtures of benzyl benzoate with acetophenone and NN- dimethylformamide over the entire composition range at 30, 40 and 50°C. The data are presented in Table 1. Experimentally measured velocities along with the theoretically evaluated velocities at 30°C employing the five theories – FLT, CFT, NOMOTO, VANDEAL and JUNJIE are compared in Figs. 1-2. The maximum percentage deviations observed at 30°C are - 1.98, 0.71, - 0.48, - 3.95 and - 0.49 and - 2.70, - 2.69, - 1.08, - 13.23 and - 1.13 in the mixtures with acetophenone and dimethylformamide respectively. The behavior is similar at other temperatures also. These deviations decrease with temperature. An examination of the deviations reveals that CFT, NOMOTO and JUNJIE have a sharp edge at all concentrations and at all temperatures as well.

Various parameters (acoustical and allied) have been computed from the measured data as a function of mole fraction of benzyl benzoate. It is observed that compressibility and free length decrease with concentration and increase with temperature. Regular variation in the first mixture i.e., with acetophenone is observed. In the second mixture i.e., with dimethylformamide more or less similar behaviour is seen for all the parameters at all temperatures. As the excess parameters play a vital role in the direction of indicating the intermolecular interactions in the binary form, the excess parameters are computed and variation of these excess parameters is shown clearly with the mole fraction of benzoate. In the acetophenone system as observed from Figs. 1(a)-1(c), the behaviour of all excess parameters with the mole fraction can be understood. β^E is generally negative and becomes more negative as the temperature increases from 30 to 50°C with a minimum at ~ 0.40 m. L_f^E is also more or less the same. In this system regular and systematic excess parameters refer to the amicable mutual behaviour of the two pure liquids, benzoate and acetophenone in the mixed state. Excess molar volumes are negative throughout at 30°C while negative upto 0.6m and positive at high concentrations at 40 and 50°C in the acetophenone system. An examination of Figs. 2(a) - 2(c) reveals that the behaviour of NN-dimethylformamide is also good and systematic in the binary mixture with benzoate. In this system also β^E and L_f^E show negative values with a minimum at ~ 0.30 m at all temperatures. Excess molar volume is negative at low concentrations which turns

Table 1—Variation of ultrasonic velocity and density with mole fraction of benzyl benzoate in the two mixtures of Benzyl benzoate

Mole fraction of BB	Velocity (ms^{-1})	Density ($kg\ m^{-3}$)	Mole fraction of BB	Velocity (ms^{-1})	Density ($kg\ m^{-3}$)
Benzyl benzoate + acetophenone			**Benzyl benzoate + NN-dimethyl formamide**		
			30°C		
0.0000	1448.0	1010.49	0.0000	1434.0	0939.48
0.0591	1455.0	1029.11	0.0430	1453.2	0965.62
0.0986	1462.0	1038.25	0.0919	1464.0	0983.12
0.2125	1472.0	1057.31	0.2125	1476.0	1012.49
0.2881	1476.0	1067.54	0.2881	1482.0	1025.57
0.3778	1480.0	1078.97	0.3778	1488.0	1038.70
0.4857	1484.0	1087.82	0.4857	1495.0	1054.55
0.6176	1488.0	1098.98	0.6182	1500.0	1070.51
0.7849	1496.3	1108.93	0.7135	1501.7	1084.36
0.8937	1501.0	1112.24	0.8047	1503.7	1097.15
1.0000	1506.0	1119.35	0.9145	1505.4	1111.05
			1.0000	1506.0	1119.35
			40°C		
0.0000	1419.5	1008.12	0.0000	1404.0	0930.01
0.0591	1428.0	1020.58	0.0430	1413.6	0963.18
0.0986	1434.0	1029.62	0.0919	1422.0	0983.07
0.2125	1443.6	1048.51	0.2125	1436.4	1011.32
0.2881	1449.0	1055.56	0.2881	1443.0	1019.29
0.3778	1454.0	1063.46	0.3778	1448.4	1034.26
0.4857	1458.0	1071.39	0.4857	1455.0	1045.61
0.6176	1462.0	1081.39	0.6182	1461.0	1063.97
0.7849	1466.7	1094.13	0.7135	1463.1	1073.25
0.8937	1469.3	1100.89	0.8047	1467.0	1088.26
1.0000	1471.4	1109.77	0.9145	1468.7	1100.46
			1.0000	1471.4	1109.77
			50°C		
0.0000	1403.7	1004.62	0.0000	1369.0	0922.03
0.0591	1406.5	1016.74	0.0430	1380.0	0965.17
0.0986	1409.8	1024.93	0.0919	1390.0	0976.19
0.2125	1416.8	1049.29	0.2125	1404.0	1001.41
0.2881	1420.8	1057.76	0.2881	1410.0	1018.71
0.3778	1424.0	1063.29	0.3778	1416.0	1034.72
0.4857	1428.0	1071.97	0.4857	1422.0	1050.07
0.6176	1432.0	1077.69	0.6182	1428.0	1064.82
0.7849	1435.7	1090.68	0.7135	1430.2	1080.39
0.8937	1438.2	1097.39	0.8047	1433.6	1089.06
1.0000	1440.0	1107.09	0.9145	1436.5	1100.43
			1.0000	1440.0	1107.09

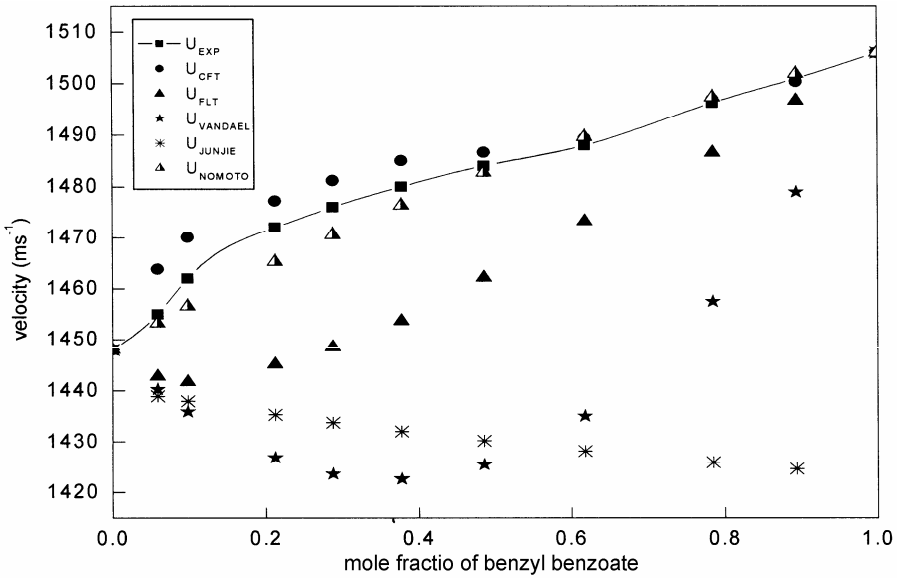

Fig. 1—Variation of ultrasonic velocities with mole fraction of benzylbenzoate at 30°C in the mixture BenzylBenzoate + Acetophenone

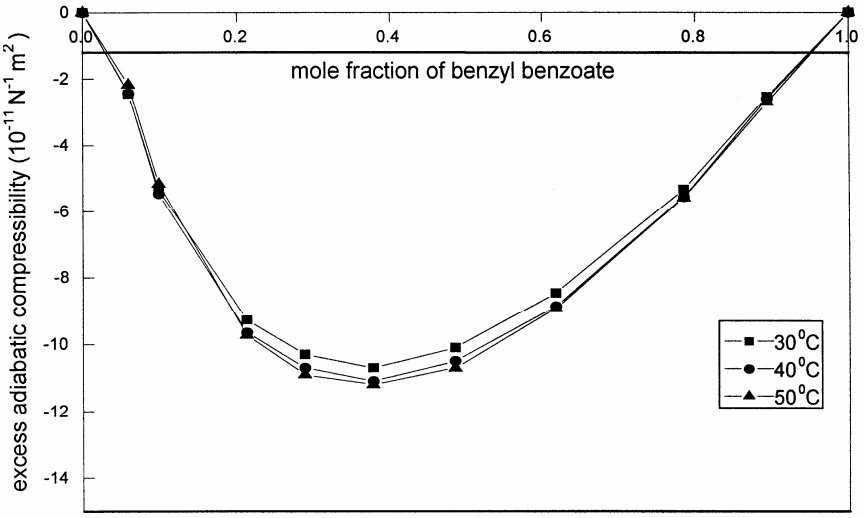

Fig.1 (a)—Variation of excess adiabatic compressibility with mole fraction of Benzyl Benzoate in the mixture Benzyl benzoate + acetophenone

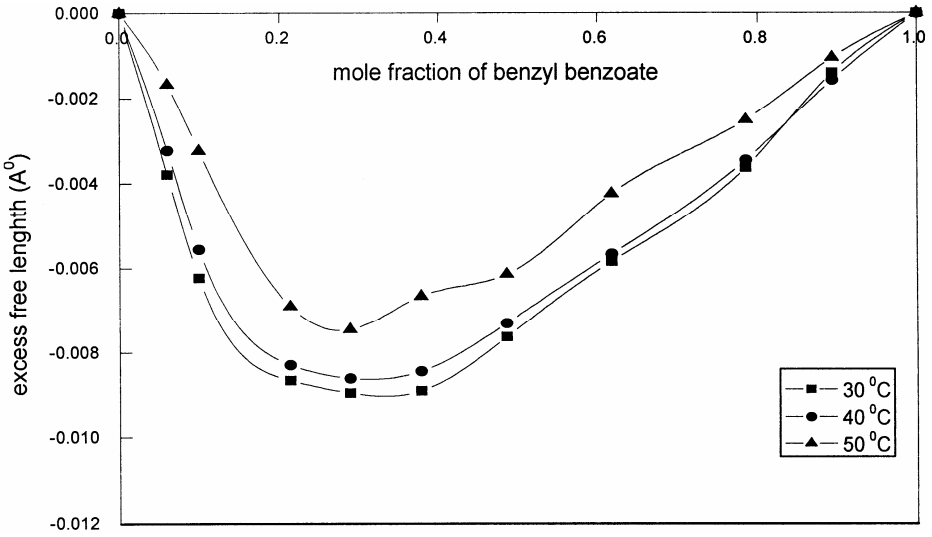

Fig. 1(b)—Variation of excess free length with the mole fraction of Benzyl Benzoate in the mixture Benzyl benzoate + acetophenone

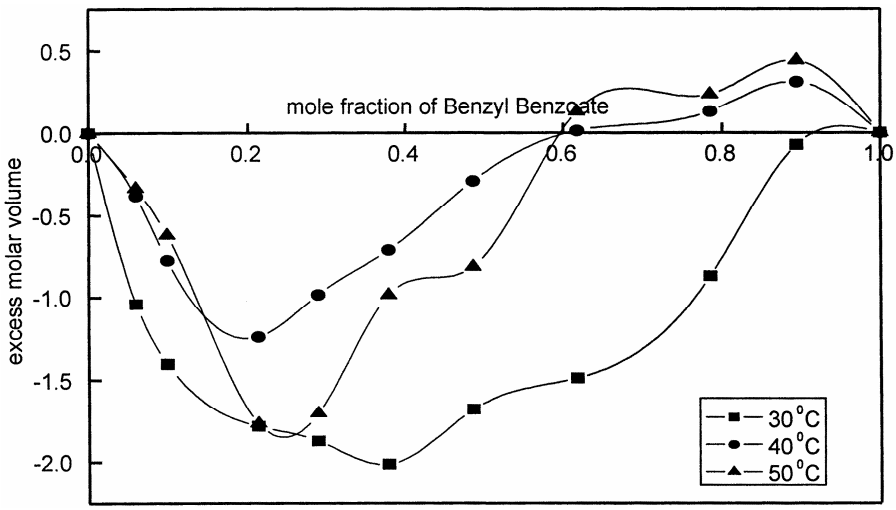

Fig.1(c)—Variation of excess molar volume with mole fraction of benzyl benzoate in the mixture Benzyl Benzoate + Acetophenone

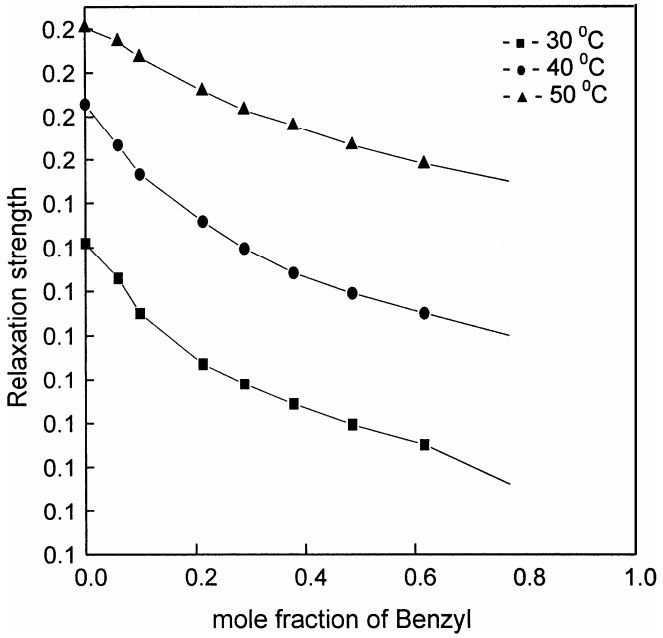

Fig.1(d)—Variation of Relaxation Strength with mole fraction of benzyl benzoate in the mixture: Benzyl benzoate + acetophenone

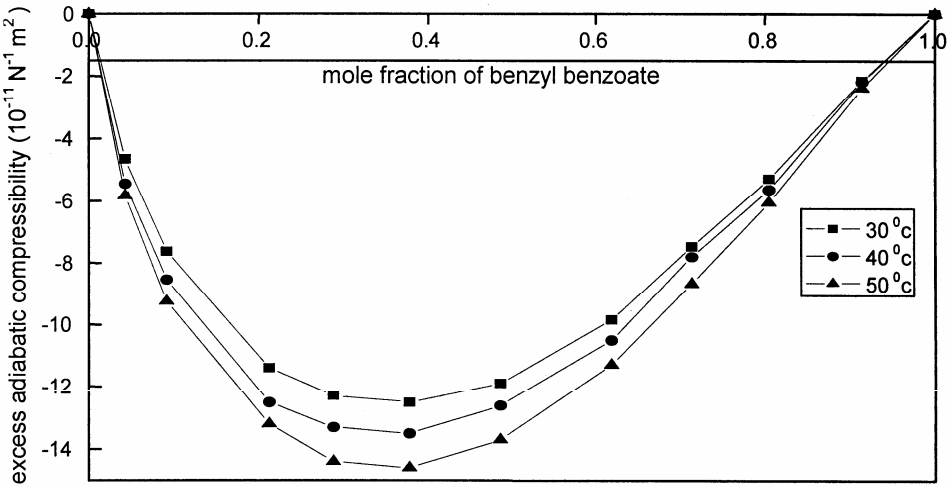

Fig. 2(a)—Variation of excess adiabatic compressibility with the mole fraction of Benzyl Benzoate in the mixture Benzyl benzoate + NN-dimethylformamide

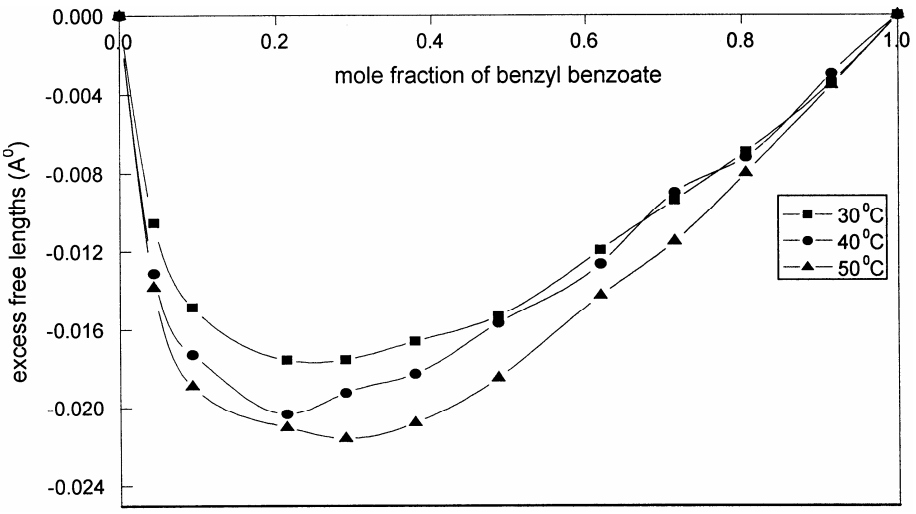

Fig. 2(b)—Variation of excess free length with mole fraction of benzyl benzoate in the mixture Benzyl benzoate + NN-dimethylformamide

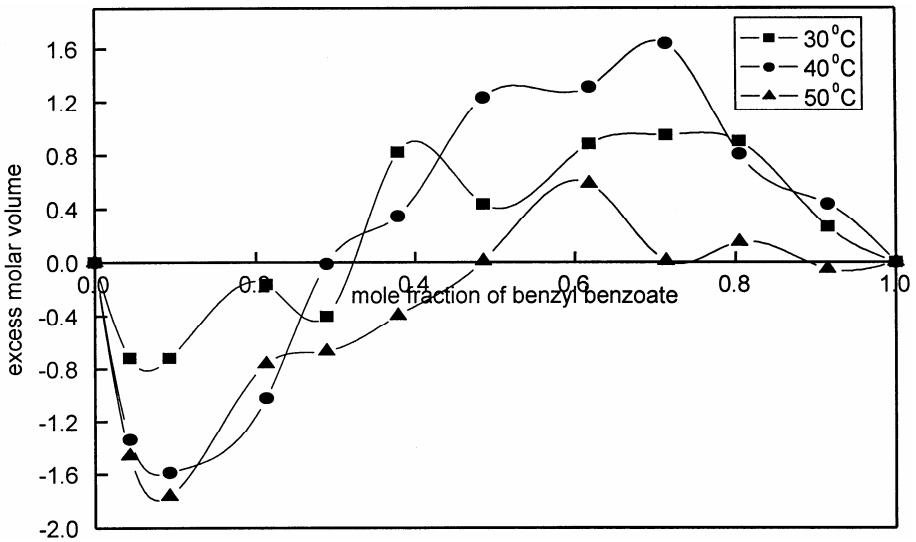

Fig.2(c)—Variation of excess molar volume with mole fraction of benzyl benzoate in the mixture Benzyle Benzoate + N-N dimethyl formamide

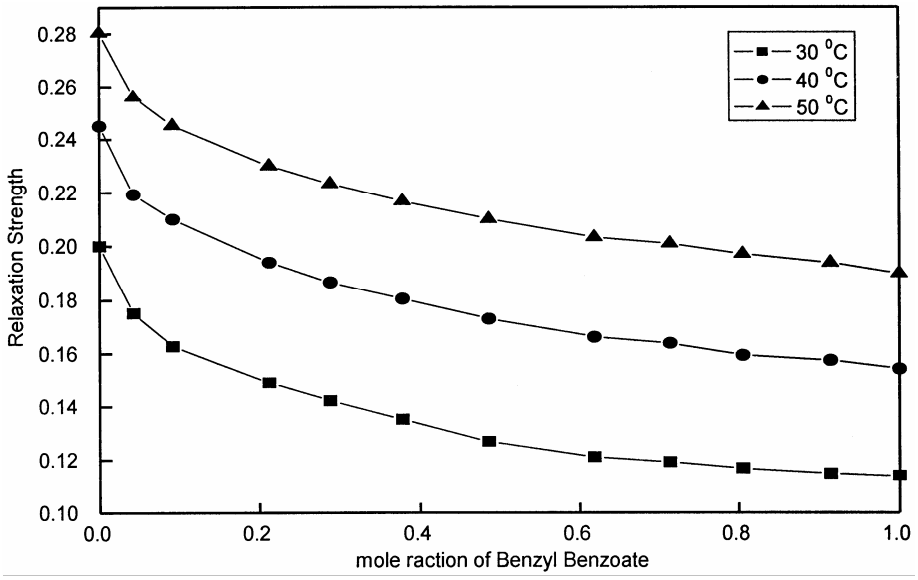

Fig. 2(d)—Variation of Relaxation Strength with mole fraction of benzyl benzoate in the mixture BB + N-N dimethylformamide

Table 2—Various parameters A_0,A_1,A_2,A_3 along with standard deviation σ using Redlich-kister method

Name of the system	β^E (10^{-10} m^2 N^{-1})				
	A_0	A_1	A_2	A_3	σ
Benzyl benzoate + acetophenone					
30°C	179.3	-6.26	0.01	-4.22	406.9
40°C	26.4	-0.11	0.24	-0.12	1.12
50°C	449.8	-6.66	0.11	-4.39	495.5
Benzyl benzoate + NN-dimethyl formamide					
30°C	-10.92	-7.27	0.13	-5.49	626.37
40°C	-14.83	-7.68	0.14	-5.93	836.37
50°C	-16.47	-8.18	0.15	-6.67	951.10

into positive at high concentrations in the DMF system. From the negative values of β^E and L_f^E in both the mixtures it can be understood that there exists strong interactions between the two constituent molecules besides dipole-dipole interactions. The Redlish-Kister polynomial is fitted to the excess parameters β^E and the constants are presented in Table 2.

To have some more clarity, relaxation strengths have also been calculated and are presented in Figs. 1(d)) and 2(d) for both the systems respectively.

In both the systems relaxation strength decreases with concentration of benzoate and increases with temperature. Reference may be made at this point for comparing our results with those of other workers in similar systems[9-12]. The systems of acetonitrile and dimethylformamide with DMSO have been studied in the direction of molecular interactions. Acetones with DMSO and acetophenones with iso-propanol also have yielded similar result. Recently Naidu and Ravindra Prasad have made an extensive study of binary mixtures of DMSO with acetonitrile and NN-dimethylformamide[12]. With benzyl benzoate as common component, several binary systems have been studied by the present authors[1-6]. Excess parameters in the mixtures of benzyl benzoate in dichloromethane and iso-butanol and several alcohols, aliphatic and aromatic alkanes, substituted aromatic alkanes, halogene substituted alkanes also have yielded the molecular interactions in the mixed state. A comparison of benzyl benzoate with acetophenone can be made with that of benzoate with the two ketones studied, methyl ethyl ketone and butyl methyl ketone at 30°C. From the positive values of π^E, H^E etc., weak interactions and dispersive forces are predicted in these mixtures and endothermic type of chemical reactions is suggested in the two ketone systems. In the present investigation also, similar type of strong interactions besides dipole-dipole interactions are suggested at all temperatures. In both the systems of present study, endothermic nature of reaction is suggested.

It may be noted that the opposing tendencies in various excess parameters is due to lack of a single theory taking into account all the factors like collision, free length etc., and hence the interpretation is based on the variation of majority of the parameters.

Acknowledgements

One of the authors (J.G) is grateful to the University Grants Commission for the award of RGNF. The authors are thankful to the Special officer, S. V. U. P. G Center, Kavali for the facilities provided.

References

1 Sivasankar, J., Geetalakshmi, M., Subramanyam Naidu, P., and Ravindra Prasad, K., Excess parameters of the binary mixtures of benzyl benzoate in dichloromethane and isobutanol. *J. Pure Applied Ultrason.*, 29 (2007) 82.

2 Jaya Madhuri, N., Subramanyam Naidu, P., and Ravindra prasad, K., Ultrasonic investigation of molecular interactions in the binary mixture of benzyl benzoate with dimethyl sulphoxide. Paper presented at the NCEM July 18-19th at NBKR Sciences and Arts college, Vidyanagar (A.P) (2009).

3 Geetalakshmi, M., Subramanyam Naidu, P., and Ravindra Prasad, K., Molecular interactions in the binary mixtures of benzyl benzoate in alcohols. *J. Pure Appl. Ultrason.*, 30 (2008) 18.

4 Ramesh, P., Geetalakshmi, M., Jaya Madhuri, N., Subramanyam Naidu, P., and Ravindra Prasad, K., Molecular interactions in the binary mixtures of benzyl benzoate in benzene and substituted benzenes-an ultrasonic study .Invertis Journal of Science and Technology 4 (2011) 1.

5 Mallikarjun, P., Jaya Madhuri, N., and Ravindra Prasad, K., Molecular interactions in the binary mixtures of benzyl benzoate – an ultrasonic study, *J. Pure Appl. Ultrason.*, 32 (2010) .(in press)

6 Jaya Madhuri, N., Glory, J., Subramanyam Naidu, P., and Ravindra Prasad, K., Study of molecular interactions in the binary mixtures of benzyl benzoate in carbon disulphide and diethylether presented XVIII national Symposium on Ultrasonics (NSU XVIII – 2009) 21 – 23 Dec 2009 at VIT University, TamilNadu, India.

7 Furniss, B.S., Hannaford, A.J., Rogers, V., Smith, PWG., and Tachall, AR., Vogel's Text Book of Practical Organic chemistry Fourth Edition, Longmann (1980).
8 Greenspan, M., and Tschieff, C.E., *J.Res.Natl.Bur.Stan*., 59 (1957) 249.
9 Chauhan, M.S., Sharma, K.C., Gupta, S., Sharma, M., and Chauhan, S., Ultrasonic velocity, viscosity and density studies of binary solvent system at different temperatures DMSO – MEOH, DMF – MEOH and DMSO – DMF, *Acous.Letters.,* 18 (1995) 233.
10 Das, A.K., and Jha, B.L., Ultrasonic study of binary mixtures of some nonhydroxy alcohols, acetones and nitrobenzene with DMSO. *J. Mol. Liq*., 59 (1994) 161.
11 Yanadi Reddy, N., Subramanyam Naidu, P., and Ravindra Prasad, K., Ultrasonic study of acetophenone in binary mixtures containing iso-propanol as common component. *Indian J. Pure & Appl Phys.*, 32 (1994) 958.
12 Subramanyam Naidu, P., and Ravindra Prasad, K., Ultrasonic study in the binary liquid mixtures of Dimethyl sulphoxide. *J. Pure Appl. Ultrason.,* 24 (2002) 18.

Journal of Pure and Applied Ultrasonics

VOLUME 33 NUMBER 4 OCT. - DEC.- 2011

CONTENTS

Website : www.ultrasonicsindia.com

A Publication of — Ultrasonics Society of India

Information for authors

1. Type of Contribution

JOURNAL OF PURE AND APPLIED ULTRASONICS welcomes original research papers and articles related to the subject of ultrasonics. The contributions may be in the areas of physical ultrasonics, medical ultrasonics, ultrasonic non-destructive evaluation including NDT, high power ultrasonics, underwater acoustics, ultrasonic transducers, transducer materials & devices and any other related topic. These may fall into one of the following categories.

ResearchPapers **-** These should be on original research work contributing to scientific developments. They should be written with a wide readership in mind and should emphasize the significance of the work.

Reviews Articles **-** Includes critical reviews and survey articles.

Research and Technical notes **-** These should be short descriptions of new techniques, applications, instruments and components.

Letters to the editor **-** Letters will be published on points arising out of published articles and papers and on questions of opinion.

Miscellaneous **-** Miscellaneous contributions such as conference reports, Ph.D. thesis reviews and news items are also accepted. Recommended lengths of contributions are: Research papers 2000-4000 words, reviews articles 2000-5000 words; conference reports 500-1500 words; news items, research and technical notes up to 1000 words.

2. Manuscripts

Manuscripts should be typed on one side of the paper in double spacing with 25 mm margins on all side of A4 size paper. A soft copy of the manuscript in MS WORD for text and MS EXCEL for illustrations and a PDF file thereof may be sent by e-mail or CD/DVD. Colour images should be formatted as JPEG files. Figures submitted in colour would be published in colour. Colour should be avoided unless it is required in order to convey a message or serve a purpose in the image.

Title **-** Titles should be short and indicate the nature of the contribution. About 5 keywords may be given after the abstract.

Abstract **-** An abstract of 100-200 words should be provided on the title page of paper and review article. This should describe the full scope of the contribution and include the principal conclusions.

Mathematics **-** Mathematical expressions should be arranged to occupy the minimum number of lines consistent with clarity e.g., $(x^2+y^2)/(x-y)^{1/2}$

References **-** References should be indicated in the text by its number only. The reference number should be given as superscript. The corresponding reference shall contain the following information in order; names and initials of author(s)in bold, full title of the work, journal or book title in italic, volume number in bold, the year of publication in brackets and the page number. As example: Vasanth B.K., Palanichamy P., Jayakumar T. and Sankar B.N., Assessment of residual stresses in a carbon steel weld pad using critically refracted longitudinal (L_{CR}) waves, *J. Pure Appl. Ultrason*., 28 (2006) 66-72.

Units and Abbreviations **-** Authors should use SI units wherever possible.

3. Reprints

One copy of the issue in which the paper is published is sent to the author free of charges.

J. Pure Appl. Ultrason. 33 (2011) pp. 73-76

Design of a hydrophone for use in off-shore oil exploration

Laly Joseph, K. P. B. Moosad And R. M. R. Vishnubhatla

Transducer Group, Naval Physical and Oceanographic Laboratory Kochi – 682 021 (Kerala), India

E-mail: ravimoosad@gmail.com

Design of a hydrophone to be used in off-shore oil exploration is presented. Design is done with the help of Finite Element Modeling using the commercial package ATILA. Three different configurations are modeled and best one is selected for fabrication. Prototypes met the performance specifications and the technology was transferred to a production agency.

Key words*: Hydrophone design, FEM, flexural disc*

1. Introduction

In off-shore oil-exploration, layers of earth under sea-bottom are analysed using acoustic radiation emanating from the huge projectors called "air guns" fitted on the survey ships. The high intensity acoustic impulses produced by these projectors penetrate the bottom of the sea and get reflected from the various layers therein. These echoes are received by long arrays of hydrophones (known as streamers), which are towed behind the vessel. Typical systems consist of a few kilometers of arrays, fitted with one hydrophone for every one-meter length of the array. Because of the large length of these arrays, maintainability is generally built-in. It is possible to replace the hydrophones, whenever required.

The objective of the study reported in this paper was to arrive at a design of a hydrophone for use in the streamers. Because of the large numbers required for the system, total design considerations included aspects like dimensional limitations, cost etc. However, the scope of discussion in this paper has been limited to the functional aspects only.

2. Design Considerations

Flexural disc hydrophone, which is perhaps the simplest design for hydrophones was considered appropriate for this application, since the depth of operation of the hydrophones is limited to less than 100 m. Flexural disc hydrophones make use of the flexural modes of vibrations of metallic discs, to sense the acoustic waves incident on them. These vibrations get transferred onto a piezoelectric ceramic disc attached to the metallic disc and generate electric charges in it. Measurement of this charge gives a measure of the pressure waves that has induced the vibration in the metallic disc.

Although flexural disc hydrophones are quite familiar to transducer scientists and engineers, published literature on the subject is limited. Electro-acoustic transducers making use of this concept have been known in literature since mid-fifties[1-5], but most of them relate to the use of flexural disc transducers for in-air applications, in radio and telephone industries. Woollett[6] appears to be the only author to have described the use of flexural disc transducers for hydrophone applications. In a comparatively recent paper, Delany[7] has studied flexural disc transducer (Bender transducer) for projector applications, in the frequency range 800 Hz – 20,000 Hz. At a drive level of 2 – 4 kV/cm, a Transmitting Voltage Response of the order of 136 dB//µPa is reported to have achieved, in a typical case. A few authors have described polymer flexural disc hydrophones, wherein piezoelectric polymer films are used in place of the piezoelectric ceramic discs[8-10].

In most of the references cited above, thickness of the metallic disc is nearly the same as that of the piezoelectric ceramic disc attached on it. At NPOL, we have development experience with several flexural disc hydrophones of various designs. In all these, the thickness of the piezoelectric ceramic disc is much smaller compared to the thickness of the metallic disc. Use of thin piezoelectric ceramic disc results in higher capacitance for the hydrophone, which is useful in the design of pre-amplifiers for the hydrophones. In streamers, the pre-amplifier modules are placed at about 100 m intervals and therefore average length of cable from hydrophones to preamplifiers will be about 50 m. To reduce the effect of the cable capacitance, it is desirable to have a large capacitance for the hydrophones. Therefore a design with thin piezoelectric ceramic disc was preferred for the present application.

Since the hydrophone is meant for an application wherein it is in continuous motion (towing) while in

use, it is better to have an acceleration-compensated design.This means that the hydrophone should have a plane of symmetry, on either side of which there are piezoelectric ceramic discs. These are then connected in parallel, so that any signals induced by mechanical movement of the hydrophones (in a direction perpendicular to the plane of symmetry) will get cancelled.

Size of the hydrophone and therefore the diameter of the metallic and piezoelectric ceramic discs were determined by the constraints of the application. The acceptable diameter of the hydrophone assembly was around 25 mm and thickness 9 mm.Modeling of two variants were carried out within these dimensional limits in order to choose an appropriate design.

3. Modeling Studies

Two models were made in ATILA viz., one with a flat ring and another with a tapered ring and their performances have been examined. Details are given in the following sub-sections.

Model of a flat ring Flexural disc hydrophone: The components and assembly of the hydrophone are indicated in Fig. 1.

Diameter of the piezoceramic disc is 14.75 mm and thickness 0.3 mm. Diameter of the metallic disc is 25 mm, and thickness is 1.5 mm. The ring has an outer diameter of 25 mm, inner diameter of 22 mm and a thickness of 1.5 mm. These dimensions were chosen since the components were readily available and therefore immediate comparison with experimental results was possible.

Two dimensional axisymmetric model was made using the preprocessors PREFLU and PREATI. Only one quarter of the hydrophone was modeled. Fig. 2 shows the Finite Element Mesh used for computations. The maximum dimension of the element is determined by the largest frequency of interest (should be less than $1/5^{th}$ of the wavelength) and the size of the water column is determined by the lowest frequency of interest (should be more than $1/5^{th}$ of the wavelength). The frequency range chosen for analysis is 500 Hz to 2000 Hz and therefore, maximum size of the element used is 0.15 m. Size of the water column was chosen as 0.6 m. Voltage excitation was used for the analysis and the sensitivity values were directly obtained from the program. Results are summarized in Table 1. The resonance frequency and sensitivity values predicted were not acceptable for the system and therefore a different design was attempted.

Model of a tapered ring Flexural disc hydrophone: In this case, the metal ring in the centre was made to have tapered ends. A schematic is shown in Fig. 3. Modeling was carried out as in the previous case. Results are summarized in Table 2.

Final model: From Table 1 and 2, it is obvious that the tapered ring design is advantageous. In the final model, the tapering of the ring was replaced by a

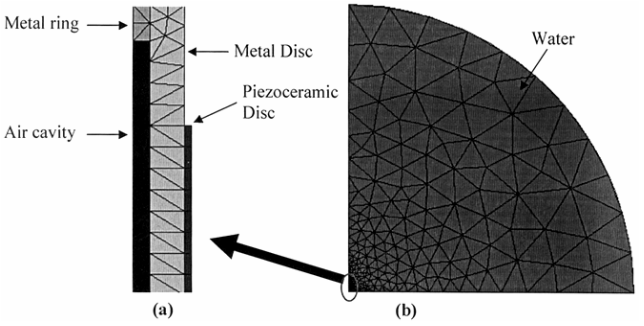

Fig. 2—Finite Element Mesh used for the modeling. (a) shows the hydrophone only and (b) shows hydrophone with the water envelope.

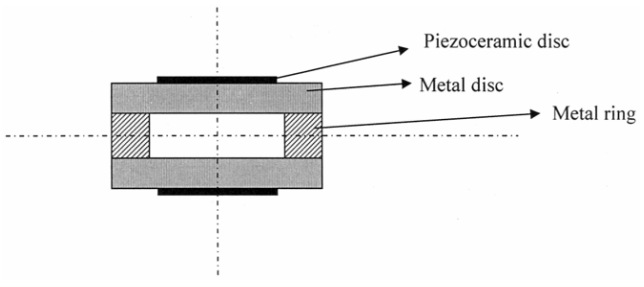

Fig. 1—Geometry of the flat ring flexural disc hydrophone

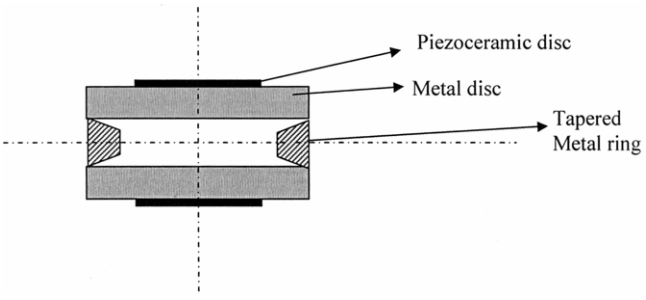

Fig. 3—Geometry of the tapered ring flexural disc hydrophone

Table 1—Summary of the results of modeling of flat ring flexural disc hydrophone

Sl. No.	Analysis done	Piezo-ceramic material	Metal disc/ring	Losses included	Resonance frequency kHz	Receiving sensitivity dB//V/microPa at 1 kHz
1	2d, axisymmetric, in-water Harmonic analysis	PZT 5H	Brass	Nil	14.25	-199

Table 2—Summary of the results of modeling of tapered ring flexural disc hydrophone

Sl. No.	Analysis done	Piezo-ceramic material	Metal disc/ring	Losses included	Resonance frequency kHz	Receiving sensitivity dB//V/microPa at 1 kHz
1	2d, axisymmetric, in-water Harmonic analysis	PZT 5H	Brass	Nil	7.505	-191

Table 3—Summary of the results of modeling of flexural disc hydrophone – final model

Sl. No.	Analysis done	Piezo-ceramic material	Metal cups	Losses included	Resonance frequency kHz	Receiving sensitivity dB//V/microPa at 1 kHz
1	2d, axisymmetric, in-water Harmonic analysis	PZT 4	Brass	Nil	11.2	-201.4

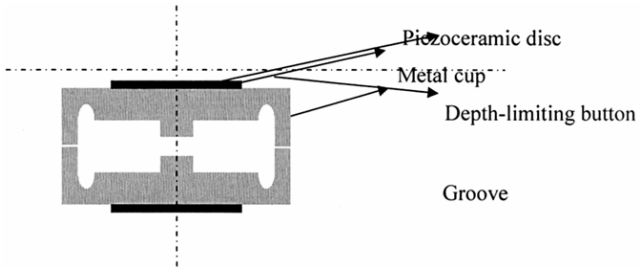

Fig. 4—Geometry of the final hydrophone

groove on the disc. This was done basically on production considerations. Several other modifications were also made to suit the system requirements. A schematic is shown in Fig. 4. Instead of three metal components, only two are used. A central tip is given on the inside of the metal cups to act as depth-limiting buttons. When the hydrophones are immersed to depths more than 100 m these two projections butt with each other, protecting the Piezoceramic discs from breaking.

Effect of changing the depth and width of the groove was checked by running several models, and an optimized value was adopted in the final design. Summary of the results of modeling obtained using this geometry is given in Table 3.

4. Results from prototypes

Prototypes fabricated in the final model showed performance comparable with the predicted values. Exact matching of the values was not obtained, probably due to the difference in the material properties used for modeling. However, the models have helped in making a choice between the various possible designs. The final product (shown in Fig.5), made water-worthy by polyurethane potting and rubber encapsulation, was subjected to quantity production (500 Nos.) by a production agency. Several of these hydrophones have been tested in streamers and the results are found to be comparable with those of the original hydrophones in the system.

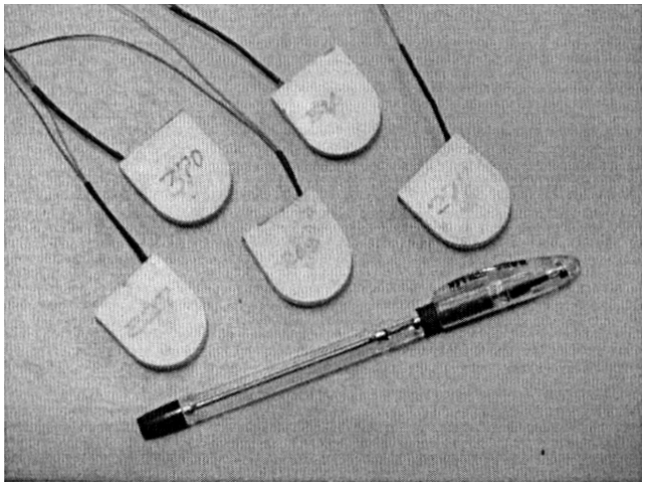

Fig. 5—Finished hydrophones

5. Conclusions

Design of a flexural disc hydrophone for use in off-shore oil exploration is described. Commercial Finite Element Modeling package ATILA has been used as a tool for the design. Prototypes fabricated have shown very good results and the technology has been transferred to a production agency for mass production.

Acknowledgements

Authors are thankful to several of their colleagues at NPOL, for their involvement in the hydrophone development, in various capacities that facilitated the timely completion of the development. Various encouraging discussions with D D Ebenezer, Group Head, Transducer Group, are thankfully acknowledged. Director, NPOL, is acknowledged for the encouragement and guidance provided and for permitting to publish this paper.

References

1 C. B. Sawyer, “The use of Rochelle salt crystals for electrical reproducers and microphones”, Proc. IRE, Vol.19, Nov.1931, pp.2020-2029

2 C. P. Germano, “Study of multi-morph, a new and improved ceramic element for use in phonograph pickup applications”, Proc. NEC, Vol.12, Oct. 1956, pp 667-688

3 J. Roos and J. Koorneef, “Thin bilaminar piezodisks used in microphone and telephone membranes”, J. Audio Eng. Soci., Vol.17, Apr 1969, p.174

4 Y. Tomita and T. Yamaguchi, “A study of piezoelectric receiver”, Rev. Elect. Commun. Lab., Vol13, July-Aug 1965

5 C. P. Germano, “Flexure Mode Piezoelectric Transducers”, IEEE Trans. Audio & Electroacoustics, Vol AU 19, No.1, March 1971, pp 6-12

6 R. S. Woollett, “Theory of piezoelectric flexural disk transducer with applications to underwater sound”, USL Res. Report 490, Dec.5, 1960

7 John L Delany, “ Bender transducer design and operation”, Journal of Acoust. Soc. Am. 109(2), Feb. 2001, pp.554-562

8 T. D. Sullivan and J. M. Powers, “Piezoelectric polymer flexural disk hydrophone”, Journal of Acoust. Soc. Am. 63(5), May. 1978, pp.1396-1401

9 Donald Ricketts, “Model for a piezoelectric polymer flexural plate hydrophone”, Journal of Acoust. Soc. Am. 70(4), Oct. 1981, pp.929 -935

10 R. Vigel Raj. T. Nagapranay, V. Ravindra, C. Lakshmana Rao, Srinivasan M Sivakumar, and C Padmanabhan, “PVDF Based Hydrophone: Design and Sensitivity Analysis”, Proc. of ISSS 2005 (International Conf. On Smart Materials, Structures and Systems, July 28-30, 2005, Bangalore, India)

J. Pure Appl. Ultrason. 33 (2011) pp. 77-87

Ultrasound shock wave propagation and generation of harmonics in biological tissues

Narendra D. Londhe and R. S. Anand

Electrical Engineering Department, IIT Roorkee, Roorkee-247667
E-mail:ndlondhe.iitr@gmail.com, anandfee@iitr.ernet.in

In this paper, two theoretical methods for the description of nonlinear ultrasound wave generated from axis symmetric circular source and propagation in soft human tissues is described. Burgers' equation has been used to model the nonlinear propagation of single sinusoidal wave of finite amplitude. In the first method, the analytical solution of Burgers' equation was achieved by using Fubini method in preshock region while weak shock theory applied in postshock region for lossless medium. In case of lossy medium, the analytical solution of Burgers' equation is achieved by using linear diffusion equation via Hopf-Cole transformation in preshock region and Fay's equation in postshock region. In the second method the operator splitting methodology is implemented in which absorption term is solved using Crank Nicholson Finite Difference (CNFD) method in time and nonlinear term by using analytical method at each step for both lossless and lossy medium. Both the methods are solved in MATLAB. The results have been shown for waveform distortion and shock formation radiated by circular piston source for lossless and lossy tissue mediums. The analytical study of fundamental, second and third harmonic components variation along the distance of propagation has been done using both proposed methods and has been compared.

Keywords: Nonlinear Wave, Ultrasonic Imaging, Burgers' Equation, Shock Formation, Soft Tissues.

1. Introduction

High intensity ultrasonic pulses are used in medical ultrasonics, which exhibits finite amplitude effects while propagating through human tissues and these effects can't be predicted by linear approximation methods. The signal source having finite dimensions generates signals of finite amplitude and it experiences thermoviscous human tissue medium with nonlinear characteristics along with diffraction and attenuation. The study of finite amplitude plane wave propagation in biological tissues from source of finite size needs to be investigated with regard to diffraction, absorption and nonlinearity effects. Of these, nonlinear effects are important for tissue harmonic imaging (THI)[1], contrast agents[2], and acoustic output measurements. Nonlinearity is a property of a medium by which the shape and amplitude of a signal at a location are no longer proportional to the input excitation. The second and higher harmonic components are generated as ultrasound propagates through biological tissues due to the phenomenon of nonlinear wave propagation. Unlike the linear imaging that uses ultrasound at the transmitted fundamental frequency to form the image, THI uses ultrasound at twice the transmitted frequency to form the image. It makes THI superior to fundamental imaging mode due to improvement of the spatial resolution and suppression of side lobe levels[3-4]. As a measure of the nonlinearity in the pressure-density relation for a medium, the nonlinearity parameter B/A (term from the Taylor series expansion expressing the variations in pressure with density in a medium.) plays a significant role in nonlinear acoustics[5], and has been found some dependence on the compositions and structure features of biological tissues[6-7]. Therefore this parameter has been assumed as a new parameter for tissue characterization, and has some potential applications in ultrasonic diagnosis.

2. Theory

A. Shock wave formation in nonlinear wave propagation

During propagation of ultrasound wave in biological tissues, the nonlinearity alters the ultrasound wave pattern progressively in shape assuming the tissue to be a lossless medium. This change in shape is due to change in speed of sound in the tissues because of their structural changes (density perturbations). The instantaneous sound speed for acoustic plane waves in ideal fluid is dependent on particle velocity u, and coefficient of nonlinearity $\beta=(1+B/2A)$.

$$c = c_0 + \beta u \qquad \ldots (1)$$

When the velocity magnitude is high, the sound speed deviates from c_0. However, due to the oscillatory nature of waves, the speed of sound will either increase or decrease according to the relative phase of the wave. In other words, the regions of compression

will travel faster than c_0, while the regions of rarefaction will travel slower than c_0 (Fig. 1).

This shift in sound speed is important when amplitudes are large and causes waveform steepening. As the waveform continues to steepen, a discontinuity known as a shock is formed. For an initially monofrequency wave, the necessary propagation distance to form a shock is known as the shock formation distance, where the shock is defined as when the rise from a trough to a crest takes less than one-tenth of the period of the wave. The shock formation distance ($\bar{z}$) is calculated for plane waves:

$$\bar{z} = \frac{1}{\beta\varepsilon\kappa} \quad \ldots (2)$$

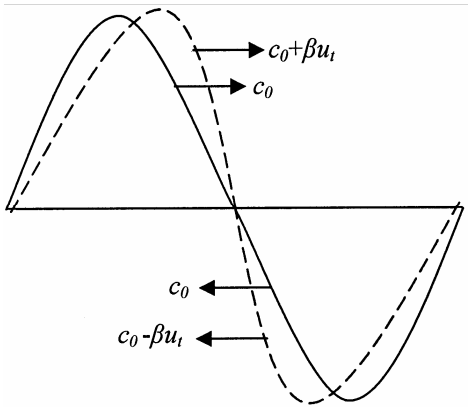

Fig. 1—Transmitted sinusoidal wave pattern: the positive portion of a waveform will travel faster than the negative portion.

where ε, the acoustic Mach number, is u_0/c_0, where u_0 is the particle velocity at the source, and κ is the wave number. From this equation, it is apparent that shocks form quicker for greater Mach numbers (i.e. higher amplitudes), higher frequencies and higher coefficients of nonlinearity.

For convenience, distance is often normalized by the shock formation distance to create a dimensionless distance σ defined as $z/\bar{z}$ for plane waves, normally called as shock parameter. A value of σ less than one would represent any distance before the shock has formed, known as the preshock region, while σ > 1 would represent distances larger than a shock formation distance[2] (Fig. 2).

B. Burgers' equation

The KZK (Khokhlov-Zabolotskaya-Kuznetsov) parabolic wave equation takes into account the combined effects of diffraction, absorption and nonlinearity in directive acoustic beams, and is expressed as:

$$\frac{\partial^2 p}{\partial z \partial t'} = \frac{c_0}{2}\left(\frac{\partial^2 p}{\partial r^2} + \frac{1}{r}\frac{\partial p}{\partial r}\right) + \frac{\delta}{2c_0^3}\frac{\partial^2 p}{\partial t'^2} + \frac{\beta}{2\rho_0 c_0^3}\frac{\partial^2 p^2}{\partial t'^2} \quad \ldots (3)$$

Diffraction Absorption Nonlinearity

where δ is the sound diffusivity of the medium, $\tau = t - z/c_0$ is the retarded time variable and t is time.

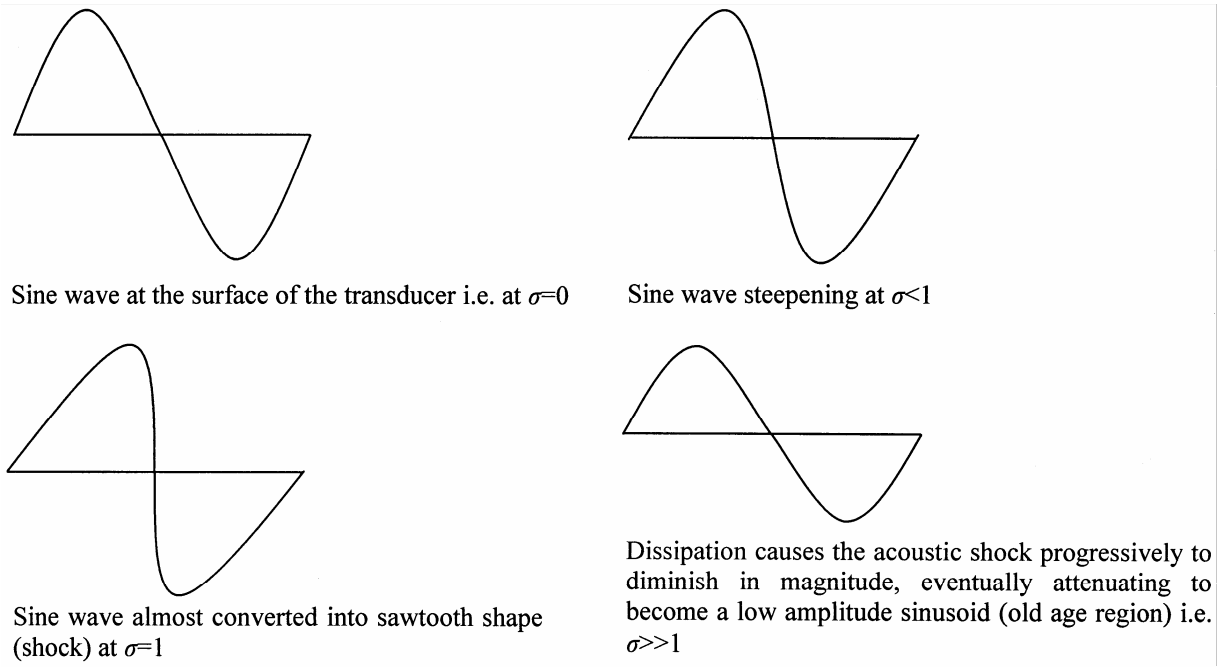

Fig. 2—Transmitted sinusoidal wave pattern for different values of propagation distance defined in terms of dimensionless axial distance σ. A sine wave steepens up and forms a shock due to nonlinear propagation. Eventually the sine wave became the sawtooth wave.

This nonlinear wave equation is very complicated and in general does not have an analytical solution. However, several of the important effects can be shown for simple cases. Also, a series of approximations can be made which allow for solutions in specific cases that effectively demonstrate many of the fundamental nonlinear acoustics phenomena.

The KZK equation without diffraction term represents the Burgers' equation. The Burger's equation is the simplest model equation that accounts for nonlinearities, losses and geometrical spreading of plane wave in one dimension. The generalized form of the Burgers' equation for plane waves is expressed as:

$$\frac{\partial p}{\partial z}=\frac{\delta}{2c_0^3}\frac{\partial^2 p}{\partial t'^2}+\frac{\beta}{2\rho_0 c_0^3}\frac{\partial p^2}{\partial t'} \quad \ldots (4)$$

As shown in Fig. 3, the geometrical system considered, consists of circular source situated at the centre of the coordinate system and plane wave propagation occurs in positive z-direction.

The plane circular source acoustic field calculation is done in the following section using analytical methods and time domain algorithm generated by Lee et al[8] for both the lossless and lossy conditions.

II. Solving Methods

It is convenient to start by considering a theoretical concept i.e. the infinite plane wave traveling in a lossless medium. This makes it possible to ignore the near-field diffractive variations resulting from the finite size of the ultrasound source, and also any changes in pressure amplitude and frequency spectrum resulting from attenuation. An equation which describes nonlinear plane wave propagation lossless medium in positive z direction can be obtained by discarding the absorption term in the Burgers' equation.

$$\frac{\partial p}{\partial z}=\frac{\beta}{2\rho_0 c_0^3}\frac{\partial p^2}{\partial t'} \quad \ldots (5)$$

A. Analytical method

A1. For Lossless medium:

Consider the continuous sinusoidal source condition given by $p=p_0\sin\omega_0 t$ at z=0. The corresponding solution of equation (5) in terms of a Fourier series is as follows [9-10]:

$$\frac{p}{p_0}=\sum_{n=1}^{\infty}\frac{2J_n(n\sigma)}{n\sigma}\sin n\omega_0 t' \quad \ldots (6)$$

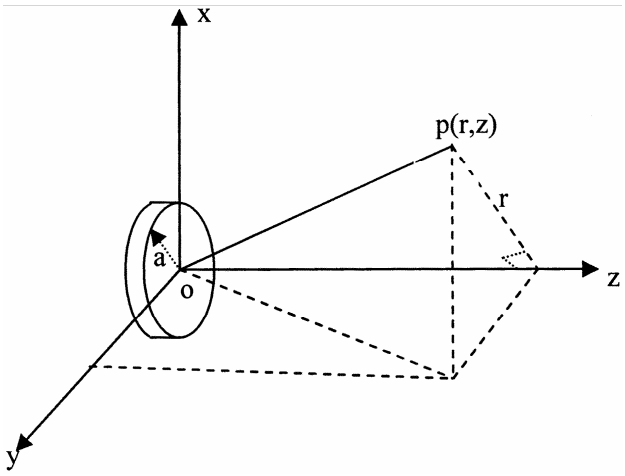

Fig. 3—Axis-symmetric circular piston source located at z=0

where J_n is the Bessel function of the first kind of order n, n is the harmonic number. Equation (6) is referred as the Fubini solution. The Fubini solution is valid in the preshock region for values of $\sigma \leq 1$. The pressure solution is clearly in terms of Fourier components B_n, with each component's amplitude defined in terms of Bessel functions according to $B_n = 2J_n(n\sigma)/n\sigma$. As σ approaches 1, more n^{th} order Bessel functions are non-negligible, and therefore more Fourier components are included in the solution.

Beyond the shock, the Fubini solution produces the multivalued waveform. So weak shock theory is employed to find a solution; however, the resulting analytical solution takes an integral form. For the values σ>3, the following explicit solution[10] is given:

$$\frac{p}{p_0}=\sum_{n=1}^{\infty}\frac{2}{n(1+\sigma)}\sin n\omega_0 t' \quad \ldots (7)$$

A2. For Lossy medium

The Burger's equation in equation (4) describes the propagation of nonlinear progressive waves in an absorbing medium. A general solution to the Burgers' equation for a sinusoidal driving pressure, derived by transforming the nonlinear equation into a linear diffusion equation via the Hopf-Cole transformation discussed in[9] is given as:

$$\frac{p}{p_0}=\frac{-4}{\Gamma}\frac{\sum_{n=1}^{\infty}n(-1)^n I_n(\Gamma/2)\exp\left(-n^2\sigma/\Gamma\right)\sin n\omega_0 t'}{I_0(\Gamma/2)+2\sum_{n=1}^{\infty}n(-1)^n I_n(\Gamma/2)\exp\left(-n^2\sigma/\Gamma\right)\cos n\omega_0 t'} \quad \ldots (8)$$

where I_n is the modified Bessel function of the first kind of order n, $\Gamma = 1/\alpha_0 \bar{z}$ is the Gol'dberg number which indicates the ratio of nonlinearity to absorption of medium. This solution is converges very slowly when Γ>>1 (strong nonlinear medium), so the following Fay's equation can be used for Γ>>1 and σ>3[10]

$$\frac{p}{p_0} = \frac{2}{\Gamma}\sum_{n=1}^{\infty}\frac{\sin n\omega_0 t'}{\sinh\left[n(1+\sigma)/\Gamma\right]} \quad \ldots (9)$$

B. Time domain Method

Lee *et al*[8] developed the solution of KZK equation exclusively in time domain for pulsed finite amplitude sound beams radiated from axisymmetric sources in homogeneous thermoviscous fluids popularly known as Texas code. It also includes effects due to multiple relaxation phenomena, each of which introduces dispersion as well as absorption, with time-domain calculations.

We used the same approach modified for Burgers' equation to model the plane wave propagation in nonlinear, thermoviscous medium.

Equation (4) is solved in the following dimensionless form of the equation:

$$\frac{\partial p}{\partial \sigma} = P\frac{\partial P}{\partial \tau} + \frac{1}{\Gamma}\frac{\partial^2 P}{\partial \tau^2} \quad \ldots (10)$$

where $P(\sigma,\tau) = p/p_0$, p_0 is the peak source pressure, σ=z/$\bar{z}$, $\bar{z} = \rho_0 c_0^3/\beta\omega_0 p_0$ is the shock formation distance for plane wave, $\tau = \omega_0 t'$, $\Gamma = 1/\alpha\bar{z}$ is the Gol'dberg number, $\alpha = \delta\omega_0^2/2c_0^3$ the thermoviscous attenuation of medium at frequency ω_0.

Using the Lee and Hamilton methodology, the transformed equation is decomposed in the following equations:

$$\frac{\partial p}{\partial \sigma} = P\frac{\partial P}{\partial \tau} \quad \ldots (11)$$

and $$\frac{\partial p}{\partial \sigma} = \frac{1}{\Gamma}\frac{\partial^2 P}{\partial \tau^2} \quad \ldots (12)$$

Equations (11) and (12) are solved independently over each incremental step size Δσ.

Equation (11) is satisfied by the Poisson solution for propagation of the waveform from σ to σ+Δσ

$$P(\sigma+\Delta\sigma,\tau) = P(\sigma,\tau+P\Delta\sigma) \quad \ldots (13)$$

for $\tau_i^{k+1} = \tau_i^k - P_i^k\Delta\sigma$ where i is the i[th] sample of the time waveform and k is the k[th] step in σ. The step size is restricted to $\Delta\sigma < \Delta\tau/\max(P)$ to avoid the multivalued waveforms. Linear interpolation is used to resample the waveform and thus reestablish a uniform time sample spacing Δτ (time sample increment).

Equation (12) is solved using the Crank Nicholson Finite Difference (CNFD) method with standard forward-space, centered time finite differences.

3. Results and Discussions

The results of numerical simulations of field of plane circular transducer are presented here for both lossy and lossless medium using both analytical method and time domain methods. The simulation parameters used in both lossy and lossless medium cases are similar. The code for both analytical and time domain solutions of Burgers' equation has been written in MATLAB.

A. For Lossless medium

The simulation parameters used are given as below:

For soft human tissues, β=4.5 (with low fat content), acoustic speed c_0=1540 m/sec, density ρ=1000 kg/m^3. The initial function at z=0 is represented by $p = p_0 \sin\omega_0 t$ with central transducer frequency f_0=2 MHz. The source is assumed to be placed at centre of the coordinate system. The calculated shock formation distance $\bar{z}$ at p_0=5MPa is 12.9 mm.

A1. Analytical Solution

Waveforms at various distances from the source along z-axis generated using analytical solution of Burgers' equation are shown in Fig. 4). Comparison of magnitude variation of (i) fundamental, (ii) second and (iii) third harmonic for lossless medium (analytical solution) are shown in Fig. 5)

A2. Time domain solution:

Waveforms at various distances from the source along z-axis generated using time domain solution of Burgers' equation are shown in Fig. 6. Comparison of magnitude variation of (i) fundamental, (ii) second and (iii) third harmonic for lossless medium (time domain solution) are shown in Fig. 7.

Fig.4 and 6 shows the behavior of acoustic sine wave propagation from plane circular piston source in tissue medium and frequency spectrum of the respective waveform as well. It is observed from

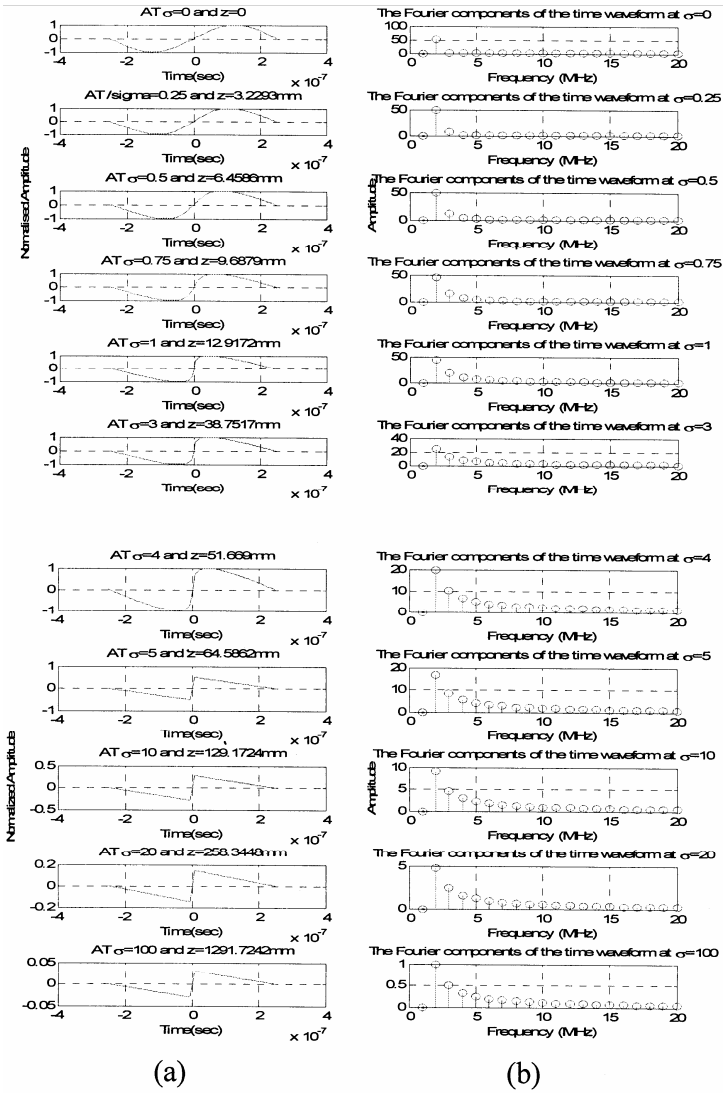

Fig. 4—Waveforms at various distances from the source along z-axis generated using analytical solution of Burgers' equation. . Fubini's equation in preshock region ($z \le \bar{z}$) while weak shock theory for $z > 3\bar{z}$ (a) shock formation along the direction of propagation, (b) Fourier components of the corresponding waveform showing harmonics generated, in lossless medium.

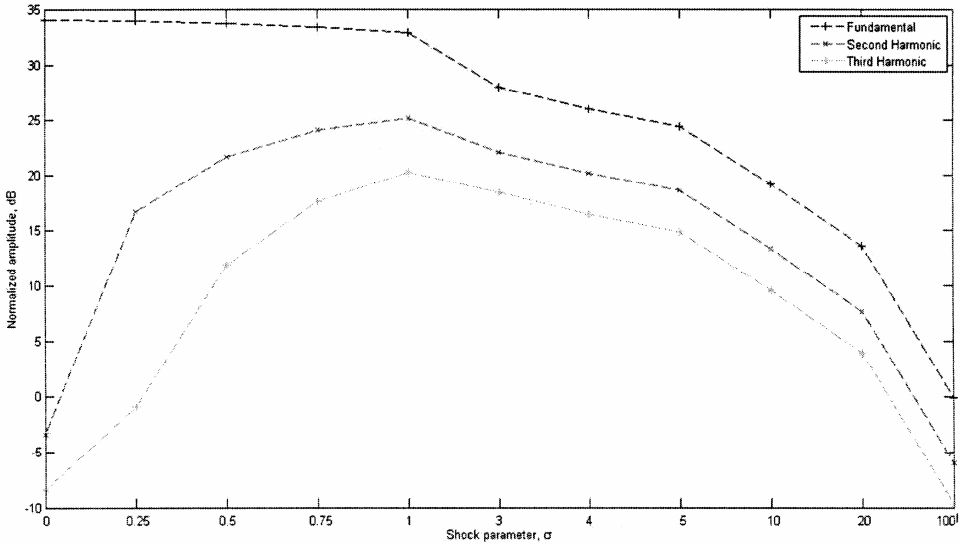

Fig. 5—Comparison of magnitude variation of (i) fundamental, (ii) second and (iii) third harmonic for lossless medium (analytical solution)

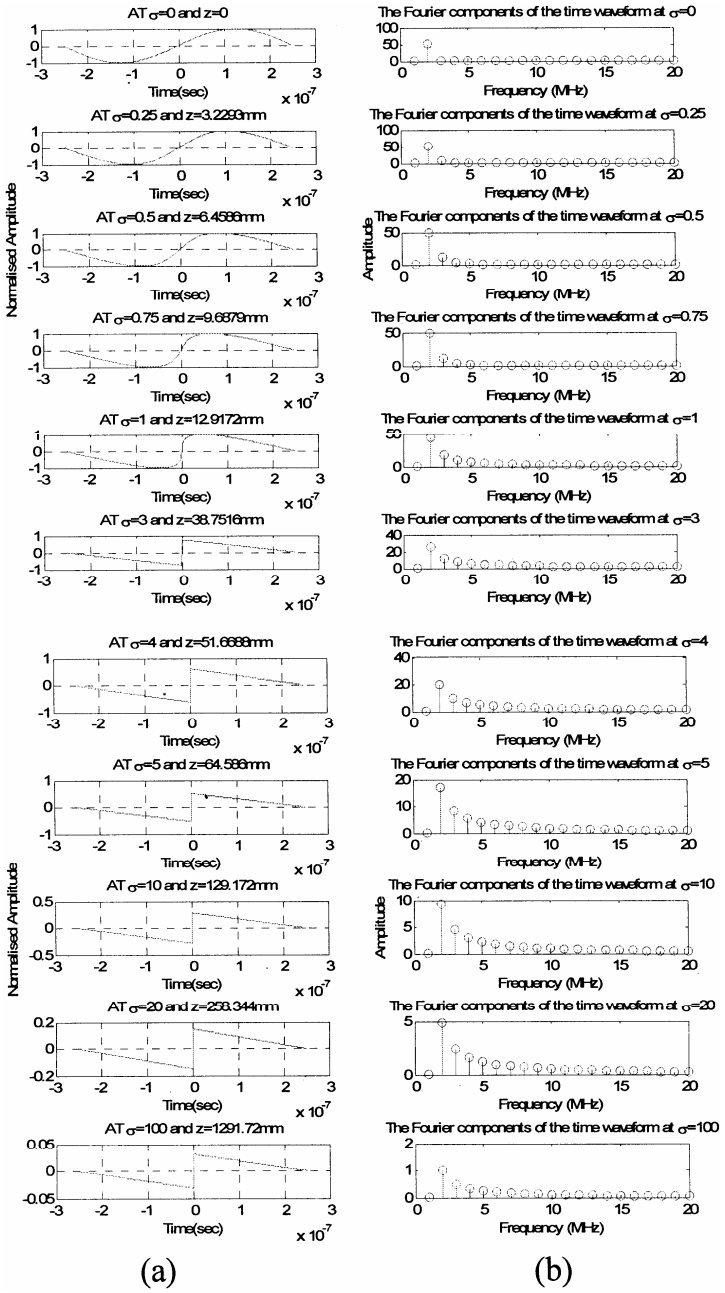

Fig. 6—Waveforms at various distances from the source along z-axis generated using time domain solution of Burgers' equation (a) shock formation along the direction of propagation, (b) Fourier components of the corresponding waveform showing harmonics generated, in lossless medium.

Fig.4 and 6 that the sine wave starts to change progressively at t=τ=0 and changes gradually towards sawtooth shaped shock waveform as it propagates in the z direction. A wave enriches in harmonics progressively with increase in z. In Fig. 4, the Fubini (equation 6) and weak shock theory (equation 7) solutions, each holds in a different region of the flow; the Fubini solution close to the source as shocks begin to form and the weak shock theory solution far from the source as shocks begin to decay. In Fig.6, the progressive conversion of sine wave to sawtooth wave using time domain method is shown. In time domain algorithm, the absorption flag set to zero while nonlinear term of dimensionless Burgers' equation is evaluated analytically in time domain. Fig.4 and 6 indicates that as the shock wave propagates, dissipation of energy occurs even no absorption is included in analytical method and time domain

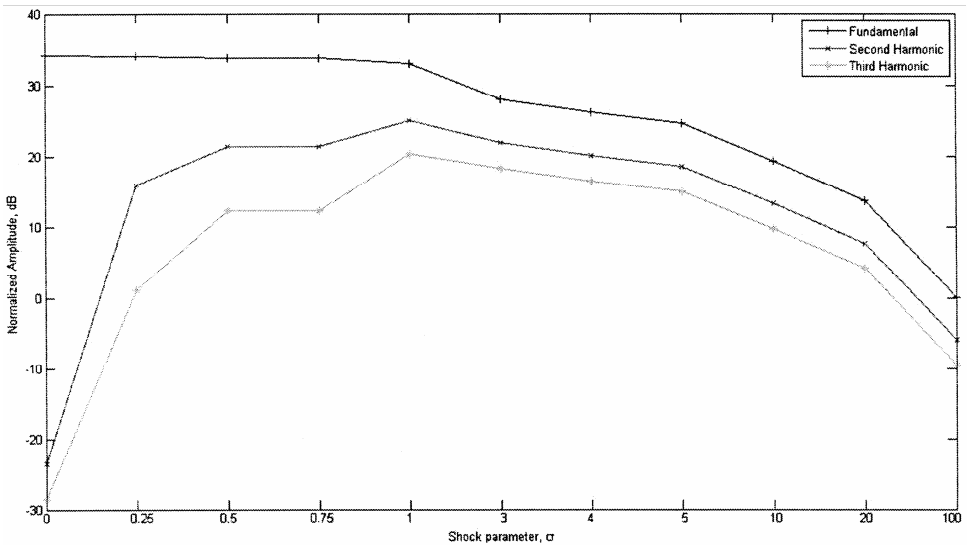

Fig. 7—Comparison of magnitude variation of (i) fundamental, (ii) second and (iii) third harmonic for lossless medium (time domain solution)

method. This happens because of finite amplitude effects generates multivalued waveforms which are corrected here by weak shock theory. Weak shock theory converts the multivalued waveforms into single valued waveforms by inserting pure shocks. According to weak shock theory, the location and amplitude of shock are determined by using Rankine-Hugoniot relations and correctly include the amount of energy dissipation at the shock. The weak shock theory is accounted analytically to include the propagation for σ>1in equation (7) by using equal area rule. While in case of time domain method, the weak shock theory is explicitly applied.

Fig. 5 and 7 shows the variation of harmonics amplitude with respect to distance of wave propagation. The acoustic field distortion numerically mainly depends on nonlinearity parameter β or the indirect parameter Gol'dberg number Γ. As shown in Fig.5, as z increases the magnitude of fundamental reduces while the amplitudes of second and third harmonics increases till the shock formation distance later they also starts reducing. The fundamental wave shows extra dissipation of energy which is transformed into harmonic waves according to the law of energy conservation.

B. For Lossy medium

The frequency dependant attenuation α [dB/mm] is generally described by following equation[12]:

$$\alpha = af^b \qquad \ldots (10)$$

where f is the transducer central frequency, exponent value *b* is widely taken as 1 for biological tissues at frequencies less than 10 MHz. The value of *a* for soft tissues is taken as 0.3 dB/cm-MHz.

For soft human tissues again, β=4.5 (with low fat content), acoustic speed c_0=1540 m/sec, density ρ=1000 kg/m^3. The initial function at z=0 is represented by $p = p_0 \sin \omega_0 t$ with central transducer frequency f_0=2 MHz. The source is assumed to be placed at centre of the coordinate system. The calculated shock formation distance $\bar{z}$ at p_0=5MPa is 12.9 mm and Gol'dberg number Γ =11.22.

B1. Analytical solution

Waveforms at various distances from the source along z-axis generated using analytical solution of Burgers' equation in lossy mediumare shown in Fig. 8. Comparison of magnitude variation of (i) fundamental, (ii) second and (iii) third harmonic for lossy medium at Γ=11.22 are shown in Fig. 9.

Waveforms at various distances from the source along z-axis generated using time domain solution of Burgers' equation in lossy medium is shown in Fig.10. Comparison of magnitude variation of (i) fundamental, (ii) second and (iii) third harmonic for lossless medium at Γ=11.22 are shown in Fig.11.

Fig. 8 and 10 shows the shock formation and their respective frequency spectrum shows harmonics generation by using analytical and time domain method respectively. In thermo viscous medium, the distortion of wave depends on Gol'dberg number (Γ) which is the ratio on nonlinearity to the dissipation of the medium. Here too as the sine wave propagates, it distorts and enriches in harmonics. In shock transition region i.e. 1<σ<3, very small change in any dependent variable gives high alterations in the waveform and

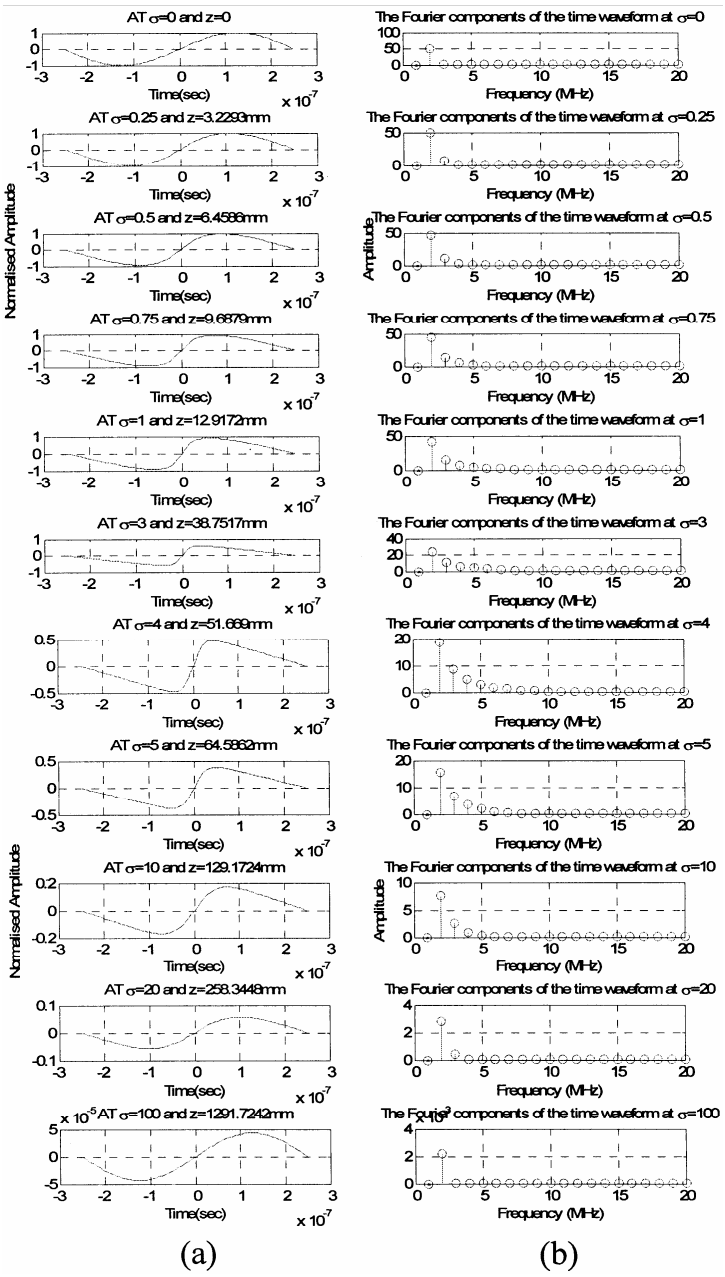

Fig. 8—Waveforms at various distances from the source along z-axis generated using analytical solution of Burgers' equation. Linear diffusion equation via the Holf-Cole transformation in preshock region ($z \le \bar{z}$) while Fay's equation for $z > 3\bar{z}$ (a) shock formation along the direction of propagation, (b) Fourier components of the corresponding waveform showing harmonics generated, in lossy medium.

harmonic content. In Fig. 8, the explicit method (equation 8) is applied in the region for σ<1 and Fay method (equation 9) for σ>3 to solve the Burgers' equation. The explicit solution is valid for all distance values but its convergence is slow if Γ>>1. In fig. 10, the time domain solution of Burgers' equation is shown at calculated value of Γ=11.22 which is the ratio of dimensionless absorption coefficient and nonlinearity coefficient.

In Fig. 9 and 11, it is seen that amplitudes of fundamental, second and third harmonics increases in the preshock region while start reducing in the postshock region and gradually decreases. As shown in Fig.8 and 10, the sine wave converted into sawtooth wave at $z = \bar{z}$ and the harmonics generated will contribute heavy attenuation because of its frequency dependence. So now the wave will be attenuated speedily. Still the healthy shock and

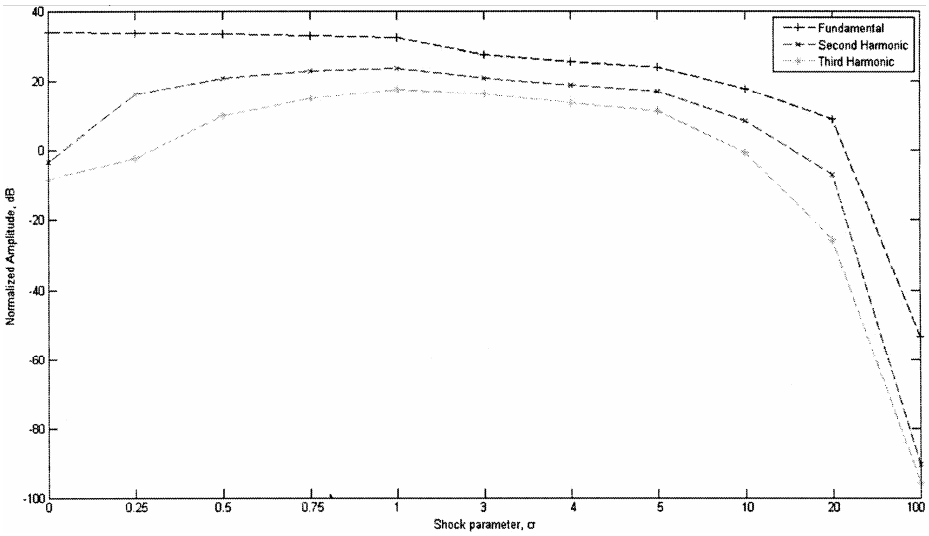

Fig. 9—Comparison of magnitude variation of (i) fundamental, (ii) second and (iii) third harmonic for lossy medium at Γ=11.22

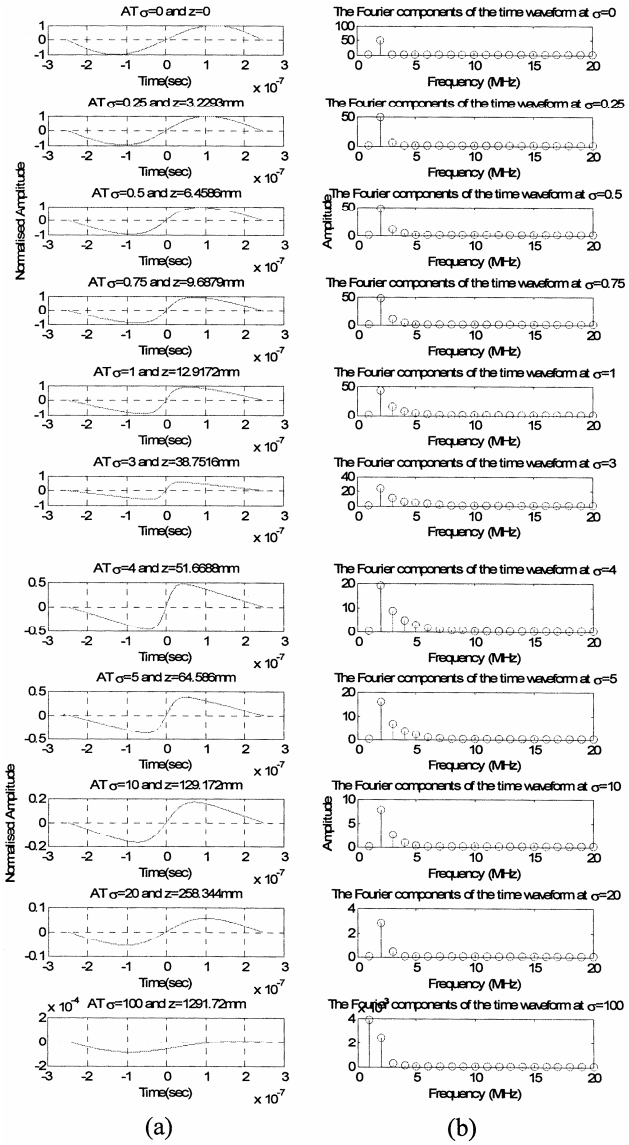

Fig. 10—Waveforms at various distances from the source along z-axis generated using time domain solution of Burgers' equation. (a) shock formation along the axis of propagation, (b) Fourier components of the corresponding waveform showing harmonics generated, in lossy medium.

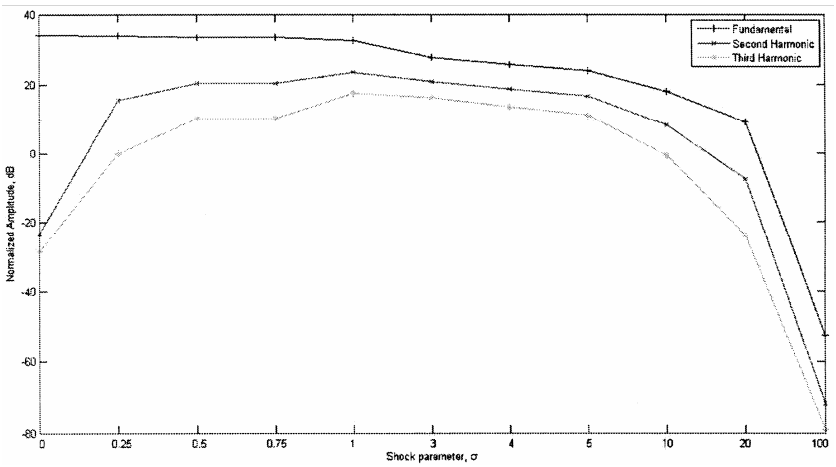

Fig. 11—Comparison of magnitude variation of (i) fundamental, (ii) second and (iii) third harmonic for lossless medium at Γ=11.22

harmonics are present in the medium up to σ=5. So the harmonic imaging is possible till the harmonics present in the medium and transducer need to be quite sensitive up to a particular distance. Later the absorption eventually reduces the amplitude of the waveform, the nonlinearly generated harmonics are lost and the wave regains its sinusoidal shape as shown in Fig.8 and 10.

4. Comparison of two methods

The results of numerical simulations of the nonlinear acoustic field propagation in lossy and lossless tissue medium conditions are presented here and comparison has been done for both analytical and time domain method in Figs. 12, 13 and 14. The Fig. 12 shows comparison of amplitude variations of fundamental and first two harmonics (second and third) for both lossless and lossy mediums. Axial distributions of harmonics calculated by time domain algorithm are in good agreement with analytical solutions at all ranges shown. Some discrepancies are observed in numerical results at the distances very close to the source. Fig. 13 and 14 are pressure-time waveforms calculated at dimensionless distance σ=1 and σ=5 i.e. at exact shock formation distance and five times of it away from the source. The results of both methods are in excellent agreement at σ=1, even both curves are indistinguishable visually at σ=1 while at σ=5 peak amplitude difference is present.

5. Conclusions

In this paper, two theoretical models are presented for the description of nonlinear ultrasound wave propagation in biological tissues. In the available literature, many researchers analyzed the shock formation but in water medium only while in this paper the methods are applied to soft tissue medium

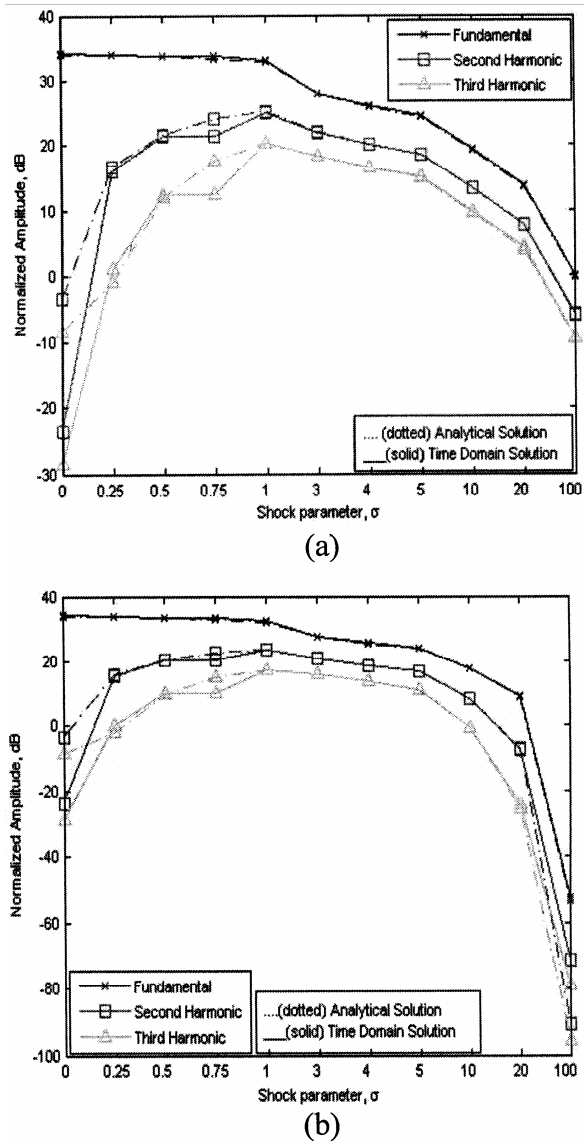

Fig. 12—Comparison of analytical method and time domain method solution of Burgers' equation. Shock parameter σ is chosen within 0 to 100. (….dotted lines) Analytical solution and (____solid lines) Time domain solution. (a) lossless medium (b) lossy medium

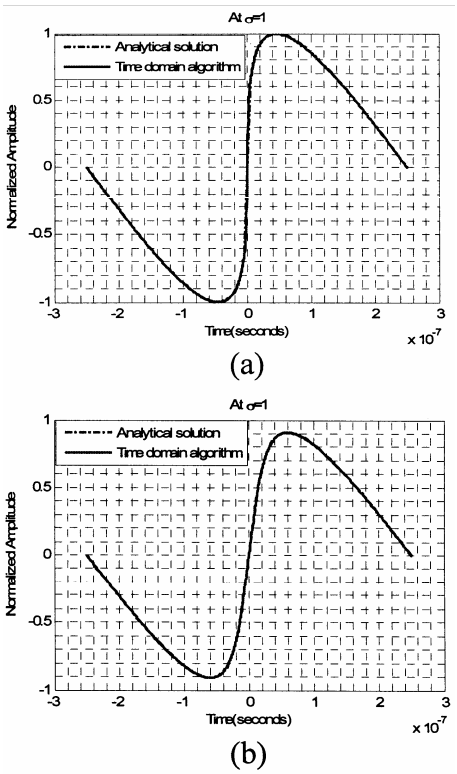

Fig. 13—Comparison of analytical method and time domain method solution of Burgers' equation. Shock parameter σ=1. (….dotted lines) Analytical solution and (____solid lines) Time domain solution. (a) lossless medium (b) lossy medium

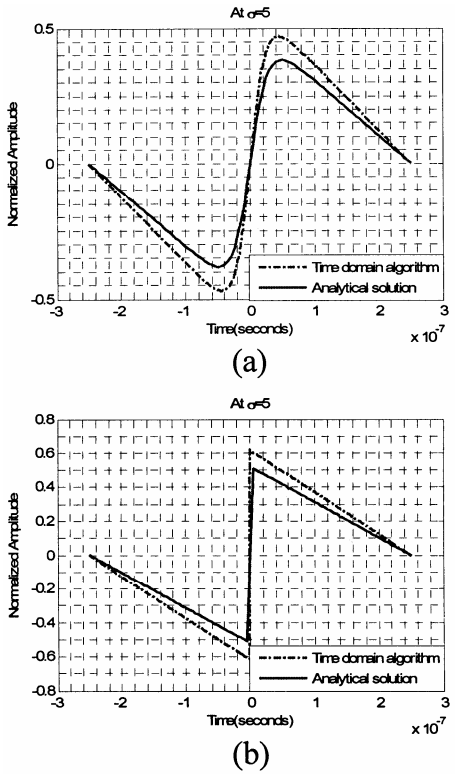

Fig. 14—Comparison of analytical method and time domain method solution of Burgers' equation. Shock parameter σ=5. (….dotted lines) Analytical solution and (____solid lines) Time domain solution. (a) lossless medium (b) lossy medium

and codes are written in MATLAB as well. It is demonstrated that shock formation and propagation plays a very important role in ultrasonic diagnosis of human physiology. Nonlinearity of medium generates harmonics which helps in enhancing the image quality. The harmonics are produced till the shock persist i.e. after particular distance the harmonics will not be present and the reflected harmonic signals will be of very low amplitude and may not be easy to pick up them by the transducer. So the distance of propagation will be less in harmonic imaging as compared to fundamental imaging. The numerical simulations give the understanding of the behavior of ultrasound wave propagation in tissues. Time domain approach enables us to effectively simulate nonlinear waves with shocks at all ranges even in the shock transition region.

References

1 Averkiou, M. A., "Tissue harmonic imaging," IEEE Ultrason. Symp. Proc., 1561-1566, 2000.

2 De Jong, N., Cornet, R., Lancee, C. T., "Higher harmonics of vibrating gas-filled microspheres. Part one: Simulations," Ultrasonics 32:447–453, 1994a.

3 Duck, F. A., "Nonlinear acoustics in diagnostic ultrasound," Ultrasound in Med. and Biol., Vol. 28, No. 1, pp. 1–18, 2002.

4 Humphrey, V. F., "Nonlinear propagation in ultrasonic fields: Measurements, modeling and harmonic imaging," Ultrasonics 38, 267-272, 2000.

5 Beyer, R. T., "Parameter of nonlinearity in fluids," J. Acoust. Soc. Am., 32:719–721, 1960.

6 Errabolu, R. L., Sehgal, C. M., Bahn, R. C., Greenleaf, J. F. "Measurement of ultrasonic nonlinear parameter in excised fat tissues," Ultrasound Med Biol.,Vol. 14:137–146, 1988.

7 Sehgal, C. M., Brown, G. M., Bahn, R. C., Greenleaf, J. F., "Measurement and use of acoustic nonlinearity and sound speed to estimate composition of excised livers," Ultrasound Med Biol., 12:865–874, 1986.

8 Lee, Y. S., Hamilton, M. F., "Time-domain modeling of pulsed finite-amplitude sound beams," J. Acoust. Soc. Am., vol. 97, pp. 906–917, 1995.

9 Blackstock, D. T., "Conection between the Fay and Fubini solutions for plane sound waves of finite amplitudes," J Acoust. Soc Am., 39:1019-1026, 1966.

10 Blackstock, D. T., "Thermoviscous attenuation of plane, periodic, finite amplitude sound waves," J Acoust. Soc Am., 36(3):534–542, 1964.

11 Cleveland, R. O.,Hamilton, M. F. and Blackstock, D. T., "Time domain modeling of finite amplitude sound in relaxing fluids" , J Acoust. Soc Am., 99(6):3312-3318, 1996.

12 Nakajima, K., Kudo, N., Yamamoto, K., Mikami, T., and Kitabatake, A., "A study of frequency dependence of ultrasound attenuation of biological tissues in the frequency range of 2-40 MHz," IEEE Ultrasonics Symposium, pp. 1381-1384, 1999.

J. Pure Appl. Ultrason. 33 (2011) pp. 88-91

Compatibility studies and evaluation of ultrasonic velocity and percentage deviation of ternary mixture of cyclohexane, toluene and 2-propanol at 303.15 k & 308.15 k.

[1]J. Thennarasu, [2]G. Meenakshi

[1]Assistant Professor, Physics, Sri Aravindar Engineering College, Villupuram

[2]Associate Professor, Physics, KMCPGS, Govt. of Pondicherry. Pondicherry

In recent years ultrasonic investigation of critical phenomena in ternary mixtures of liquids have been the subject of intensive research of both theoreticians and experimentalists. Particularly the Anomalous increase of Ultrasound attenuation near the critical region of ternary liquid mixtures has been widely studied. The experimental study of the above liquids have been carried out at 303.15 K & 308.15 K and the data can be described with its compatibility studies over a wide range of composition ranging from 0-100% of above different liquids. The result of ultrasonic velocity and its derived percentage deviation have been used to discuss the statistical approach of the blend under study. These discussion revealed that the blend is weakly polar in an ideal mixing relation. Using this data, the interaction parameters of molecular radius (r_m), molar sound velocity (R_{mix}) and molar volume (V_{mix}) were computed. The ultrasonic velocity results are further confirmed by density and percentage deviation results. For the ternary mixtures, the observed results shows that the Nomoto method seems to give good results for the evaluation and compared to Van-Dael's method.

Keywords: Ternary Mixtures, Acoustical Parameters, Ultrasonic Velocity, Polar liquids, Molecular interactions

1. Introduction

With the growth of scientific knowledge, it became increasingly necessary to specialize in the theoretical and experimental investigation by putting much effort. The material structures and contents may be achieved only if the scientist knows about theoretical background and technological aspect of the materials to be studied. Hence it is decided to evaluate the theoretical parameters of the selected components, when it is exposed to ultrasonic waves.

The ultrasonic wave through the solution is used for knowing the nature and strength of intermolecular interaction in pure liquids and the mixtures. The Ultrasonic velocity in three ternary liquid mixtures of cyclohexane, toluene and 2-propanol have been measured by Kannappan and V. Rajendran[1] of different proportions and also compared the relative merits of Flory's statistical theory and junjie's thermo dynamical approach for theoretical evaluation of sound velocity in mixtures. Nomato and bhimseenachel et al made successful attempts to evaluate the sound velocity on ternary liquid mixtures. Van Dael ideal mixing relation has also been carried out successfully to investigate the acoustical behavior. For theoretical evaluation of sound velocity; other researcher found that Van Deal ideal mixing relation gives minimum deviation from the experimental values.

In this paper a comparative study[2] of relative merits of the different methods becomes essential and the present work has been attempt in this direction. In this paper, it is aimed to find the suitable theoretical[3] method to evaluate the sound velocity on ternary mixtures of cyclohexane + toluene + 2-propanol at the temperature of 303.15 k & 308.15 k.

2. Theoretical studies

Nomoto's empirical formula for sound velocity in ternary liquids mixtures in terms of molar sound velocity R_{mix} and molar volume V_{mix} as

$$U_{mix} = \left\{ \frac{R_{mix}}{V_{mix}} \right\}^3 \quad \ldots (1)$$

$$U_{mix} = \left\{ \frac{X_1R_1 + X_2R_2 + X_3R_3}{X_1R_1 + X_2R_2 + X_3R_3} \right\}^3 \quad \ldots (2)$$

where,

$$R = \left(\frac{M}{\rho} \right) \; U^{1/3} \quad \ldots (3)$$

where, R Rao's constant
X_1, X_2, X_3 Concentration of first, second & third Liquids.
V_1, V_2, V_3 Sound Velocity
ρ Density of Liquids.

Van-Deals expression for sound velocity in ternary mixtures is

$$\frac{1}{X_1M_1 + X_2M_2 + X_3M_3}\frac{1}{(U_{im})^2} = \frac{X_1}{M_1U_1^{\,2}} + \frac{X_2}{M_2U_2^{\,2}} + \frac{X_3}{M_3U_3^{\,2}} \quad \ldots (4)$$

Schaff's and Nutsch – Kunhkies expression for sound velocity in ternary liquid mixture is

$$U_{mix} = U\alpha\{X_1S_1 + X_2S_2 + X_3S_3\}\left(\frac{X_1B_1 + X_2B_2 + X_3B_3}{Vm}\right) \quad \ldots (5)$$

where,

$U\alpha = 1600\ ms^{-1}$

S_1, S_2, S_3 & B_1, B_2, B_3 are collision factors and actual volume of the molecules per mole of first, second and third components respectively.

r_m – molecular radius which can be obtained from the formula

$$d^{5/2} = \frac{1}{7.2\times10^3}\ \frac{V\sigma^{1/4}}{T_C^{\,1/4}} \quad \ldots (6)$$

σ = Surface tension

The degree of intermolecular attraction α is given by

$$\alpha = \frac{U_{exp}^{\ 2}}{U_{im}^{\ 2}} - 1 \quad \ldots (7)$$

The experimental value of ultrasonic velocity and density of the ternary mixtures cyclohexane + toluene + 2-propanol are taken from the work of G. Arul et al[4].

3. Results and discussions

Ultrasonic velocity and density[5] for the pure components: cyclohexane, toluene, and 2-propanol are given in Table 1. Ultrasonic velocity experimental and theoretical derivation of ternary mixture cyclohexane + toluene + 2-propanol at the temperature of 303.15 k & 308.15 k is evaluated in Table 2 & 3.

The percentage deviations of theoretically calculated[6] ultrasonic velocity from the experimental results are also given in Table 1 & 2. The calculated values of $(U_{exp}^{\ 2}/U_{idl}^{\ 2})$, alpha, excess velocity (U^E), excess impedance Z^E and excess volume V^E with mole fraction are given in Table 4 & 5.

From Tables 2 & 3 it is observed that the average percentage deviation of the calculated values of sound velocity from the experimental values at 303.15K & 308.15K shows that the Collision factory theory[7] and Nomoto's method are in better agreement with the experimental values followed by ideal mixing relation.

Cyclohexane is a Non-polar liquid[8] whereas toluene is a weakly Polar and 2-Propanol is a polar liquid. The calculated values of alpha, excess velocity, and excess impedance are positive and decrease with increase in concentration of 2-ol[9] whereas the excess volume is negative. The Negative

Table 1—Ultrasonic velocity & Density of pure Components for ternary mixtures at 303.15 K & 308.15K

Component	303.15 K		308.15K	
	Density (ρ) 10^3 kg m^3	Velocity (V) ms^{-1}	Density (ρ) 10^3 kg m^3	Velocity (V) ms^{-1}
Cyclohexane	766.9	1229.5	767.7	1230.3
Toluene	587.8	1285.3	857.8	1287.2
2-Propanol	762.1	1112.0	762.1	1112.0

Table 2—Ultrasonic velocity and percentage deviation of the ternary mixture cyclohexane + toluene + 2-Propanol at 303.15k

Mole fraction (x_1)	Mole fraction (x_3)	Density ρ_{mix}^{*} (kg m^3)	Ultrasonic Velocity U_{Expt}^{*} (ms^{-1})	U_{nomoto} (ms^{-1})	$U_{Van\text{-}dael}$ (ms^{-1})	U_{cft} (ms^{-1})	Percentage Deviation (ΔU/U) Nomoto	(ΔU/U) VanDael	(ΔU/U) Cft
0.5000	0.0990	798.53	1208.6	1244.2	1221.7	1243.9	-2.94	-1.09	-2.02
0.3990	0.2020	800.69	1205.8	1234.7	1196.8	1234.1	-2.40	0.74	-2.35
0.3000	0.3000	802.95	1201.3	1225.4	1176.7	1224.5	-2.01	2.04	-1.93
0.2000	0.3990	806.97	1197.2	1215.5	1159.5	1214.3	-1.53	3.15	-1.43
0.0990	0.4990	810.13	1194.2	1204.9	1144.8	1203.5	-0.89	4.14	-0.78
0.0000	0.6008	813.54	1190.6	1193.1	1132.4	1191.6	-0.21	4.89	-0.09
							-1.66	2.31	-1.58

X_1, X_3 - refers mole fractions of cyclohexane & 2-propanol
*-Experimental values taken from the work of G.Arul et al[3].

Table 3—Ultrasonic velocity and percentage deviation of the ternary mixture cyclohexane + toluene + 2-Propanol at 308.15k

Mole fraction (x_1)	Mole fraction (x_3)	Density ρ_{mix}* (kg m^3)	Ultrasonic Velocity U_{Expt}* (ms^{-1})	U_{nomoto} (ms^{-1})	$U_{Van\text{-}dael}$ (ms^{-1})	U_{cft} (ms^{-1})	Percentage Deviation (ΔU/U) Nomoto	(ΔU/U) VanDael	(ΔU/U) Cft
0.5000	0.0990	794.37	1197.8	1228.3	1206.0	1228.1	-2.55	0.69	-2.53
0.3990	0.2020	794.98	1191.1	1219.2	1181.7	1218.7	-2.36	0.79	-2.31
0.3000	0.3000	797.78	1182.5	1210.3	1162.0	1209.4	-2.35	1.73	-2.28
0.2000	0.3990	802.30	1179.6	1200.8	1145.2	1199.6	-1.79	2.92	-1.70
0.0990	0.4990	807.43	1172.9	1190.5	1130.8	1189.2	-1.50	3.59	-1.39
0.0000	0.6008	810.97	1169.6	1179.2	1118.7	1177.7	-0.82	4.36	-0.69
			Average				-1.90	2.12	-1.81

X_1, X_3 - refers mole fractions of cyclohexane & 2-propanol
*- Experimental values taken from the work of G.Arul et al[3].

Table 4—Excess parameters in the Ternary Mixtures of Cyclohexane + toluene + 2-propanol – 303.15k

Mole fraction (x_1)	Mole fraction (x_3)	Ultrasonic Velocity (U_{idl} ms^{-1})	$\frac{U_{Expt}^2}{U_{idl}^2}$	Alpha	Excess Velocity (V^E) ms^{-1}	Excess impedance (Z^E) 10^3kg m^{-2} s^{-1}	Excess Volume (V^E) 10^{-3} m^3 ms^{-1}
0.5000	0.0990	1241.41	0.4138	-0.5862	-442.88	-54.42	0.7246
0.3990	0.2020	1229.11	0.4244	-0.5756	-428.42	-44.10	0.4869
0.3000	0.3000	1217.57	0.4349	-0.5651	-414.62	-34.75	0.2876
0.2000	0.3990	1205.92	0.4478	-0.5522	-398.98	-25.30	-0.1034
0.0990	0.4990	1194.14	0.4603	-0.5397	-384.01	-15.76	-0.3606
0.0000	0.6008	1181.94	0.4738	-0.5262	-368.40	-05.43	-0.6630

X_1, X_3 - refers mole fractions of cyclohexane & 2-propanol

Table 5—Excess parameters in the Ternary Mixtures of Cyclohexane + toluene + 2-propanol – 308.15k

Mole fraction (x_1)	Mole fraction (x_3)	Ultrasonic Velocity (U_{idl} ms^{-1})	$\frac{U_{Expt}^2}{U_{idl}^2}$	Alpha	Excess Velocity (V^E)ms^{-1}	Excess impedance (Z^E) 10^3kg m^{-2} s^{-1}	Excess Volume (V^E) 10^{-3} m^3 ms^{-1}
0.5000	0.0990	1225.67	0.4201	-0.5799	-431.30	-56.69	0.7415
0.3990	0.2020	1213.75	0.4290	-0.5710	-418.77	-46.92	0.7233
0.3000	0.3000	1202.59	0.4401	-0.5594	-404.81	-38.09	0.4670
0.2000	0.3990	1191.32	0.4535	-0.5465	-389.02	-29.18	0.0266
0.0990	0.4990	1179.93	0.4683	-0.5317	-372.50	-20.17	-0.4435
0.0000	0.6008	1168.10	0.4820	-0.5180	-357.13	-10.37	-0.7368

X_1, X_3 - refers mole fractions of cyclohexane & 2-propanol

excess volume indicates the formation of molecular clusters and complexes and may involve even charge transfer complexes[10]. As the components have poor and zero dipole moments, the dipole-dipole interaction is weak in the pure state. The decrease in magnitude of the excess parameters suggests the close packing of molecules inside the shield, which may be brought about by the increasing magnitudes of interactions[11]. The positive and decreasesing excess parameters with increasing 2-ol concentration is due to a weak bond of a type between a conventional localized hydrogen bond and the formation of charge transfer complex occurring between the components of mixtures[11]. The excess volume studies also confirm the weakening of dipolar interaction between the components of the liquid mixture.

4. Summary and conclusion

In the ternary system cyclohexane + Toluene + 2-propanol, cyclohexane is a weakly polar liquid and Toluene is a non-polar and 2-propanol is a polar liquid. The excess studies confirm the weakening of dipolar interaction between the components of the mixtures. The increase of 2-ol concentration may cause charge transfer complexes due to the localized weak hydrogen bond between the components of the mixtures. The study gives quite satisfactory results with all the theories. Collision factor theory and Nomoto's methods are better agreement with the experimental values.

In this study a trial has been made to evaluate the theoretical parameters of ultrasonic waves when it passes through ternary liquid mixtures. Three methods have been chosen namely (Nomoto's method, Van

Dael's ideal method and Schaff's collision factor theory) for the theoretical evaluation. Also an attempt is made to identify the suitable method to compute the ultrasonic velocity theoretically. Suitable interpretations are based on hydrogen bonding of dipole-dipole interaction and charge transfer complexes. The work gives very interesting results and out of three different methods the Nomoto method is found to be the best for ternary mixturesdue to the closeness in values obtained with respect to the experiment.

References

1 Kannappan A.N. and Rajendiran.V., study of molecular interaction in ternary mixtures at 303K, 308K and 313K, *Indian journal of pure & Applied physics* 30(1992) 240-252.

2 Srinivasoly.U and Naidu P.R. volumetric and thermodynamic studies of molecular interaction in ternary liquid mixtures at different temperatures, *Journal of Pure & applied. ultrasonics,* 43 (1995)123

3 Fort R.T and Moore W.R. acoustical studies on binary liquid mixtures of some aromatic hydrocarbon at 303K, *Transfarady Soc.(Great Britain),* 61 (1965) 2102

4 Arul.G, molecular interaction studies with evaluation of ultrasonic velocity and percentage deviation of some ternary mixtures, *Physics of Ultrasonics*, 34 (1989)898

5 Prigogine.R, study of molecular interaction in ternary liquid mixtures by ultrasonic velocity measurements, *The molecular theory of solutions(North-Holand, Amsterdam)*, 4(1957)487

6 Letcher T.M and Nevine J.A, ultrasonic study of n-alkanes in toluene with benzene, *Journal of Chemical thermodynamics,* 26 (1994)697

7 Rajendiran.V & Christopher.R, study of molecular interaction in ternary mixtures *, Newton Benny Acoustics letters,* 17(1993)2

8 Palaniappan.L. ultrasonic studies in acoustical parameters, *Ph.d., ,thesis, Annamalai university*, 71(1998) 276-287

9 Eigen & meyer, ultrasonic velocity measurements in liquids with high-resolution techniques, selected application and percspectives, *Acoustics letters (in technique of organic chemistry)*, 8 (1963)859

10 Acoust R.P*,* thermodynamic properties of molecular interaction in ternary liquid mixtures, *Acoustics letters*, 6(1983)53

11 Scaff's .W ultrasonic study of binary mixtures at different temperatures, *Physics of Ultrasonics,* 4(1975) 69,110,114,115

12 Nomoto, deviation from linearity of the concentration dependence of the molecular sound velocity in liquid mixtures, *journal of pure & Applied physics* 13(1958)1528

J. Pure Appl. Ultrason. 33 (2011) pp. 92-95

An ultrasonic study of aqueous solutions of various drugs used for cough – Jacobson's theory of compressibility

N. Jaya Madhuri[1], J. Glory, P.S. Naidu And K. Ravindra Prasad

Department of Physics, S.V.U.P.G. Centre, Kavali - 524 201.

Email : nissi.joicy@gmail.com

Six drugs belonging to one class which are used for reducing cough have been chosen for an ultrasonic study. These solutions have in them as major components- Chlorpheniramine maleate / diphenydramine hydrochloride / ambroxol hydrochloride / terbutalline sulphate / codeine phosphate / herbal syrup. Ultrasonic velocity and density have been measured in the aqueous solutions of these systems at 303.15K. Deviations in velocity and compressibility have been computed. Also the effect of these systems on the structure of water has been analysed employing Jacobson's theory of adiabatic compressibilities.

Keywords: Ultrasonic velocity, adiabatic compressibility, Jacobson's theory, aqueous solutions, structural properties.

1. Introduction

Jacobson's theory of compressibilities[1] provides an easy and accurate method of determining the nature of the properties of solutes in their aqueous solutions even at a lower temperature (compared to TVM, TACM etc.,) provided higher concentrations are studied. For this, one needs the value of a dimensionless parameter μ (>1 structure breaker and <1 structure maker). This method has been employed by a few workers only in aqueous solutions of many organic liquids[2-8]. In our recent paper[8], a study of aqueous solutions of some ophthalmic solutions in aqueous medium has been made employing Jacobson's theory. The present investigation aims at an understanding of the structure making / breaking effect of various drugs used for cough in their aqueous solutions at 30^0C (303.15K). The six drugs commercially obtained have the major components as chlorpheniramine maleate (zencoff), diphenydramine hydrochloride (benadryl), ambroxol hydrochloride (ambrolite), terbutalline sulphate (bro-zedex), codeine phosphate (siricodin) and herbal syrup.

2. Experimental

Ultrasonic velocities were measured employing a single crystal variable path ultrasonic interferometer working at 2MHz with an accuracy of ± 0.05%. For density measurement, a double stem capillary type pyknometer was used, the accuracy being 2 parts in 10^5. Details of measurement are dealt with elsewhere[8].

3. Theoretical

According to Jacobson, the molecules of the solvent are bound to each other by association and the dissolved molecules also have an association tendency to the solvent, Now the compressibility of the resulting solution is

$$\beta = \nu \beta_2 + (1- \nu) \beta_1 + K \qquad \ldots (1)$$

where β_2, β_1 and β are the compressibilities of the solute, solvent and the solution respectively, ν, the volume fraction of the solute (ν = CV/1000, C, the weight fraction, V, the molar volume), K, the correction factor, given by (1- ν) (1-θ) Gζ. θ designates a hydrogen bonding factor which gives the fraction of bond between water and solute per molecular surface of the solute in relation to the mean value for water on an equally large inside surface of water at the given temperature. ζ is the change in compressibility following the breaking of hydrogen bond association from fully formed association at the given temperature. G is the ratio of the number of hydrogen bonds broken due to the addition of the solute to the number of hydrogen bonds present in water. Now with higher concentrations a certain amount of the surface of the solute will be ineffective in the breaking of hydrogen bonds, as the molecules of the surface will touch each other and do not come in to contact with the solvent. This reduction of total surface γ_2 is difficult to estimate depending interalia on the mutual association energy and form of the molecules. The surface tension should be a function of the total surface ν^{μ}, where μ is a constant for each substance and is always a positive quantity. μ is a constant giving the mutual association tendency of the dissolved molecules.

Substitution of $\frac{\nu(1-\nu^{\mu})}{1-\nu}$ B for in (1) yields

$$\beta = \nu\,\beta_2 + (1-\nu)\,\beta_1 + \nu\,(1-\nu^{\mu})((1-\theta)\,B\zeta \qquad \ldots (2)$$

Now $\Delta\beta = (\beta - \beta_2) = \beta$ solution $- \beta$ solvent and

$$\frac{\Delta\beta}{\nu} = (\beta_2 - \beta_1) + (1-\theta)\,(1-\nu^{\mu})B\zeta \qquad \ldots (3)$$

Now the slope of the plot $\frac{\Delta\beta}{\nu}$ against ν is obtained by

$$\frac{d}{d\nu}\left[\frac{\Delta\beta}{\nu}\right] = -\mu\,\nu^{\mu-1}(1-\theta)\,B\zeta = \Gamma \qquad \ldots (4)$$

Now if Γ_a, Γ_b are two slopes at different volume fractions ν_a and ν_b,

μ is given by $\mu = \frac{\log \Gamma_a / \Gamma_b}{\log \nu_a / \nu_b} + 1$

Now from the values of μ, one can determine whether the solute is a structure maker (μ < 1) or a structure breaker (μ > 1).

4. Results And Discussion

Ultrasonic velocity and density have been measured in aqueous solutions of all the six cough drugs as a function of the weight fraction of the solutes at 303.15K and the velocity is present in Fig. 1 against the weight fraction of the solute. Utmost care has been taken in measuring the velocity and density. Velocity change Δu ($u_{solution} - u_{solvent}$) is also plotted versus a weight fraction in Fig. 2. Fig. 3 portrays the behaviour of adiabatic compressibilility (β) versus weight fraction of the solutes. Change in compressibility Δ β, ($\beta_{solution} - \beta_{water}$) has also been shown in Fig. 4.

For all systems, velocity increases with weight fraction of the solute and deviation in velocity Δu is positive. Velocity is slightly greater in ambrolite and benadryl at lower concentrations of the solute and at higher concentration in zencoff and siricodin.

Table 1—Variation of ultrasonic velocity, density with volume fraction of solute in aqueous solutions at 30^0C

BENADRYL + WATER			ZENCOFF + WATER			AMBROLITE + WATER		
Weight fraction of solute	Velocity (ms^{-1})	Density x 10^3 ($kg\ m^{-3}$)	Weight fraction of solute	Velocity (ms^{-1})	Density x 10^3 ($kg\ m^{-3}$)	Weight fraction of solute	Velocity (ms^{-1})	Density x 10^3 ($kg\ m^{-3}$)
0.0000	1508	0.99567	0.0000	1508	0.99567	0.0000	1508	0.99567
0.1132	1542	1.03148	0.1132	1513	1.01630	0.1357	1539	1.01986
0.2034	1551	1.04825	0.2003	1522	1.02998	0.2390	1548	1.04092
0.2769	1557	1.06492	0.2731	1533	1.03743	0.3202	1554	1.05470
0.3380	1566	1.08535	0.3338	1543	1.04897	0.3858	1560	1.06433
0.3896	1569	1.09949	0.3851	1551	1.06064	0.4398	1566	1.07172
0.4337	1575	1.11465	0.4297	1558	1.06665	0.4851	1572	1.07861
0.4891	1581	1.11913	0.4844	1577	1.07645	0.5408	1578	1.08995
0.5610	1591	1.12285	0.5561	1589	1.08787	0.6109	1584	1.10389
0.7539	1615	1.12569	0.7451	1627	1.12568	0.7856	1609	1.13834
0.9199	1634	1.13105	0.9185	1657	1.16961	0.9339	1624	1.17885
TULSI + WATER			SIRICODIN + WATER			BRO-ZEDEX + WATER		
Weight fraction of solute	Velocity (ms^{-1})	Density x 10^3 ($kg\ m^{-3}$)	Weight fraction of solute	Velocity (ms^{-1})	Density x 10^3 ($kg\ m^{-3}$)	Weight fraction of solute	Velocity (ms^{-1})	Density x 10^3 ($kg\ m^{-3}$)
0.0000	1508	0.99567	0.0000	1508	0.99567	0.0000	1508	0.99567
0.1066	1520	1.01748	0.1531	1524	1.00634	0.1454	1528	1.0343
0.1927	1529	1.03445	0.2656	1536	1.01691	0.2574	1545	1.04995
0.2636	1538	1.04325	0.3517	1548	1.02970	0.338	1559	1.06039
0.3231	1549	1.04692	0.4197	1557	1.04464	0.4051	1567	1.07001
0.3737	1557	1.05107	0.4748	1566	1.07324	0.4598	1575	1.07777
0.4173	1562	1.05333	0.5203	1576	1.10231	0.5053	1581	1.08626
0.4723	1568	1.05840	0.5756	1585	1.12356	0.5607	1587	1.09511
0.5441	1577	1.06896	0.6439	1598	1.13952	0.6299	1594	1.10673
0.7357	1614	1.10977	0.8084	1639	1.15858	0.7988	1612	1.12635
0.9148	1647	1.15100	0.9421	1676	1.18098	0.9387	1625	1.12963

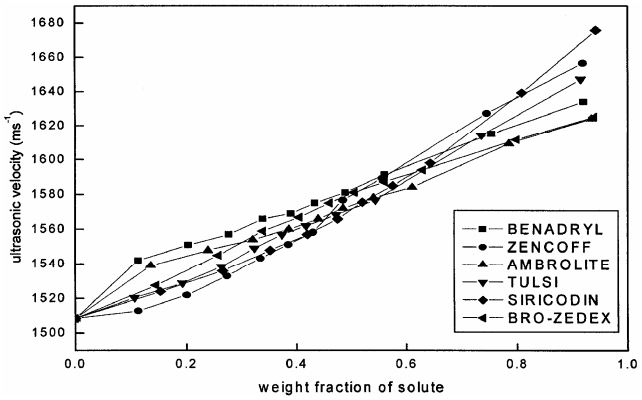

Fig. 1—Variation of ultrasonic velocity as a weight fraction of the solute in the aqueous solutions at 30 °C

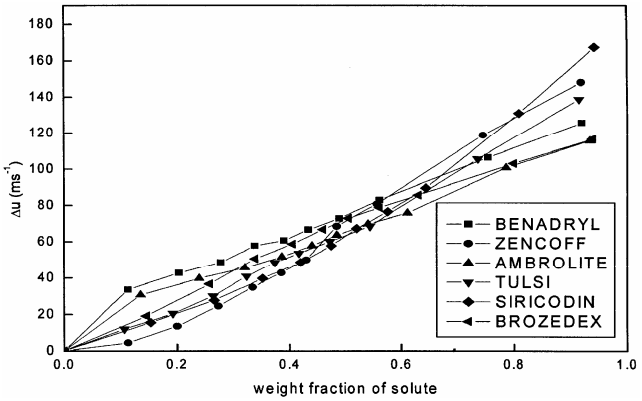

Fig. 2—Variation of deviation in velocity (Δu) with weight fraction of the solute in the aqueous solutions at 30 °C

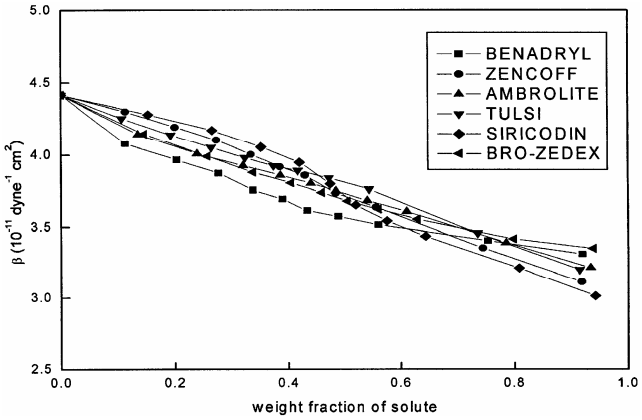

Fig. 3—Variation of adiabatic compressibility (β) with weight fraction of the solute in the aqueous solutions at 30 °C

At ~ 0.5 weight fraction concentrations of the solute, very nearly equal velocities are obtained. Adiabatic compressibility (β) shows decreasing trend with the concentration of all the solutes. Deviations or change in adiabatic compressibility (Δβ) is negative in all the aqueous solutions of all six drugs. Though the behaviour is the same in all the drugs i.e.,

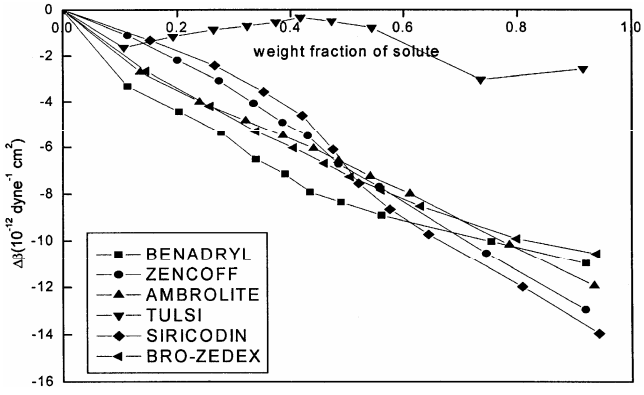

Fig. 4— Variation of β with weight fraction of the solute in the aqueous solutions at 30 °C

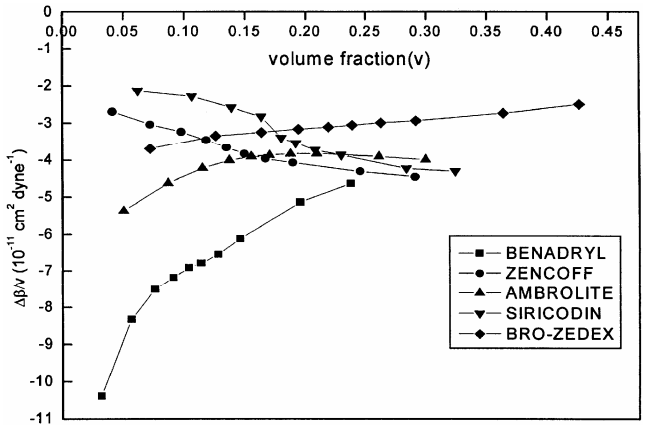

Fig. 5—Variation of Δβ/v as a function of volume fraction of the solute (v) in the aqueous solutions at 30 °C

Δβ is decreasing with concentration, the behaviour is peculiar for the herbal syrup, Tulsi. In all the cases, all the above parameters, u, Δu, β and Δβ record almost linear variations, though totally Δβ is slightly nonlinear.

Now at higher concentrations, the Jacobson's theory of compressibilities is made in the aqueous solutions of all the solutes in their aqueous solutions to study the structural properties of the solutes. The value of μ (a dimensionless parameter) which indicates the mutual association tendency of the dissolved molecules in relation to association tendency with the solvent (water), determines the effect of the solute on the structure of water in its aqueous solutions. If μ >1, mutual tendency of dissolved molecules is small and hence the solute is more effective in breaking the hydrogen bonds in water and the solute is called structure breaker. If μ < 1, mutual association tendency is more and the solute is termed structure promoter / builder / maker.

(Δβ/v) versus v is plotted for five systems (except for Tulsi, herbal syrup). From Fig. 5, the μ values

obtained are 2.82, 5.04, 10.42, 1.65 and 2.644 for benadryl, zencoff, ambrolite, siricodin and bro-zedex respectively. Zencoff, benadryl, ambrolite, bro-zedex and siricodin act as structure breakers ($\mu > 1$) in their aqueous solutions at higher concentrations at 30°C. Though μ could not be calculated for the sixth drug, Tulsi (herbal), from the similar behaviour of velocity, compressibility and the deviations, it may also be considered as structure breaker in its aqueous solutions qualitatively.

Solute – Solvent interactions are also estimated by the recent workers in the aqueous solutions of cefadroxil and other drugs[10] from a study of the values of β_w / β.

If $\beta_w / \beta > 1$, it means that the attractive force among the molecules of the solutes is not weaker than the among molecules of water used as solvent and reflects the presence of structure change of water in the cefadroxil solutions. In our system $\beta_w / \beta > 1$ in all the aqueous solutions of six drugs indicating the presence of structural change of water in the solutions confirming our results from Jacobson's theory.

Also from the plot of Δu/u versus c, the limiting slope A can be calculated ($\Delta u = u_{solution} - u_{solvent}$ and c is the molar concentration). The stacking interaction constant Δ and association constant k for any aqueous solution can be obtained from the intercept and the slope of the plot $((A - \Delta u/uc)/c)^{1/2}$ and $(A - \Delta u/u)$. (If $\left(A - \frac{\Delta u}{u}\right) = x$, plot is between $(x/c)^{1/2}$ and x). If Δu/u versus c is nonlinear, strong solute-solute interactions. The value of k confirms the presence of stacking phenomena in aqueous solution. The compressibility of stack is less than the corresponding monomers in the cefadroxil aqueous solution[9]. Δ indicates the degree of interaction among the solute molecules and if Δ is negative, it indicates the compressibility of monomer is more than that corresponding stack. This clearly reflects dominance of number of molecules in the solution at the temperature of measurement. For zencoff and siricodin Δ is negative and positive for benadryl, bro-zedex and ambrolite.

It may be concluded that majority of the drugs act as structure breakers and strong interactions are noticed.

References

1 Jacobson, B., *The adiabatic compressibility of aqueous solutions, Arkiv Kemi* 2 (1950) 177.

2 Muralikrishna, C., *TVM and TACM studies in aqueous solutions, M.Phil. Dissertation submitted to S.V.University,* (1978).

3 Ravi Meher, E.L., *Ultrasonic studies in liquid mixtures Ph.D., thesis submitted to S.V.University,* (1984).

4 Ravindra Prasad, K., and Reddy, K.C., *Effect of solutes on the structure of water – Jacobson's theory of compressibilities, J. Pure. Appl. Ultrason.* 9 (1987) 4.

5 Muralidhara Rao, G., and Ravindra Prasad, K., *Ultrasonic study of the aqueous solutions of 1, 4 dioxan and pyridine – Jacobson's theory of compressibilities, ibid* 14 (1992) 51.

6 Muralidhara Rao, G., *Ultrasonic studies in aqueous solutions - Jacobson's theory. M. Phil, dissertation submitted to S.V. University,* (1986).

7 Muralidhara Rao, G. and Ravindra Prasad, K., *Ultrasonic studies in aqueous solutions - Jacobson's theory of compressibilities, J. Pure & Appl. Ultrason.* 18 (1996) 37.

8 Ravindra Prasad, K. and Subramanyam Naidu, P., *Ultrasonic study of some ophthalmic solutions in aqueous medium, Indian J. Pure & Appl. Phys.* 41 (2003) 686.

9 Roumana, C., Velraj, G., Roumaisa, and Mohammed Kamil, M.G., "*Acoustical investigation of molecular interaction in aqueous antibiotic solution", J. Pure Appl. Ultrason.,* 30 (2008) 97.

10 Baluja, S., Solauki, A., and Kachchada, *An ultrasonic study of some drugs in solutions, J. Physical Chemistry, A Focus on Chemistry* 81 (2007) 5.

AUTHOR INDEX
Volume 33, January-December 2011